2-5-2019 1:00 PM

A Network Approach to Interdependent Infrastructure Resilience Assessment for Natural Hazards

Howard Tong, *The University of Western Ontario*

Supervisor: Simonovic, Slobodan P., *The University of Western Ontario*

A thesis submitted in partial fulfillment of the requirements for the Master of Engineering Science degree in Civil and Environmental Engineering

Abstract

Natural disasters are increasingly costly to society as they disrupt basic infrastructure functions. Infrastructure managers face challenges from growing urbanization, climate change, and aging infrastructure. Infrastructure resilience is an emerging concept that has been suggested as a solution to this problem; however, it is not yet mature. This thesis proposes to extend an existing dynamic infrastructure resilience quantification methodology to include infrastructure growth capabilities while relaxing some of the original constraints. The methodology uses a complex networks approach to model infrastructure interdependencies that is applied to a case study in the City of Toronto using a newly developed web tool.

Keywords

Resilience, Resilience Quantification, Complex Networks, Infrastructure Growth Interdependency, Critical Infrastructure, Risks, Decision Support, Cascading Failure

Acknowledgments

I would first like to thank my Supervisor, Professor Simonovic, for all the guidance and support he has provided during my time as a Master's student. From the initial opportunity of presenting an interesting research topic in the area of quantitative resilience on decision support to the final corrections of my Master's thesis, my journey has been filled with abundant personal development.

Second, I would like to thank Andre for his support throughout my research endeavors. All of the proposed concepts would remain theoretical without his contributions to developing a decision support tool.

The City of Toronto infrastructure staff as well as Toronto Hydro and Toronto Region Conservation Authority (TRCA) members also contributed to discussions and data collection related to the project.

Next, I would like to thank the Facility of Decision Support and its members for creating a home away from home for me. A special mention goes to Patrick who helped me throughout my time in and out of academia.

I am thankful to the overall Western community, ranging from student services to the Civil and Environmental Engineering Department to Western Water Chapter, for enriching my life as a graduate student.

Finally, I would like to thank my family and friends for their support throughout this chapter of my life.

Table of Contents

List of Tables

List of Figures

Section 1

1 Introduction

The changing climate is driving larger, more intense, and more frequent storms that pose ever-increasing risks to municipal infrastructure around the world. These risks are further exacerbated by urban population growth, which puts even more pressure on aging systems that are interdependent. In this respect, if a hurricane shuts down an electrical grid, a city's water supply may be subsequently cut off.

Losses can take multiple forms, such as physical infrastructure replacement/repair costs, disruptions to economies and businesses, and a decreasing quality of life because of infrastructure failure. Critical municipal infrastructure includes systems, facilities, networks, assets, and services that are essential to the effective functioning of a city. Some examples of critical infrastructure include electrical networks and water distribution and transportation systems. It is crucial that these function properly, but critical infrastructure is becoming increasingly vulnerable to failure, creating a challenging infrastructure management problem. Infrastructure resilience is emerging as a potential means to address these issues. Infrastructure resilience is defined as the ability of an infrastructure system and its component parts to absorb, accommodate, or recover from the effects of a system disruption in a timely and efficient manner, including through the preservation, restoration, or improvement of its essential basic structures and functions (UNISDR, 2017).

1.1 Research Problem

Infrastructure resilience as a concept has been garnering attention in both the scientific literature and the infrastructure management community, but it has not yet been sufficiently developed to provide standards for addressing specific infrastructural issues. Risk is generally considered an important criterion in infrastructure management decision making. Regrettably, these have been shown to have inadequacies when faced with increasingly complex environments. Infrastructure resilience, as a decision-making criterion, is gradually gaining acceptance but is generally qualitative or superficial. Quantifiable objectives are useful to guide good decision making, but there is no standardized quantitative infrastructure resilience approach.

1.2 Thesis Objective

The thesis proposes a quantitative infrastructure resilience approach that calculates a set of infrastructure resilience values to facilitate infrastructure decision making. The infrastructure resilience approach is based on the network theory applied to complex interdependent infrastructure systems. This thesis extends the existing approach, developed by Kong and Simonovic (2016), in five aspects. These are (i) the introduction of spatial impact areas, (ii) adjustable damage representation, (iii) a new subdivision infrastructure development method, (iv) an infrastructure expansion capability for existing networks, and (v) the application of the method through a newly developed web-based tool in the form of a case study in the City of Toronto.

1.3 Approach to Achieve Objective

Kong and Simonovic (2016) used a network approach to represent individual critical infrastructures as layers. Service links between individual layers characterize the interdependencies that exist between them. Hazard scenarios and impact assessments are utilized to determine potential damage to infrastructure layers and functionality. The approach and its implementation accommodate the possibility of multiple hazards and impact relationships. With resulting damage and loss of performance, interdependencies can show the cascading effects that occur over time due to the initial hazard(s). Adaptation measures and recovery priorities are considered that reduce the impacts of hazard(s) and improve system performance. Infrastructure resilience is calculated for each time step, making it a quantitative dynamic measure.

The thesis's infrastructure resilience approach extends the work developed by Kong & Simonovic (2016) in five key ways. First, data types are no longer restricted to network nodes and edges format, as spatial impact areas are now included. For example, infrastructure and buildings can be represented with spatial polygon areas. Second, operational infrastructure network components, such as hydraulic flows in water distribution pipes, can have partial system performance. Originally, Kong and Simonovic's (2016) methodology restricted infrastructure network components to binary, functional, or non-functional, 1-0 system performance values. Third, a feature that takes the form of creating new infrastructure networks in the context of a new subdivision is added. This allows the creation of new suburban road networks. Other critical infrastructure networks, such as water pipes, electrical distribution, gas, and telecommunications, tend to use subdivision roads as a reference for their own development. Fourth, a method of expanding existing critical infrastructure networks is added. The method uses a critical infrastructure's demand, added efficiency, and cost as guiding input parameters. Both the third and fourth added features are tied to different forms of infrastructure growth. Finally, the thesis uses a newly developed web-based tool called ResilSIMt (www.resilsimt-uwo.ca) to apply the proposed methodology and showcase the benefits to infrastructure management decision making. This is accomplished through a case study set in the City of Toronto. The case study contains municipal infrastructure and building elements that are impacted by flooding and wind hazards. The case study is only used to illustrate the capabilities of ResilSIMt and thesis contributions due to the unavailability of real infrastructure data and impact relationships.

1.4 Desired Impacts

The thesis's refinement of an existing quantitative resilience approach aims to contribute to standardizing a quantitative resilience methodology and its use in infrastructure management. A standardized approach can remove one of the impediments preventing resilience use in infrastructure decision making.

The proposed methodology has been adapted into a web-based tool that can be used in the management of complex infrastructure. Through this avenue, quantified resilience can be streamlined into a useable tool for system management, with particular emphasis on handling emerging and future hazards. Using the approach and implemented tool can aid decision support for prioritizing infrastructure and policy investments when overall system resilience is a key objective. For example, the incremental gain in resilience from implementing adaptation measures may prove to be valuable to infrastructure decision makers.

The concept of resilience has the potential to change how decision makers think about how to properly prepare their systems for disruptions to key services such as energy, water, transportation, healthcare, communications, and financial services. The approach and implementation provide the next step in making this vision a reality.

1.5 Organization of Thesis

Section 2 provides a literature review on resilience and how it has been applied to infrastructure. The review identifies the issues encountered during the lifecycle of infrastructure, ranging from planning to maintenance. The quantification of resilience is also explored. Section 3 presents the methodology for this resilience quantification approach, divided into the five key subsections representing infrastructure, hazards, impact, adaptation, and resilience. Section 4 presents a case study in the City of Toronto. Section 5 concludes the thesis and summarizes the key points. Finally, Section 6 discusses potential directions for future research using this approach.

Section 2

2 Literature Review

Section 2 begins with identifying the typical infrastructure management problems and challenges that managers face over the lifecycle of infrastructure. Infrastructure management includes planning, design, and operations and maintenance phases. Subsequently, a literature review of the resilience concept as it has been applied to infrastructure management is provided. Finally, deterministic infrastructure resilience quantification approaches and metrics are presented.

2.1 Infrastructure Management Problems

Infrastructure management can be described as an optimization problem, where maximizing certain objectives is desirable while meeting certain constraints. Each phase of infrastructure management has its own set of challenges due to the state of infrastructure and systems in place. The general format for the following three sections includes a description of the infrastructure management phase, phase implementation, objectives and constraints, and finally, challenges encountered within the management phase. The state of Canadian infrastructure is described, and a summary of challenges is presented.

2.1.1 Infrastructure Planning

Critical municipal infrastructure planning entails connecting systems of production to consumption. These systems come in various forms, such as networks, facilities, assets, and services. Infrastructure planning ensures that these essential systems remain functional over the long term for a city. This is a reflection of societal interest based on the manifestation of social interactions and dynamics and inherently reveals a society's priorities and preferences, whether intentional or not. For example, Ancient Rome's water system was built to prioritize public fountains first, then public baths, and finally, individual homes when there was insufficient flow (Graham & Marvin, 2001). Infrastructure planning is characterized by a long time horizon, as its effects can last decades.

Infrastructure ownership and, subsequently, its planning process, can be private or public. When privatized, multiple utilities may compete to provide various added value services to a profitable market segment. An example of an added value service is when a conscientious green utility provider promotes and secures renewable electrical energy to gain consumer favour.

Cost-benefit analysis is a typical mechanism used in decision making, whereby benefits are based on forecasted demand and usage, and costs include construction and ongoing operations (Flyvbjerg, 2009; Mostafavi, 2017; Van Wee & Tavasszy, 2008). Costs and benefits are quantified in monetary terms to the extent possible. Cash flow diagrams and financial metrics are applied to evaluate the desirability of projects (Van Wee & Tavasszy, 2008).

The overall objectives are different for private and public infrastructure planners. Privatized firms attempt to maximize organizational profits when planning infrastructure. In contrast, public infrastructure planning attempts to maximize benefits and infrastructure services to society at the lowest cost (Simmins, 2011). This is a reflection of whom infrastructure planners ultimately serve. Regardless of whether infrastructure is private or public, both attempt to accommodate the growing demands of modern society, improve productivity while reducing production costs, minimize general business interruptions during implementation, and provide high-quality service to consumers (Flyvbjerg, 2009; Graham & Marvin, 2001; Kelman & Soberman, 2010). Constraints can exist in traditional project management forms, including resources, time, and quality. Regulations and laws must also be abided. For example, there may be restrictions or conditions on the placement of infrastructure to avoid negative environmental impacts (Simmins, 2011).

A few prominent challenges exist for infrastructure planners. First, infrastructure planning involves high levels of uncertainty because of long-term planning horizons and complex interactions (Flyvbjerg, 2009). Within such a long-term timeframe, infrastructure planning can involve multiple parties that have conflicting interests (Flyvbjerg, 2009; Kelman & Soberman, 2010), and project scopes can shift due to changing priorities (Flyvbjerg, 2009; Kelman & Soberman, 2010; Simmins, 2011). Second, infrastructure cost overruns and benefit shortfalls pose a significant challenge to infrastructure planners (Flyvbjerg, 2009; Kelman & Soberman, 2010; Simmins, 2011; Van Wee & Tavasszy, 2008). There are various causes, including proponent strategic behaviour, optimism bias, changes in project specification, inappropriate lifecycle period selection, demand forecasting, value of reliability, and robustness of policies. The value of reliability refers to consumers' trust in key infrastructure. For example, if a hazardous event disrupts infrastructure service, there could be a loss in confidence on the infrastructure. This results in lower than projected infrastructure usage causing a benefit shortfall. Third, asset planning is generally evaluated individually and not in conjunction with how they function to the overall system-of-systems (Mostafavi, 2017). This can make an asset susceptible to cascading failures and perpetuate these failures. This problem can be exacerbated by the amount of aged infrastructure that is still relied on.

2.1.2 Infrastructure Design

Critical infrastructure design entails an application of technical knowledge to generate acceptable specifications of infrastructure elements. The process can include creating models to predict an infrastructure's behaviour over time. Experts also use technical manuals and guidelines as references.

The design of infrastructure varies among different sectors; however, designs share similarities in that they each address core need(s). Designs are translated into objective variables. Given the scale of many critical infrastructure projects, laws and professional bodies usually regulate them. Laws and regulations are termed constraints, or requirements that must be met for the design to be eligible for consideration. Ideally, multiple alternative solutions are proposed that satisfy all of the conditions, but there are various tradeoffs in regards to maximizing the benefits of the set objectives. Decision makers would typically weigh the incremental trade-off benefits and decide on the design solution.

The design of stormwater management systems is used to illustrate the process, though variants of the process may be applicable to other key infrastructure systems. Stormwater designs have multiple objectives. Examples include minimizing flood and erosion risk (Chin, 2006; Ontario Ministry of Environment, 2003) while maintaining water quality (City of Stratford, 2016; Ontario Ministry of Environment, 2003). Fulfilling these objectives has important implications for society, such as the protection of property from surcharge and backwater flooding during storm events (Ontario Ministry of Environment, 2003).

Generally, in Canada, municipalities set specific design criteria and standards. Examples of constraints include the sizing and configuration of components for inlets, outlets, filter media, and distribution pipes (Ontario Ministry of Environment, 2003). Slope and velocity control is used to prevent sediment deposition and scouring (Chin, 2006). This effectively reduces the likelihood of clogging, which can lower system performance. Preventing scouring reduces the chance of earlier component replacement, which can result in higher costs. When stormwater components are combined with other infrastructure components, such as municipal roads that can act as floodways, additional constraints exist. These may include servicing, alignment, safety, and gradient, among others. By extension, additional constraints act on the other critical infrastructure. For example, the depth at the crown should not exceed 150mm for arterial roads when they are used as a floodway (Ontario Ministry of Environment, 2003). Other regulatory constraints may apply to stormwater system designs from other jurisdictions and professional bodies in the form of regulations and design guidelines. For example, the Fisheries Act contains regulations for runoff and its effect on aquatic life.

Stormwater drainage flow models are typically based on a rational method that employs the design peak flow (Chin, 2006; Ontario Ministry of Environment, 2003). Design peak flows normally rely on historical data and return period information. Subsequently, Darcy-Weisbach or Manning flow equations are usually applied for sizing storm sewers.

Many infrastructure designs are based on historical climate data (Chin, 2006; Ontario Ministry of Environment, 2003). As climate change shifts trends in historical data, prior assumptions may no longer be accurate (Boyle, Cunningham, & Dekens, 2013; Upadhyaya, Biswas, & Tam, 2014). This poses a problem because if design assumptions are no longer appropriate, this can create the risk of failure. New design data must be based on modelled predictions, which have uncertainty due to climate forcing and changes due to land cover. Unfortunately, climate change modelling is not sufficiently developed to the point that it can output specific design parameters, such as intensity, duration, frequency of storms, geographical location, and timing for reliable stormwater design modelling (Upadhyaya et al., 2014). In some cases, this is due to limited credible data over a sufficiently long timespan that can be used for modelling climate change impact (Ontario Ministry of Environment, 2003). For example, historical records of the Mississippi River's limit the ability to make adequate prediction for 100 and 500 year return flows when faced with possible changes in climate forcing and land use (Park, Seager, Rao, Convertino, & Linkov, 2013). This issue of insufficiently developed design parameters that adapt the various uncertainties is further voiced in a 2012 survey of Canadian infrastructure engineers reported by the Canadian Standards Association. The survey showed that the main barriers of adapting infrastructure included the "lack of requirements in codes, standards or policy; [the belief that] the changing climate having no effect on engineering practice; and lack of information and resources" (CSA Group, 2012).

When infrastructure investors prioritize recognized risks, it can be at the expense of flexibility, resulting in a rigid design. This makes infrastructure difficult or costly to expand once its construction is complete, as potential future expansion was not considered. For example, this is applicable to situations where there is a future demand for space due to urban growth. Zhao and Tseng (2003) illustrate the value of flexibility with a case study that showed that if an appropriate value was not assigned to flexibility, certain alternative solutions would have been underestimated. In the case of stormwater collection systems, the issue is further magnified by urban population growth that would lead to larger amounts of impervious surfaces that affect the design flow (Upadhyaya et al., 2014).

2.1.3 Infrastructure Maintenance and Operations

Operations and maintenance are usually grouped together as a management phase, although they have separate functions. Operations deals with maintaining the safe and efficient functioning of existing infrastructure components and systems, while maintenance revolves around the actions needed to keep the infrastructure components and systems in working condition. Operations typically deals with choosing the desired state of functionality. Maintenance deals with the deterioration of infrastructure due to environmental stressors that act on it through time and how to handle these. Maintenance personnel decide on the infrastructure components that need attention, along with the process and timing required to keep performance above a minimum acceptable threshold (Sánchez-Silva et al. 2016).

Common sense and heuristic decision making are frequently used when creating a maintenance policy. When maintenance models are employed to help with developing a policy, they typically incorporate some form of a reliability measure or index for infrastructure that is expected to degrade. These measures inform actions that include regular inspections, maintenance, rehabilitation, decommissioning, and replacement (Sánchez-Silva et al. 2016). Digital tools can be employed to aid the process, such as remote sensing, which has been utilized to identify infrastructure conditions and save costs (American Society of Civil Engineers, 2017).

Operations and maintenance objectives typically include maximizing service usage, lifecycle performance, and safety while minimizing lifecycle costs. Constraints include the amount of resources available and safety and reliability considerations (Sánchez-Silva et al. 2016). For some infrastructure operations, there may be capacity constraints due to physical limitations or congestion (American Society of Civil Engineers, 2017).

The World Economic Forum has commented that many governments have been unable to do well in operations and maintenance, partly owing to insufficient funding. There also seems to be a political bias towards new infrastructure while maintenance is neglected (World Economic Forum, 2014). Insufficient funds for infrastructure investment in the past led to a decline in the physical state of infrastructure, resulting in increased costs to renew infrastructure later down the line (Canadian Construction Association et al., 2016). Insufficient funds can also lead to a lack of system monitoring automation, which can result in the malfunction of key components in electrical settings (Agostino & Scala, 2014). A lack of funds can also translate to the absence of needed field condition assessments, which creates greater uncertainty and reliance on assumptions (Ahmad, 2015; Harvey et al., 2017; Ontario Sewer & Watermain Construction Association, 2018).

Furthermore, growth in the population, economy, and urbanization exacerbate the situation, with infrastructure forced to operate beyond its expected capacity. For example, updates to environmental legislation also require local governments to hasten the upgrade of infrastructure (Canadian Construction Association et al., 2016). The lack of adaptive action can materially affect the lifespan and capability of key Canadian infrastructure.

Climate change also poses a challenge for operations and maintenance management. The increased frequency and severity of extreme weather events create larger losses. For example, Hurricane Irene caused more bridge deterioration in the timespan of one day than in multiple years in Vermont (Mostafavi, 2017). Additionally, the composition of material can be affected by changing climate conditions. For example, wood-based designs in drier conditions are increasingly susceptible to fire. Likewise, changing climate, in terms of variability, may affect the weathering of existing materials in structures, effectively reducing the lifecycle of infrastructure (Boyle et al., 2013). The 2017 American Infrastructure Report Card cautioned that aging equipment, capacity bottlenecks, increased demand, and climate impacts are factors that will create more power interruptions in terms of frequency and severity (American Society of Civil Engineers, 2017). For example, the incorporation of wind energy and trans-border flow can result in infrastructure being operated beyond the capacity of the original design (Agostino & Scala, 2014).

2.1.4 State of Infrastructure in Canada

Much of the infrastructure that current Canadian municipalities depend on needs renewal. Half of the Canadian electrical sector generation infrastructure was built before 1980 (Baker, Sklokin, Coad, & Crawford, 2011). Twelve percent of potable water infrastructure is in poor or very poor condition. For wastewater and stormwater infrastructure, these percentages are 11% and 7%, respectively (Canadian Construction Association et al., 2016). Thirty-four percent of roads, bridges and culverts are in poor conditions (Ahmad, 2015). Despite the deteriorating conditions of critical infrastructure, the current reinvestment rate is lower than the required target rate needed to maintain infrastructure in good quality for the coming years (Canadian Construction Association et al., 2016). In a recent report, 20% of linear infrastructure for potable water, stormwater, and wastewater was in poor or worse condition (Ontario Sewer, 2018). Deteriorating infrastructure increases the risk of system performance disruption and subsequent failure (Ahmad, 2015; Baker et al., 2011; Canadian Construction Association et al., 2016; Harvey et al., 2017; Ontario Sewer & Watermain Construction Association, 2018; Upadhyaya et al., 2014).

Common themes emerge from the sets of infrastructure problems present in the Canadian setting. These include urban growth, climate change, and aging infrastructure (Ontario Sewer & Watermain Construction Association, 2018; Simonovic, 2016; Upadhyaya et al., 2014). Municipalities are constantly faced with the pressure to provide more services and maintain high reliability and standards while being limited to existing resources. At the same time, reliability is a valued measure in engineered systems (Hosseini, Barker, & Ramirez-marquez, 2016). Preventing infrastructure failure and loss makes financial sense. Infrastructure resilience has been cited as a concept that can address several of these infrastructure management challenges within the planning, design, and operations and maintenance phases (Ayyub, 2015; Mostafavi, 2017; Simonovic, 2016). Interest in and popularity of infrastructure resilience within the research community and among practitioners have grown in recent years (Mcaslan, 2010). Although disaster vulnerability analysis and subsequent management have historically been used in infrastructure management, there is a shift towards resilience as it is considered more proactive (Simonovic, 2016; Simonovic & Peck, 2013).

2.2 Resilience as an Infrastructure Management Criterion

2.2.1 Background of Resilience

Given the potential that infrastructure resilience holds in addressing infrastructure management challenges, it is worthwhile to explore the background of the term. The term "resilience" was originally used to describe the elasticity of a solid material (Mcaslan, 2010; Rankine, 1867). In the 1970s, Holling applied the term in the field of ecology to describe the ability of a system to absorb shocks (Holling, 1973). This shift in definition marked an increased usage of the term resilience in many other disciplines and contexts (Park et al., 2013). Hosseini et al. (2016) commented that the engineering resilience domain is relatively new compared to other domains, such as the organizational, social, and economic domains. Linkov & Palma-Oliveira (2017) also noted that resilience concepts are relatively new to the risk management community.

In a review of resilience concepts, as they relate to complex engineered adaptive systems, Woods (2015) claimed that resilience can generally be organized into four categories. The first is resilience as rebound, which focuses on recovery once a disruption has occurred, given a systems' capabilities beforehand. The second is resilience as robustness, which is associated with the ability of a system to maintain functionality in the face of disruption. The third is resilience as graceful extensibility, which explores how systems stretch to accommodate unknown disaster circumstances. The fourth is resilience as architectural properties that produce sustained adaptability, which focuses on the principles that continue to provide capability, or the lack of, to respond well to disruptions. While this section is focused on the past development of the resilience concept and its usage, the next section is specifically focused on infrastructure resilience.

2.2.2 Infrastructure Resilience Definition

Although various definitions of infrastructure resilience exist, they share some common characteristics. Infrastructure resilience is based on a measure of system performance that can vary between different infrastructure systems (Ayyub, 2015; Reed, Kapur, & Christie, 2009; Simonovic, 2016). Many authors have tied infrastructure resilience to the functionality or capacity of infrastructure systems and their ability to manage the situation when faced with disruptions (Bruneau et al., 2003; Francis & Bekera, 2014; Mcaslan, 2010; Mostafavi, 2017; Park et al., 2013; Vugrin, Warren, Ehlen, & Camphouse, 2010). Examples of system performance measures include the number of functional transmission towers or kilometers of roads remaining functional during a hazard.

Resilience is threat dependent (Hosseini et al., 2016; Park et al., 2013). Infrastructure resilience has been described as an emergent property of systems (Linkov and Palma-Oliveira 2017; Francis and Bekera 2014; Hosseini, Barker, and Ramirez-Marquez 2016). This description emphasizes that it is the response of a system, rather than a constant, unchanging property. Recovery is considered to be a key component of resilience in many definitions (Hosseini, Barker, and Ramirez-Marquez 2016). The speed of recovery is also an important factor (Mostafavi, 2017).

Different definitions of infrastructure resilience can be found from various organizations and their respective documents. These include the Presidential Policy Directive on Critical Infrastructure Security and Resilience (The White House, 2013), American Society of Civil Engineers Committee on Critical Infrastructure (ASCE, 2013), National Infrastructure Advisory Council (National Infrastructure Advisory Council, 2009), Multidisciplinary Center for Earthquake Engineering Research (MCEER, 2006), and the United Nations Office for Disaster Risk Reduction (UNISDR, 2017). All definitions share similarities in that they describe mitigating damage to a system and recovering rapidly. For the purposes of this thesis, the definition provided by the United Nations Office for Disaster Risk Reduction for infrastructure resilience is used. Infrastructure resilience is defined as the ability of an infrastructure system and its component parts to absorb, accommodate, or recover from the effects of a system disruption in a timely and efficient manner, including through the preservation, restoration, or improvement of its essential basic structures and functions (UNISDR, 2017).

Simonovic and Peck (2013) presented a method to quantitatively assess dynamic resilience. They proposed a spatial-time dynamic resilience measure based on physical, health, economic, social, and organizational system performance dimensions (Simonovic & Peck, 2013). Dynamic resilience refers to an idea that resilience changes over the course of a disruption. Thus, one can observe the progression of system performance over time. Collectively, this produces a set of resilience values for a disruptive event. Not all infrastructure resilience metrics are dynamic. Many of the metrics are static and a review of quantitative approaches presented in Section 2.3 reinforces this point. However, there are practical benefits to using a dynamic infrastructure resilience metric. This is discussed further in Sections 2.2.3 and 2.2.4. Simonovic and Peck (2013) were the first to introduce dynamic resilience measures in the context of flood management (Irwin, Schardong, Simonovic, & Nirupama, 2016; Irwin, Simonovic, & Nirupama, 2016; Simonovic & Arunkumar, 2016).

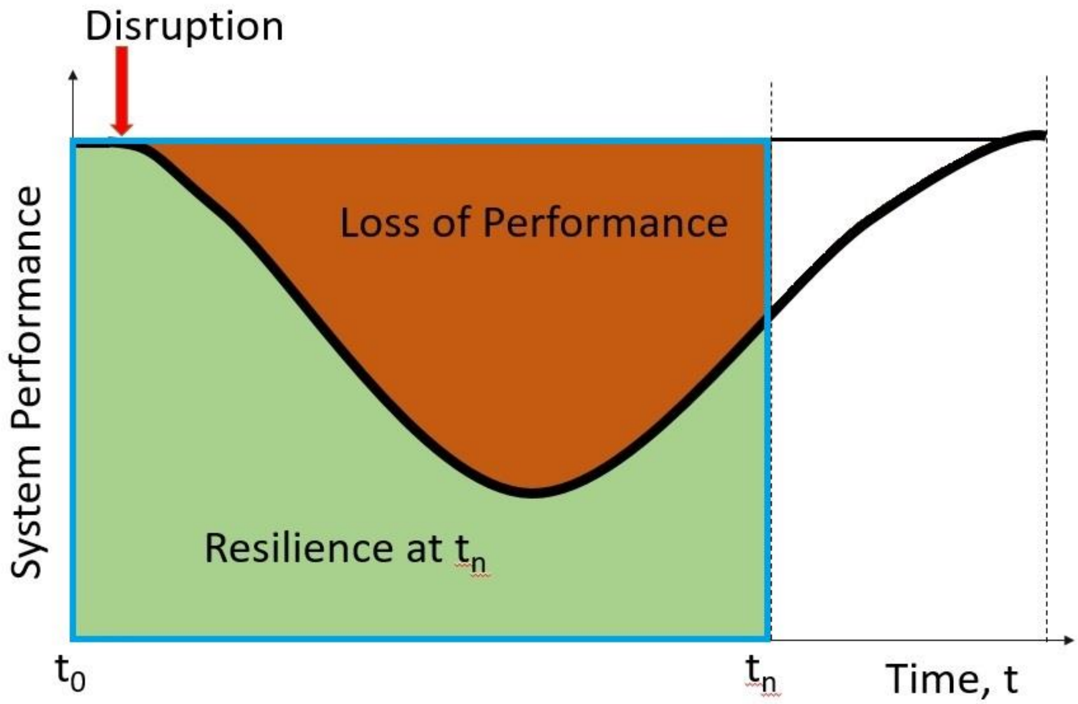

Figure 1 Method to quantify infrastructure resilience from system performance

Figure 1 presents a graphical interpretation to assess infrastructure resilience based on the work of Simonovic and Peck (2013). The curve shows how system performance varies when faced with a disruption. The green area underneath the system performance curve represents the remaining performance over time. The rectangular area outlined in blue represents potential system performance the system would have provided by time t_n if there were no disruption. Note that the orange area can be interpreted as the loss of performance experienced by time t_n. Simonovic and Peck (2013) quantified this loss of performance in equation (1).

$$\rho^i(t,s) = \int_{t_0}^{t} [\,P_o^i - P^i(t,s)]dt, \qquad where\ t \in [t_0, t_1] \tag{1}$$

where $\rho^i(t,s)$ is the performance loss of a specific impact at a specific time, t, and space, s. P_o^i is the initial performance prior to disruption, and t_o is the initial time of disruption. t_1 is the final time step under consideration. $P^i(t,s)$ is the performance indicator of a specific impact at a given time and in a given space.

By knowing the potential performance that could have occurred and the loss in system performance during a disruptive event, the resilience of a single impact for a single infrastructure, r^i, can be calculated in equation (2).

$$r^i(t,s) = 1 - \frac{\rho^i(t,s)}{P_o^i \times (t - t_o)} \quad \textbf{(2)}$$

Referring back to Figure 1, infrastructure resilience is based on the ratio of remaining system performance and the potential performance a system could have had. Note that this formulation effectively normalizes the resilience measure to a value ranging from 0 to 1.

If the performances of multiple infrastructure systems are under consideration, individual resilience values calculated from (2) can be combined to form a single set of resilience values using equation (3).

$$R(t,s) = \left\{\prod_{i=1}^{M} r^i(t,s)\right\}^{\frac{1}{M}} \quad \textbf{(3)}$$

where R is the set of resilience value, and M is the total number of infrastructure impacts.

Bruneau et al. (2003) also quantitatively assessed disaster resilience; the authors claimed that resilience consists of four properties that are common among physical and social systems, namely robustness, redundancy, resourcefulness and rapidity. Robustness refers to the ability of a system to maintain a minimal level of functionality despite shocks and stressors. Redundancy refers to the level of substitutability of system components, resulting in a lower loss of functionality than otherwise expected. Resourcefulness refers to the ability of a system to prioritize resources to adapt to the disruptive situation. Rapidity refers to the ability of a system to efficiently return to a desirable stable state

(Bruneau et al., 2003). Simonovic & Arunkumar (2016) took these four properties further by considering them as part of adaptive capacity and proposed a quantification for each of them, as shown in Figure 2.

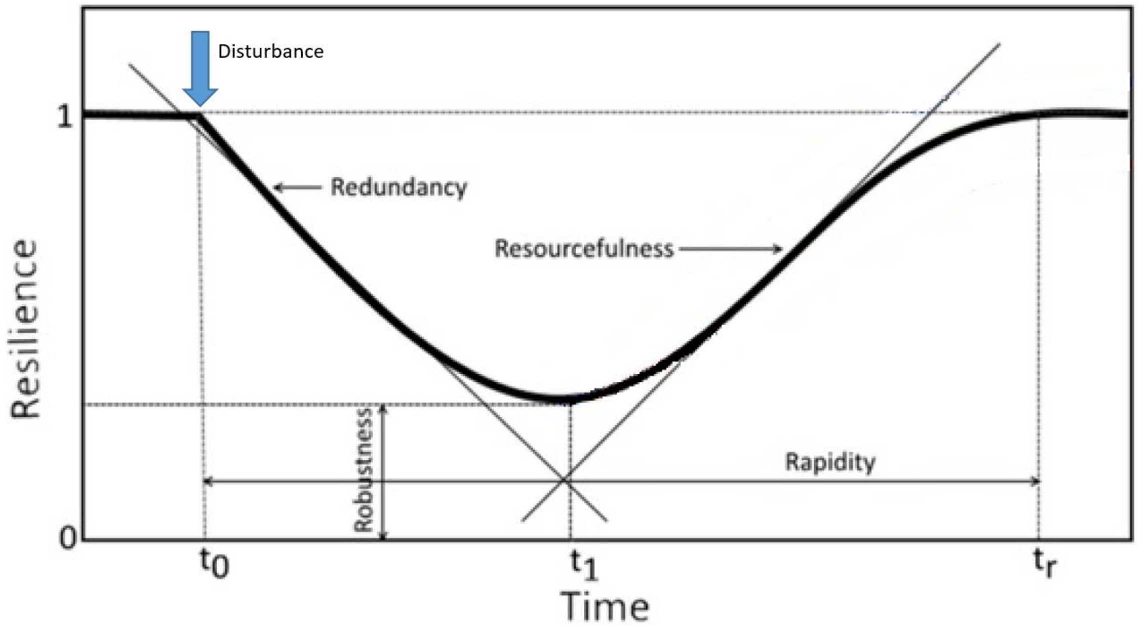

Figure 2 Quantification of resilience properties, including robustness, redundancy, resourcefulness and rapidity. Adapted from Simonovic and Arunkumar (2016)

The variable t_0 in the above graph refers to the time of disturbance, t_1 refers to the time associated with the minimum resilience of the overall system and t_r refers to the time of full recovery. As displayed in the figure, robustness is the lowest level of resilience that occurs in the simulation, associated with the remaining system performance of the overall system. Redundancy is interpreted to be the downward slope after the disturbance has occurred, with the end point being the minimum performance encountered. Resourcefulness is the upward slope associated with the recovery phase. Finally, rapidity is the time required before the system is fully recovered.

Many resilience definitions, including the one used for this thesis, advocate for mitigation and recovery efforts. These ideas relate to the infrastructure system's absorptive capacity and adaptation measures. Kong and Simonovic (2016) proposed that absorptive capacity is comprised of a proactive absorptive capacity component and reactive absorptive capacity component. Proactive absorptive capacity is attributed to the remaining system performance once a disruption occurs throughout time if no recovery measures or initiatives are set in place. Reactive absorptive capacity refers to the added system performance over time as a result of recovery measures or initiatives. Reactive absorptive capacity typically refers to the resources that are expended during and after a disaster to improve system performance recovery, while proactive absorptive capacity is associated with long-term infrastructure planning and design (Kong & Simonovic, 2016). In this sense, the effect of adaptation measures is the enhancement of either the proactive or reactive absorptive capacities. In relation to the concepts of robustness, redundancy, resourcefulness and rapidity, the measures are enhancing these characteristics (Simonovic, 2016). Adaptation encompasses measures that help infrastructure systems cope with disruption scenarios and restore system functionality back to their pre-hazard state.

2.2.3 Infrastructure Risk-based Management vs Infrastructure Resilience

Infrastructure management generally involves some form of risk analysis. Traditional risk is defined as the potential loss that could occur as a result of a hazardous event. It is typically measured as the product of hazard, exposure and vulnerability (Francis & Bekera, 2014; Little, 2010; Simonovic, 2016). Sometimes, it is also calculated as the product of probability and severity of an event. The literature by Park et al. (2013) and Linkov and Palma-Oliveira (2017) compared the different perspectives of risk and resilience. In the following paragraphs, a comparison is made between traditional risk and dynamic resilience metrics, and four main differences are identified.

First, traditional risk differs from dynamic resilience in that metrics are aggregated into a single value. A traditional risk measure aggregates probability and consequences into a single value. Consequently, from the perspective of a decision maker who did not perform the analysis, there can be similar risk levels for different classes of events. For example, a high-severity, low-probability event can have the same overall risk value and interpretation as a low-severity, high-frequency event (Little, 2010).

Second, as traditional risk is represented as a single value, the traditional risk measure has a static nature. A single static measure does not reflect changing system behaviours that occur during a disruptive event. In comparison to risk that has a tendency to aggregate potential losses into a single monetary value, a resilience metric applies a broader framework that exceeds the idea of merely reducing monetary loss (Bruneau et al., 2003). Dynamic resilience has a temporal component (Francis & Bekera, 2014; Linkov & Palma-Oliveira, 2017), which reflects a key property of complex systems that risk analysis misses (Francis & Bekera, 2014). A set of resilience values, represented by the changing dynamics of an overall system's behaviour, captures a system's characteristics and interdependent interactions throughout a disruption (Simonovic & Arunkumar, 2016). A static measure of resilience in isolation would be unable to capture the minimum performance encountered, the time it takes to recover, and changes to system performance over time (Simonovic & Arunkumar, 2016).

The third difference is that traditional risk definitions focus on mitigating potential loss and thus lack a recovery aspect (Linkov & Palma-Oliveira, 2017). Resilience measures consider recovery to be an essential aspect of analysis (Francis & Bekera, 2014; Hosseini et al., 2016; Linkov & Palma-Oliveira, 2017; Mcaslan, 2010). Traditional risk management generally attempts to reduce pre-hazard vulnerabilities for disaster management (Hosseini et al., 2016; Linkov & Palma-Oliveira, 2017; Simonovic, 2016). Examples of traditional risk solutions often focus on hardening or reinforcing a vulnerable area or applying a fail-safe solution to make the infrastructure less susceptible to harm (Hosseini et al., 2016; Linkov & Palma-Oliveira, 2017; Park et al., 2013). In comparison, infrastructure resilience focuses on ensuring a system remains as close to optimal functionality or stability as possible and recovers quickly in the case of failure (Hosseini et al., 2016; Linkov & Palma-Oliveira, 2017; Little, 2010; Park et al., 2013).

The fourth difference identified is that traditional risk analysis relies heavily on probability estimates of hazards. Unfortunately, the reliability of probability estimates for extreme weather events can be low, partially due to a lack of available data concerning these extreme events (Park et al., 2013). Even when traditional risk analysis has the ability to identify low-probability, high-severity hazards, the exact impact on infrastructure can be uncertain. For example, it can be extremely difficult to accurately predict the failure modes that occur during cascading failures (Little, 2010). Given the inherent uncertainty that exists in predicting extreme events and the fact that their impact is material, risk analysis cannot adequately prevent system failure in the long run (Linkov & Palma-Oliveira, 2017; Little, 2010; Park et al., 2013). Although these low-probability, high-severity events are rare, they can occur, as evidenced by the September 11 terrorist attacks and the Fukushima disaster (Francis & Bekera, 2014; Linkov & Palma-Oliveira, 2017), and are arguably an inevitable occurrence (Homeland Security Council, 2007). Merz, Elmer, and Thieken (2009) cautioned that expected annual damage as a risk indicator should be used carefully as it may not align with societal priorities. This stems from the limitations of flood risk analyses that convey incomplete information, leading to a mismatch between technical risk appraisals and societal perceptions of risk (Merz et al., 2009). In this sense, Little (2010) argued that a greater focus on the consequences can yield better management guidance, citing a hypothetical scenario based on Hurricane Katrina and New Orleans with regards to infrastructure development. Therefore, traditional risk analysis may not be adequate to prepare for low-probability, high-consequence disasters that drastically affect society (Linkov & Palma-Oliveira, 2017).

Nonetheless, infrastructure management generally relies on risk analysis. In a thesis regarding infrastructure resilience, it is appropriate to define traditional risk management and compare it with infrastructure resilience. There is a remarkable emphasis now placed on resilience when it comes to disaster management as opposed to simply reducing vulnerabilities, given its proactive and positive approach (Linkov & Palma-Oliveira, 2017; Simonovic, 2016).

2.2.4 Appropriateness of Using Resilience in Infrastructure Management

Dynamic resilience can yield multiple benefits when applied to infrastructure management. As the world becomes increasingly complex with urban growth, climate change, and aging infrastructure, the drawbacks of applying traditional infrastructure risk are made more apparent with the rising number of failures observed. Infrastructure resilience can be used to characterize how infrastructure system behaviour changes during a disruptive event. Overall, it acknowledges that failures may not always be preventable but can be accepted as long as recovery is timely and graceful. Infrastructure resilience shifts the focus to minimizing critical functionality loss rather than preventing initial loss. As a metric, it integrates multiple types of performance metrics from different infrastructure systems (Simonovic, 2016). These changes create a different value proposition than traditional risk management. Infrastructure managers may find these benefits to be of greater value, particularly in a critical infrastructure setting, where functionality is emphasized. Infrastructure resilience can be applied to the different stages of infrastructure management, ranging from planning to design to operations and maintenance. Two key characteristics are recommended to make infrastructure resilience metrics more useful to infrastructure decision support, namely using a quantitative measure with a dynamic nature.

Quantitative measures are generally desirable for decision support. They convey a precise sense of extent and magnitude for the decision maker. Quantitative measures also provide a relatively consistent view in comparison to qualitative measures, which may be more easily influenced by subjectivity. In terms of infrastructure management, qualitative infrastructure resilience does not inform how to improve system resilience (Alderson, Brown, & Carlyle, 2014). A quantitative measure of resilience is essential to analyze system behaviour (Mcaslan, 2010). In the literature (Ayyub, 2015; Bruneau et al., 2003; Cutter et al., 2008; Henry & Ramirez-marquez, 2012; Simonovic & Arunkumar, 2016; Simonovic & Peck, 2013; Vugrin et al., 2010) practical benefits of applying infrastructure resilience have been discussed. For example, resilience measures can serve as a baseline for policy assessment and determining the added value of adopting different decisions (Bruneau et al., 2003; Mostafavi, 2017; Tierney & Bruneau, 2007).

Most static resilience approaches that yield a single value fail to capture changes in system performance and subsequent recovery (Simonovic, 2016; Simonovic & Arunkumar, 2016). A static resilience measure in isolation cannot reflect the essential characteristics of resilience, including robustness, redundancy, resourcefulness, and rapidity (Simonovic & Arunkumar, 2016). Dynamic resilience reflects changes to a system’s behavioural response in a given scenario. This serves as valuable insight for infrastructure decision makers and is key for evaluating system recovery strategies (Simonovic, 2016). A dynamic infrastructure resilience measure is crucial for evaluating complex and interdependent components (Kong & Simonovic, 2016; Simonovic & Arunkumar, 2016; Simonovic & Peck, 2013).

A traditional risk approach to infrastructure management may have deficiencies in that it yields a single static value based on uncertain probabilities and does not consider recovery efforts. A quantitative and dynamic infrastructure resilience measure can address these gaps. It can be applied to the various infrastructure management phases to address some of the challenges cited in Section 2.1. It can also be used to evaluate recovery strategies post hazard.

2.2.5 Interest in Raising Resilience by Infrastructure Owners

Infrastructure resilience has become a fundamental concept for any decision maker who wants to ensure sustained functionality of critical infrastructure to new forms of threats (Linkov & Palma-Oliveira, 2017). This need becomes more apparent after disasters. Examples of such large-scale disasters include Hurricane Katrina in 2005, the Haiti earthquake in 2010, the Deepwater Horizon oil spill in 2010, the Fukushima nuclear accident in 2011, and Hurricane Sandy in 2012 (Alderson et al., 2014; Simonovic & Peck, 2013). Various governments, municipalities, and infrastructure owners have declared interest in infrastructure resilience. The Homeland Security Council acknowledged the need for infrastructure resilience in critical infrastructure and included this sentiment in their 2007 National Strategy (Homeland Security Council, 2007).

The 100 Resilient Cities initiative by the Rockefeller Group was initiated to raise infrastructure resilience in cities around the world (Friedman & Lee, 2017). The group was pioneered by the Rockefeller Foundation to help global cities become more resilient to disruptions of fundamental societal functions (100 Resilient Cities, 2018). The non-profit organization aims to catalyze the urban resilience movement by creating a platform to share ideas and experiences related to urban resilience. The platform's membership consists of chief resilience officers from 100 selected cities around the world. These chief resilience officers have access to global industry leaders and innovators in various sectors, as well as a peer-to-peer network of other cities' resilience officers to share best practices, training, and information (Friedman & Lee, 2017).

Department(s) or working group(s) within an organization may also independently acknowledge and pursue making their infrastructure more resilient. For example, the Colorado Department of Transportation initiated work to raise their infrastructure resilience after a flooding event (Mostafavi, 2017). At other times, interest in infrastructure resilience arises to address specific needs. For example, through the case study of a multipurpose reservoir system that quantifies resilience using a system dynamics approach, Simonovic and Arunkumar (2016) demonstrated that a set of dynamic resilience values is valuable in selecting appropriate adaptation measures.

2.2.6 Need for Practical Resilience Measures

Given the current interest in managing infrastructure challenges of urban growth, climate change, and aging infrastructure, a traditional risk measure to guide decision makers is insufficient. There are issues with such an approach related to how a single static risk measure cannot fully represent an infrastructure system's response to disruption. Furthermore, the probabilities associated with forecasting these disruption events contain uncertainty, and a traditional risk approach generally does not consider infrastructure recovery. An infrastructure resilience approach can be applied to address some of these gaps.

Overall, there is a need for infrastructure resilience concepts to be further developed and tested. Despite various resilience frameworks and definitions, a consistent definition and approach to resilience remains elusive (Mcaslan, 2010). Resilience is less mature than risk when it comes to quantification measures (Linkov & Palma-Oliveira, 2017). The majority of existing infrastructure resilience measures found in the literature are qualitative in nature (Alderson et al., 2014). Nonetheless, resilience metrics can range from relatively simple measures, such as those of a qualitative nature, to sophisticated ones that are limited only by the sophistication and availability of information (Linkov & Palma-Oliveira, 2017). There is a lack of quantitative infrastructure resilience approaches (Simonovic & Peck, 2013). For example, resilience indices for transportation networks are limited (Mostafavi, 2017). Accordingly, there is a need to develop, standardize, and apply an infrastructure resilience approach to infrastructure management problems in the face of natural disasters (Ayyub, 2015).

2.3 Resilience as a Criterion for Infrastructure Decision Making

Although quantitative infrastructure resilience approaches have been less developed thus far, several are available. Here, the resilience approaches relevant to critical infrastructure are explored and presented chronologically. Various types of approaches based on system analysis tools, such as complex networks, agent-based modelling, and system dynamics are identified. However, it should be noted that not all have been framed in an infrastructure resilience approach with an emphasis on critical infrastructure. For each approach, the infrastructure resilience quantification metric is shown. If the quantification of robustness, rapidity, redundancy, and/or resourcefulness is available, it is described as well. Additional formulas are also presented as they relate to the respective infrastructure resilience quantification.

Bruneau et al. (2003) looked into resilience quantification as a means to determine how to minimize the reduction of quality of life in societies faced with earthquake hazards. The authors define resilience as the remaining quality of community infrastructure, denoted as Q(t), over time, as illustrated in Figure 3.

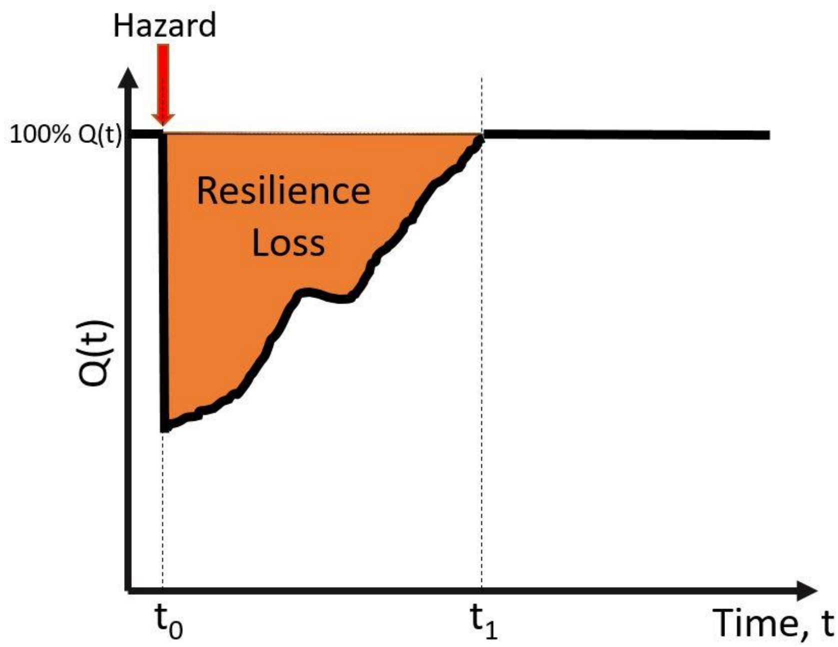

Figure 3 Bruneau et al. (2003) resilience metric. This figure is adapted from Hesseini et al. (2016).

Equation (4) below shows their resilience metric.

$$RL = \int_{t_0}^{t_1} [100 - Q(t)]dt \tag{4}$$

where RL denotes resilience loss, Q(t) is the quality of community infrastructure at time t, t_0 is when the disruption begins, and t_1 is when the community returns to its pre-disruption quality. Q(t) can be interpreted as the functional capacity of an infrastructure component and/or system. Note that the value of 100 in the figure refers to the maximum performance percentage. The formulation is considered to be a deterministic static measure for infrastructure resilience.

The infrastructure resilience approach developed by Reed et al. (2009) was influenced by the resilience metric developed by Bruneau et al. (2003). The quantified infrastructure resilience is based on the quality of the system, where quality is affected by fragilities and interdependencies. The approach applies an input-output inoperability model. The quality of a given infrastructure system at any given time is determined by equation (5).

$$Q(t) = Q_\infty - (Q_\infty - Q_0)e^{-bt} \quad \textbf{(5)}$$

where Q(t) is the quality of a particular system at a given time. The quality of a system can refer to an infrastructure system's service level, performance, or capacity. For example, it could refer to the amount of water demand met during a hazard event. In Bruneau et al.'s (2003) paper, the values of Q(t) range from 1, meaning it is fully operational, to 0, meaning it is completely inoperable. Q_∞ is the capacity of the system at full functionality, and Q_0 is the capacity of the system post-event. The variable t is the time since the beginning of the hazard event. The variable b is an empirically derived parameter from the recovery data of the event. This variable is also proposed as the rapidity of the scenario.

The robustness in this approach is interpreted to be the minimum quality of the system encountered during the hazard scenario. Infrastructure resilience is quantified by applying equation (6) below.

$$R = \frac{\int_{t_1}^{t_2} Q(t)dt}{t_2 - t_1} \quad \textbf{(6)}$$

where R is the infrastructure resilience, and Q(t) is the quality of the system at time t. The variables t_1 and t_2 are the endpoints of the scenario under consideration. If multiple infrastructure systems are under consideration, overall system resilience is derived using equation (7) below.

$$R_s = g(R_1, R_2 \dots R_i \dots R_n) \quad \textbf{(7)}$$

where R_s is the overall system resilience and comprises a combination of other subsystem resiliencies of R_1, R_2 … R_n.

Ip and Wang (2011) applied a network approach to estimate the infrastructure resilience of a Chinese railway. The network was modelled as an undirected graph with nodes as city destinations and edges as paths between cities. Each node is associated with a population, and each edge has a reliability measure. Several parameters had to be set up before the infrastructure resilience of the network could be calculated. First, two sets of weights had to be determined, as demonstrated in equation (8) and equation (9), based on the nodal population.

$$w_i = u_i / \sum_{j=1}^{n} u_j \,, \quad i = 1,2 \ldots, n \tag{8}$$

$$v_i = u_i / (\sum_{j=1}^{n} u_j - u_i) \,, \quad i = 1,2 \ldots, n \tag{9}$$

where u_i is the population of a city node at i, and n represents the total number of city nodes in the railway network. w_i is the weight of a city node calculated as the proportion of a specific city's population to the overall population of the network. v_i has a similar meaning but with the exclusion of the specific city's population from the overall amount. The second step involves identifying all of the pathways available from a specific city i to the rest of the cities in the network. The authors' provide a step-by-step guide on how to do so in their original paper (Ip & Wang, 2011). The third step involves calculating the resilience of each individual node in the network through equation (10).

$$r_i = \sum_{j=1, j \neq i}^{n} v_j \times NP(i,j) \tag{10}$$

where r_i is the resilience of a specific node i, n refers to the number of nodes in the network, v_j is the value calculated above from equation (9), and NP(i,j) refers to the number of reliable passageways available between cities i and j. Finally, the infrastructure resilience of the entire network can be estimated through equation (11).

$$R(G) = \sum_{i=1}^{n} w_i \times r_i \tag{11}$$

where R(G) refers to the infrastructure resilience of the entire graph. Again, n refers to the number of nodes. w_i is from equation (8), and r_i is from equation (10).

Henry and Ramirez-Marquez (2012) proposed a time dependent infrastructure resilience metric that can be adopted based on the fundamental definition of resilience. They applied this to a road network example using a ratio of recovery to loss that is a function of time. The metric is shown in equation (12).

$$\text{Я}_F(t_r|e_j) = \frac{F(t_r|e_j) - F(t_d|e_j)}{F(t_0|e_j) - F(t_d|e_j)} \tag{12}$$

where Я denotes the infrastructure resilience value for a specific time and event. F() is the figure-of-merit that refers to a quantifiable system performance level. Traffic is an example of a figure-of-merit that illustrates a road network's system performance. e_j refers to the condition of a specific disruptive event, t_0 is the time before a disruptive event occurs, t_d is the time of disruptive event associated with the lowest system performance, and t_r is a specific moment in time bounded between t_d and the final system state.

Simonovic and Peck (2013) provided a dynamic resilience quantification approach that uses systems dynamics to model impacts of natural disasters in coastal megacities. Their work was previously discussed in Section 2.2.2.

Francis and Bekera (2014) proposed a resilience analysis framework and metric. Their infrastructure resilience metric is obtained from three key resilience capacities, namely adaptive capacity, absorptive capacity, and recoverability (Francis & Bekera, 2014). Equation (13) expresses their infrastructure resilience metric.

$$\rho_i(S_p, F_r, F_d, F_o) = S_p \frac{F_r}{F_o}\frac{F_d}{F_o} \tag{13}$$

$$\text{Where } S_p = \begin{cases} (t_\delta/t_r^*)\exp[-a(t_r - t_r^*)] \;\; for \; t_r \geq t_r^* \\ (t_\delta/t_r^*) \;\; otherwise \end{cases}$$

where ρ_i denotes the infrastructure resilience for a specific event *i*. S_p is the recovery factor. F_o is the pre-event stable performance level. F_r is the new stable performance level, and F_d is the lowest performance level immediately after a disaster. t_δ is the slack time, t_r is the time associated with the new stable performance level, t_r* is the time associated with the onset of recovery actions, and *a* is the resilience decay factor.Francis and Bekera (2014) noted that the ratio of F_r/F_o represent the adaptive capacity. It compares the final system performance level to the original state prior to the disaster. The ratio of F_d/F_o represent the absorptive capacity and refers to the remaining performance level after an event.

Bhatia et al. (2015) applied a data-driven, quantitative network approach to determine the resiliency of an Indian rail network. The authors used nodes to represent stations and edges as origin-destination pairs and an adjacency matrix to designate the connectivity between two stations where the values are binary. As most of the origin-destination nodal pairs were bidirectional, the infrastructure was modelled as an undirected weighted graph. The authors proposed a state of critical functionality (SCF) measure as shown in equation (14) below:

$$SCF = FF/TF \tag{14}$$

where TF refers to total functionality, which reflects the number of functional nodes prior to failure. FF refers to fragmented functionality, which reflects the remaining number of functional nodes of the giant component. The giant component represents the largest connected set of nodes of a network during a single instance. SCF is interpreted to be the authors' measure of resilience.

Sela, Bhatia, Zhuang, and Ganguly (2017) further extended the work completed by Bhatia et al. (2015). They modelled critical infrastructure systems as directed graphs and considered multiple infrastructure systems. Their case study illustrates the interaction of two critical infrastructure networks, namely power and railway.

Kong and Simonovic (2016) modelled critical infrastructure through a systems approach. They represented infrastructure as network layers using a graph theory and included interdependencies between the layers. Their infrastructure resilience metric is dynamic and is derived from the three properties of robustness, resourcefulness, and rapidity, with redundancy imbedded within robustness (Kong & Simonovic, 2016). Properties of resilience are quantified by equation (15) for robustness, rapidity by equation (16), and resourcefulness by equation (17). The resilience metric for a single network layer is shown in equation (18).

$$R_{Rob}^{\phi,\zeta_1}(t^*) = \frac{n_o^{\phi}(t^*) + e_o^{\phi}(t^*)}{N^{\phi} + E^{\phi}} \quad \textbf{(15)}$$

where φ corresponds to a specific network layer, ζ is a specific hazard, t* is the time of maximum loss of performance, n_o is the number of operational nodes, e_o is the number of operational edges, N is the total number of nodes, and E is the total number of edges.

$$R_{Rap}^{\phi,\zeta_1} = t\left(R_{Rob}^{\phi,\zeta_1} = 1\right) - t_{10}^{\phi} \quad \textbf{(16)}$$

where t_{10} is the time of disturbance.

$$R_{Res}^{\phi,\zeta_1}(t) = SP^{\phi,\zeta_1}(t) - SP_0^{\phi,\zeta_1}(t) \quad \textbf{(17)}$$

where t is time, SP is the system performance at time t, and SP_0 is the baseline performance at time t without implementation of adaptation measures.

$$r^{\phi,\zeta_1}(t) = \rho_{PA}^{\phi,\zeta_1}(t) + \rho_{PR}^{\phi,\zeta_1}(t) = \frac{\int_{t_{10}}^{t} SP_0^{\phi,\zeta_1}(t)dt}{1 \times t} + \frac{\int_{t_{10}}^{t} R_{Res}^{\phi,\zeta_1}(t)dt}{1 \times t}, \quad t \leq R_{Rap}^{\phi,\zeta_1} \quad \textbf{(18)}$$

where ρ_{PA} is the proactive absorptive capacity, ρ_{PR} is the reactive absorptive capacity, and 1 x t corresponds to the total system performance that would have been available had the disruption not occurred.

Overall, limited approaches are available to quantify infrastructure resilience (Bhatia et al., 2015). This is problematic as it means there are few approaches that can translate theoretical infrastructure resilience concepts into practical tools for decision making. Current approaches and metrics do not easily provide practical guidance to infrastructure management (Ayyub, 2015).

The literature review concludes with a summary of the gaps found in the literature. Section 2.1 showed that urbanized growth, climate change, and aging infrastructure pose challenges to infrastructure managers. Infrastructure resilience is one concept believed to be helpful is assisting infrastructure owners to manage these challenges. Thus, an infrastructure resilience approach that can incorporate the ways in which infrastructure expands and changes over time and the subsequent effect on resilience is desirable.

Section 2.2 explored the infrastructure resilience concept. Notably, quantitative and dynamic characteristics in an infrastructure resilience measure have been proven worthwhile. Unfortunately, Section 2.3 also showed that there are few quantitative and dynamic resilience measures. Even fewer approaches have been developed to the point that practical tools have emerged. Thus, an improved infrastructure resilience approach that can address the infrastructure challenges cited, such as urbanized growth, while applying theoretical concepts to yield practical knowledge for infrastructure decision makers is desirable.

Section 3

3 Methodology

Given the limited number of infrastructure resilience approaches that can support infrastructure management in the literature, the thesis aims to address the gap presented in the conclusion of Section 2.3 by extending the existing approach developed by Kong and Simonovic (2016) and improving its capabilities. These gaps include the need: (1) to incorporate infrastructure growth into an infrastructure resilience approach, (2) improve the accuracy and capabilities of the existing infrastructure resilience assessment approach, and (3) apply the methodology in a readily available web tool to yield practical results.

The extension adds features that include: (i) the introduction of spatial object analysis of impacts, (ii) adjustable damage representation for edges, (iii) new subdivision road-structure development, and (iv) infrastructure network expansion. The added features are described in Section 3, and each is illustrated in Section 4.2. This section describes the procedure for the assessment of infrastructure resilience. A flowchart representation of the procedure is shown in Figure 4. The flowchart begins with describing an existing infrastructure system and ends with an assessment of infrastructure resilience. Between the two ends various phases are included, denoted as P1 through P5, which are described in detail in the following sections.

Gap (1) is addressed through features (iii) and (iv), while Gap (2) is addressed through features (i) and (ii). These features are illustrated through a case study in Sections 4.2.1 to 4.2.4. The final gap is addressed through the overall case study in Section 4.2.5.

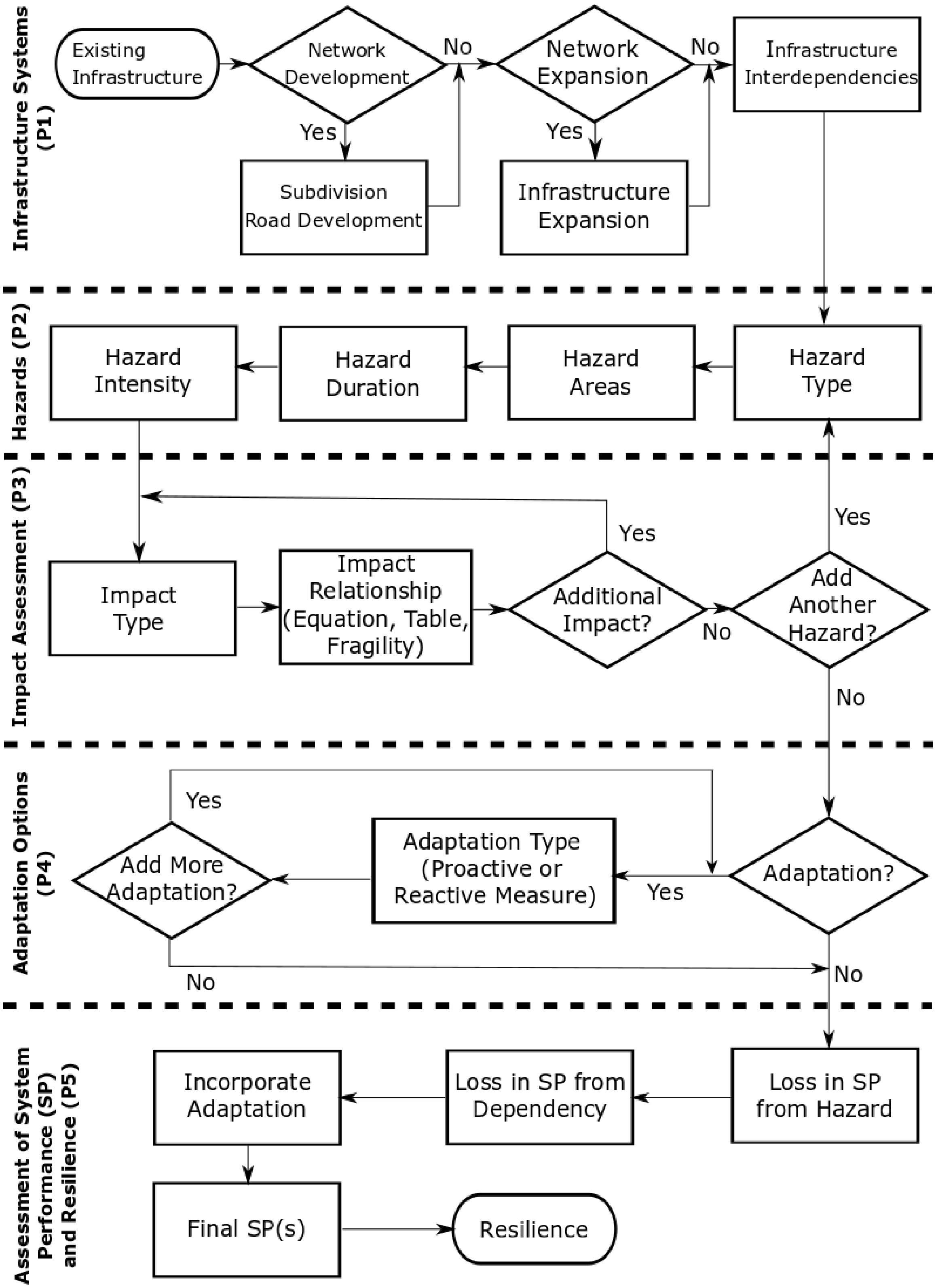

Figure 4 Flowchart of the procedure for the assessment of infrastructure resilience

3.1 Description of Infrastructure System (P1)

To implement a resilience approach for a complex infrastructure system, a model of the system's structure is required. Infrastructure systems can be described in a multitude of ways for analysis. This can come in the form of knowledge-based models, input-output inoperability models, complex network theory, PetriNet-based modelling, and agent-based modelling to name a few (Agostino & Scala, 2014). Similar to other works, a system-of-systems approach is used to describe the overall system (Kong & Simonovic, 2016; Mostafavi, 2017). Individual critical infrastructure systems and buildings are represented as infrastructure networks or layers. Network development and expansion modules are discussed in this section as well. In Figure 4, this section is referred as the first phase (P1) of the procedure.

3.1.1 Networks

Networks are one of the tools used to describe the structure of complex systems and, by extension, infrastructure (Amaral & Ottino, 2004; Brown & Dawson, 2016; Heracleous, Kolios, Panayiotou, Ellinas, & Polycarpou, 2017; Thacker, Pant, & Hall, 2017). The thesis's approach uses network representation as a means to (i) describe an infrastructure system's structure, (ii) capture its functionality, and (iii) assess its performance (flow of services provided by the infrastructure system). Networks, represented by the notation G, are composed of nodes, N, and edges, E. Different infrastructure systems can be represented by networks using the symbol ϕ. Infrastructure networks can thus be denoted as follows in equation (19):

$$G^{\phi} = f(N^{\phi}, E^{\phi}) \quad \textbf{(19)}$$

For example, a power grid network consisting of nodes and edges could be $G^P(N^P,E^P)$ while a water network might be denoted as $G^W(N^W,E^W)$. Nodes and edges represent real physical system components. Table 1 lists examples of how some critical infrastructure can be represented as networks.

Table 1 Examples of critical infrastructure represented as networks

Infrastructure Networks	Nodes	Edges
Power	• Generators • Transformers • Substations • Poles • Switches	• Power lines
Water	• Pumping stations • Water tanks • Outlets • Water towers • Reservoirs • Treatment plants • Valves • Hydrants	• Trunk watermains • Distribution watermains • Service lines
Transportation	• Traffic signals • Intersections • Diverging points • Merging points • Origin-destination pairs	• Roads

Each network can have its own measure of system performance. For example, a road performance measure might be the travel time across a road segment, the kilometers of road unaffected by a hazard, or the maximum acceptable speed limit. For power grids, a performance measure might be the amount of electricity delivered to consumers. For a water distribution network, it could be the amount of potable water being delivered or the water pressure. When such data are not readily available, the performance measure may be simplified to a binary 1 or 0 to represent whether a network component is functional or not functional. Other times, a general percentage of remaining functionality can be used when a specific unit is unidentified.

In the implementation of the network approach, nodes and edges can be sub-classified further according to the component within an infrastructure type. This allows the represented network components to respond differently when interacting with each other and with a hazard. This is shown in equation (20):

$$G^{\phi} = f(n^{\phi_1}, n^{\phi_2} \dots n^{\phi_u}, e^{\phi_1}, e^{\phi_2} \dots e^{\phi_v}) \quad \textbf{(20)}$$

where n^{ϕ} and e^{ϕ} are the nodes and edges of infrastructure ϕ of different infrastructure elements. The value from sub-classifying nodes and edges becomes apparent when estimating hazard impacts given that studies have shown losses can vary significantly depending on classifications. Examples include "…differences in construction materials, techniques and quality, and also in the quantity and nature of contents located within these structures…" (Natural Resources Canada, 2017).

3.1.2 Layers

Layers are used to present spatial infrastructure elements that may not be in network form. For example, layers may represent buildings or service areas as polygons. In these instances, they also have a functional capacity measure.

Other types of layers exist that do not play a role within the interconnected infrastructure system but supplement the infrastructure management. While not necessarily relevant to this methodology, they can play a critical role in a practical modelling scenario and enhance the presentation of results. Examples of these types of layers include digital elevation models (DEM) and regional wards. Digital elevation data can be useful in multiple ways, for example they can play a role in estimating flooded areas and/or flood depths. In this example, it can also affect resilience calculations, albeit not through the representation of infrastructure. Ward information can help provide a visual administrative sense of where impacts are likely to occur. These types of layers may not affect directly the resilience calculation but do support the infrastructure system analyses.

3.1.3 Dependencies

Once the infrastructure components and connections are modelled, it is necessary to model the flow of services that occur within a single network/layer, known as intra-dependencies, and between networks/layers, known as interdependencies. The proposed methodology considers only direct first-order impacts—that is, how one network component's functional state affects another network component's functional state.

However, it is proposed that by aggregating these direct dependencies, increasing the number of relevant networks or layers, and combining them into a system-of-systems, it becomes possible to replicate complex behaviours in real-life scenarios.

Infrastructure component dependencies of a single component can be represented mathematically as in equations (21) through (23):

$$\rho_{Func}^{\phi n_1} = f(\rho_{Func}^{n}, \rho_{Func}^{e}, \rho_{Func}^{pa}) \tag{21}$$

$$\rho_{Func}^{\phi e_1} = g(\rho_{Func}^{n}, \rho_{Func}^{e}, \rho_{Func}^{pa}) \tag{22}$$

$$\rho_{Func}^{\phi pa_1} = h(\rho_{Func}^{n}, \rho_{Func}^{e}, \rho_{Func}^{pa}) \tag{23}$$

where $\rho_{Func}^{\phi n_1}$, $\rho_{Func}^{\phi e_1}$ and $\rho_{Func}^{\phi pa_1}$ describe the functional state of a single infrastructure component of a node, edge, and polygon area, respectively. The right-hand side of the equation depicts the dependencies with other infrastructure components in the system. This can take the form of other nodes, edges, or polygon areas. At times, it may be appropriate to model an infrastructure component as dependent on a single component. At other times, it may be necessary to model a single infrastructure component's functionality as a combination of functional states from multiple components. This can arise from a mixture of various components within the same network, intra-dependency, or different networks' interdependencies.

This general formulation provides flexibility to the relationship dependencies that exist, as it can capture dependencies of a single component or multiple components. The latter allows for describing complex failure modes such as cluster and pathway dependencies.

Note that these infrastructure dependencies capture only their relationship and exclude external factors that may disturb or enhance their performance. This refers to the hazard impacts described in Section 3.3 and adaptation described in Section 3.4, respectively.

3.1.4 Development of New Networks

Development of new subdivisions of a city, capturing urban growth, can be assessed using the resilience measure. This represents one of the important contributions of this thesis. The growth of new networks can cause resilience to change and can thus play a role in making smarter decisions in infrastructure planning.

In the context of this thesis, a rapid expansion methodology based on minimal parameters is used to simulate the growth of urban subdivision development. Consequently, its impact on resilience can be quantified. By incorporating network development and expansion models into the methodology, the potential implications of infrastructure growth policies on resilience can be explored and used to guide infrastructure decision making.

In terms of their placement, storm sewers, water mains, and other infrastructure are planned for the streets of proposed subdivisions (City of Stratford, 2016). Power cables can be located below roads and are within the same area as sewers and water and gas mains (Boyle et al., 2013). With this information, it becomes apparent that critical infrastructure tends to follow the placement of roads, at least in the scenario of subdivision development.

The subdivision process for a piece of land requires the incorporation of many aspects, ranging from objectives, zoning regulations, and bylaws to development standards. The layout design is a creative and semi-subjective process (Wakchaure, 2001). Wickramasuriya et al. (2010) provided a process to divide a rectangular parcel of land into lots and streets. The process requires user inputs that include dimensions of the rectangular pieces of land and typical lot dimensions, which are also assumed to be rectangular, found in local zoning regulations. Given the inputs and the constraint that lots must have a minimum of one side connected to a road, the algorithm outputs four templates that consist of the total number of lots and streets, along with their dimensions. The chosen alternative is the one with the maximum number of lots possible, followed by the minimum number of proposed street segments (Wickramasuriya et al., 2010). This reflects the priorities of developers as they want to maximize profit, which is correlated to the number of lots, and minimize the number of roads needed, which corresponds to lower capital and maintenance costs. This thesis modifies the process slightly by replacing the secondary decision factor of the minimum number of streets with the minimum total length of streets.

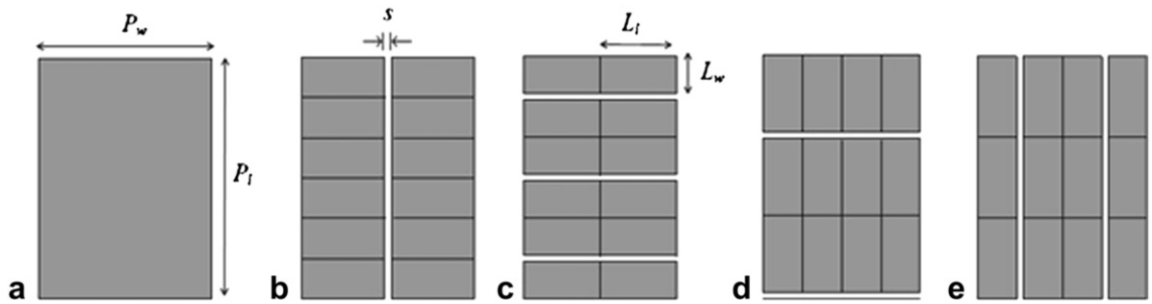

Figure 5 Subdivision process for a rectangular parcel. (a) represents the original parcel of land. (b), (c), (d), and (e) are the different templates considered when organizing the lots and streets. This figure is the property of the original authors of Wickramasuriya et al. (2011)[1]

Figure 5 shows the different layouts that are considered given a rectangular land parcel. The notations used include P_w as parcel width, P_l as parcel length, s as street width, L_l as lot length, and L_w as lot width. Most of the layouts considered use a similar process with slight changes in the calculations. A sample procedure for one of the templates is shown below. The procedure is based on the Figure 5b template.

The procedure requires certain variables to be known. These inputs include the parcel width, parcel length, street width, minimum lot length and width, and the number of existing streets adjacent to the parcel. The procedure then begins with determining the initial number of blocks, where $b_{initial}$ representing the quotient, and remaining length after the maximum number of whole initial blocks is allocated, *Rem*, as shown in equation (24).

---

[1] Republished, with permission obtained by Howard Tong, from an automated land subdivision tool for urban and regional planning: Concepts, Implementation and Testing, Wickramasuriya et al. (2011), Volume 26; permission conveyed through Copyright Clearance Center, Inc.

$$b_{initial} + Rem = \frac{P_w}{L_l} \quad \textbf{(24)}$$

Next, the number of expected streets, ns_{exp}, must be determined as an intermediate variable based on the two conditions of whether the initial number of blocks is an even or odd number, and the number of existing adjacent streets, s_{adj}. This can be mathematically represented in the following equation (25).

$$ns_{exp}\begin{cases} q+1, & when\ b_{initial}\ is\ an\ odd\ number\ AND\ s_{adj}\ is\ 0 \\ q, & when\ b_{initial}\ is\ an\ odd\ number\ AND\ s_{adj}\ 1\ or\ 2 \\ & OR\ when\ b_{initial}\ is\ an\ even\ number\ AND\ s_{adj}\ 0\ or\ 1 \\ q-1, & when\ b_{initial}\ is\ an\ even\ number\ AND\ s_{adj}\ is\ 2 \end{cases} \quad \textbf{(25)}$$

where q is the quotient of $b_{initial}/2$. Note that the variable s_{adj} takes only the number of existing adjacent streets parallel to the parcel length or width, depending on which of four templates is being considered. In the case of Figure 5b, this is the parcel length. The next step encompasses calculating the minimum total width required to accommodate the expected number of new streets, sw_{Total}, as shown in equation (26).

$$sw_{Total} = ns_{exp} \times sw \quad \textbf{(26)}$$

where sw is the street width entered earlier as an input. At this point, if the length of *Rem* is greater than or equal to sw_{Total}, then the procedure continues to the next step. However, if *Rem* is less than sw_{Total}, then $b_{initial}$ is decreased by one, resulting in the recalculation of the values up to this point. This loop continues until *Rem* is greater than or equal to sw_{Total}.

Figure 6 illustrates the logical procedure up to this point from the calculation of the number of initial blocks.

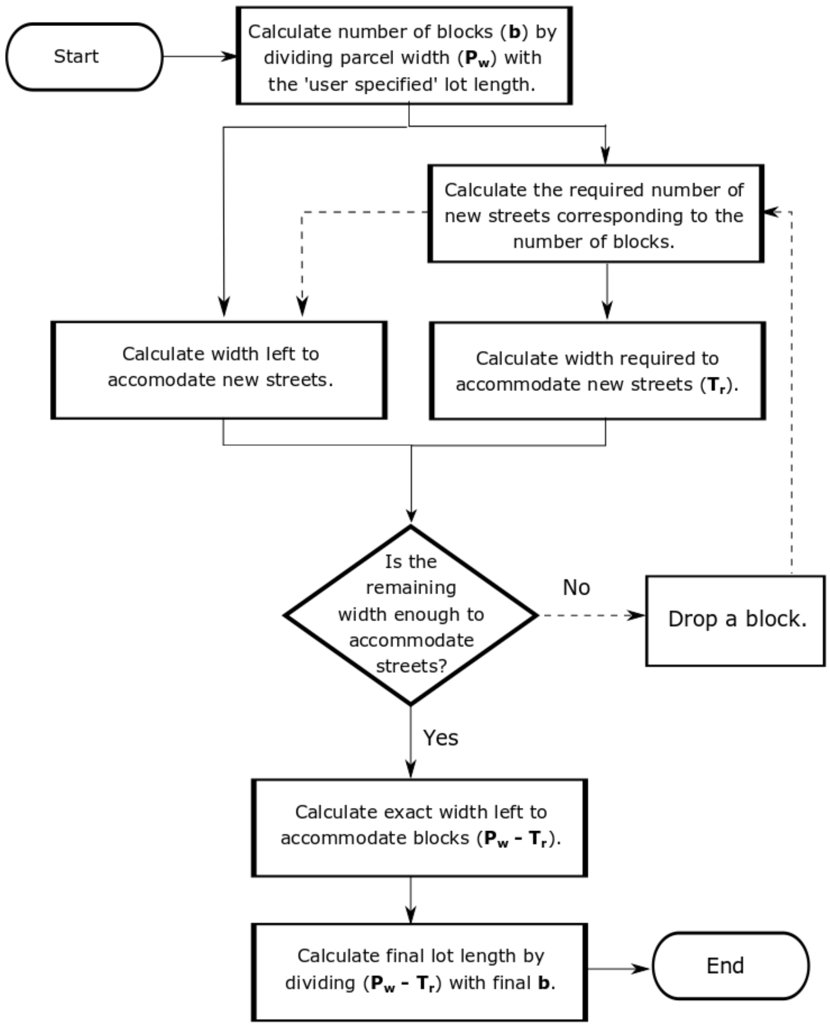

Figure 6 Feedback loop process to ensure remaining width can accommodate total street width. This figure is adapted from Wickramasuriya et al. (2011). [2]

Now that there is a sufficient length to accommodate the total number of added streets, the next step encompasses distributing the remaining length to the lot dimensions. Before this step, the remaining width, W_{rem}, is calculated by equation (27).

$$W_{rem} = P_w - (sw \times ns_{Act}) \quad \textbf{(27)}$$

---

[2] Republished, with permission obtained by Howard Tong, from an automated land subdivision tool for urban and regional planning: Concepts, Implementation and Testing, Wickramasuriya et al. (2011), Volume 26; permission conveyed through Copyright Clearance Center, Inc.

where ns_{Act} is the final number of added streets after proceeding through the feedback loop to satisfy the condition. The remaining length is distributed to the lot length or width, depending on the template. In the case of Figure 5b, it is allocated to the lot length.

The number of rows, *nr*, then needs to be calculated to determine the total number of lots that can be obtained from the design. This depends on whether there is an existing street adjacent to the parcel width in this template. If there is no existing adjacent street parallel to the parcel width, then the street width is taken from the parcel length before the following calculation in equation (28). Otherwise, it proceeds without that consideration.

$$nr = P_l / L_w \tag{28}$$

At this point, the total number of lots, *NL*, for the template design is determined as shown in equation (29).

$$NL = b_{final} \times nr \tag{29}$$

where b_{final} is the final number of blocks determined after going through the earlier feedback process. The total street lengths, sl_{Tot}, created for this layout also need to be calculated for comparison between the four different templates. This equation is shown in (30).

$$sl_{Tot} = ns_{Act} \times P_l \tag{30}$$

where ns_{Act} is the number of actual streets added parallel to the parcel length. In addition to sl_{Tot}, had the number of existing adjacent street on the parcel width been zero, it would also have been added to the parcel width.

Wickramasuriya et al. (2011) extended the algorithm such that the input is no longer restricted to a rectangular parcel of land. Based on the irregular polygon input, the process begins by creating a minimum area-bounding rectangle with an irregular shape, considering potential rotational shifts. Subsequently, the procedure continues using the previous process with a rectangular input. Once the subdivision process is complete for the rectangular shape, it is reoriented and clipped. Figure 7 illustrates this process.

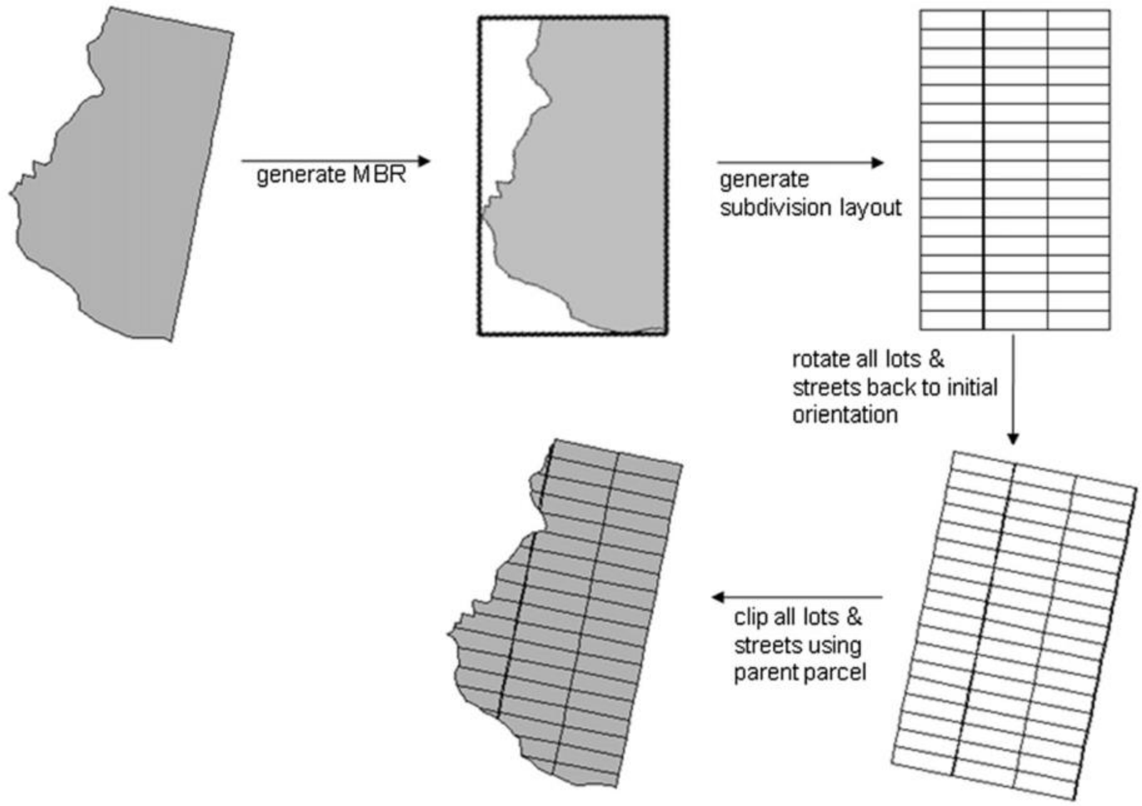

Figure 7 Subdivision process for an irregular polygon. MBR is the minimum bounding rectangle. This figure is the property of the original authors of Wickramasuriya et al. (2011)[3]

The authors compared their simulated subdivision designs to real-life designs in the United States and remarked that when the initial parcel of land was oriented in a particular direction, the street areas matched closely with the observed pattern (Wickramasuriya et al., 2011).

---

[3] Republished, with permission obtained by Howard Tong, from an automated land subdivision tool for urban and regional planning: Concepts, Implementation and Testing, Wickramasuriya et al. (2011), Volume 26; permission conveyed through Copyright Clearance Center, Inc.

3.1.5 Network Expansion

In the previous subsection, an algorithm was presented for the development of a new subdivision without direct connection with existing infrastructure. In many cases, a municipality may choose to expand a development by connecting it to existing infrastructure. The expansion of network infrastructure typically evolves in an ad hoc manner, which rarely considers interdependencies (Reed et al., 2009). However, Fu et al. (2016) presented a network growth model that is applicable for infrastructure systems expansion. The spatial distribution model considers three key factors associated with infrastructure growth to populate new nodes and edges. The factors include demand, efficiency, and costs. The model has been validated through stochastic simulation to demonstrate that with good accuracy, it can create networks that share common network properties like those in real-life infrastructure networks (Fu et al., 2016).

The thesis aims to adapt Fu et al.'s (2016) model into the infrastructure resilience approach. When there are differences from the original model, it is noted. After the input of an existing infrastructure network, the expansion proceeds in three basic steps. The first step encompasses the placement of a single node within the geographical space. The second step encompasses adding edge(s) to the new node. If no new edges are added, the node is removed, and the first step must be repeated. When the second step is successful, the third step encompasses repeating steps one and two until a desired number of nodes is added. The following is the presentation of the adapted expansion algorithm. An intermediate step of setting up the geographical boundaries is introduced after the input of the existing network but prior to step one.

The original procedure from Fu et al. (2016) assumes that all nodes are placed within a square space that can be dimensioned into a three-by-three grid. The colour within each grid space represents the level of demand for a certain infrastructure within the sub-area. This is illustrated in Figure 8a. Note that γ refers to the relationship between an infrastructure system's demand to its placement.

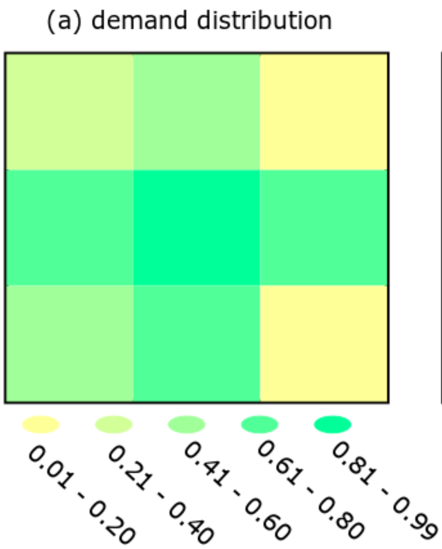

Figure 8 (a) Demand distribution for a certain type of infrastructure. (b) Nodal allocations when γ = 0. Adapted from Fu et al. (2016) CC-BY.

The proposed change includes relaxing the grid-like boundaries as actual demand is more complex. A better representation would be obtained by dividing the overall space by geopolitical boundaries, municipal boundaries, or planning areas, depending on the infrastructure of interest. These boundaries can reflect the difference in demand because of by-law regulations.

Now that the setup is complete, the first step is determining the sub-area in which to place a node. This is determined through a probabilistic function as shown in equation (31).

$$P(n \in sa) \sim \omega \times \psi(sa)^{\gamma} \qquad \textbf{(31)}$$

The equation states the probability for the next node placement, n, within a sub-area, sa. This is the result of a normalization factor, ω, multiplied by the demand density of sub-area, $\psi(sa)$, to the exponent of a factor, γ, that relates demand for a service to its geospatial placement. In the original paper, the authors used population density as a proxy for the demand density of a sub-area.

Although not explicitly explained in the original paper, the normalization factor ω is determined by equation (32) below.

$$\omega = \frac{1}{\sum_{i=1}^{Number\ of\ subareas} \psi(sa)_i^{\gamma_i}} \quad \textbf{(32)}$$

Fu et al. (2016) proposed that the γ factor can vary from -1 to 1. When γ has a positive value, this means that demand is positively correlated to the placement of an infrastructure node. This is reflected in their observations of electrical substations and road junctions, which had noticeable positive correlations with population density. A negative γ value indicates that the placement of a node would generally be inversely proportional to the demand. This was evident in the water reservoir placement. When γ values have a weak correlation (i.e., when values are close to zero), this means that the placement of infrastructure is independent of the population. An example of this is shown in Figure 8b.

The second step relates to the placement of edges attached to the newly placed node. The probability of attaching the new node to an existing node, $P(e_{ij})$, within the same infrastructure is expressed as equation (33).

$$P(e_{ij}) \sim \frac{f(k_j)}{g(d_{ij})} \quad \textbf{(33)}$$

$f(k_j)$ represents the efficiency gain for the node with the new attachment, while $g(d_{ij})$ represents the costs of the attachment. The functions are further defined in the case of the infrastructure that Fu et al. (2016) investigated, with their functions attributed to network-oriented properties. Note that more than one edge can be added to the newly formed node. If no edges are added, then the new node is removed, and another new node is formed. Both equation (34) and equation (35) are examples of functional forms proposed by Fu et al. (2016). The special scaling parameters of β and α are introduced and fitted with existing infrastructure data.

$$f(k_j) = k_j^{\beta} \quad \textbf{(34)}$$

Equation (34) expresses that efficiency is estimated as the degree of node *j* to the exponent of a scalable variable β, which has a range of values between zero and one, inclusive.

$$g(d_{ij}) = e^{\frac{d_{ij}}{\alpha}} \tag{35}$$

Equation (35) expresses the costs as the Euler constant e to the exponent of a fraction $\frac{d_{ij}}{\alpha}$. d_{ij} is the shortest geographical physical distance between the newly introduced node, *i*, and existing node, j. α is a constant for a specific infrastructure. The constant also has a range of zero to one but the value of zero is excluded.

Fu et al. (2016) suggested values for the γ, β, and α constants based on case study data of various infrastructure types. These are shown in Table 2.

Table 2 Estimated infrastructure growth parameters. Adapted from Fu et al. (2016) CC-BY

Network	α	β	γ
Electricity: national transmission network (England and Wales)	0.034	0.0	0.579
Railway network (England and Wales)	0.009	0.0	0.807
Electricity distribution network (Denwick, North East England)	0.007	0.0	0.728
Gas network (England and Wales)	0.042	0.0	-0.103
Road network (West Midlands, England)	0.008	0.0	0.716
Air traffic (European)	0.287	0.9	0.991

The final step includes repeating the first and second steps until the desired amount of network growth has occurred, as expressed by the number of nodes initially determined.

3.2 Hazard Description (P2)

Infrastructure systems face multiple forms of threats, ranging from natural, cyber, or anthropogenic to financial and others (Agostino & Scala, 2014). The focus of this thesis relates to natural hazards, specifically flooding and wind, and their potential cascading effects on complex municipal infrastructure systems. While risk may be estimated as a function of hazard, exposure, and severity, this section pertains to hazard and exposure.

Natural hazards are a complex phenomenon, so to include them within the resilience approach, simplifications must be made. The proposed approach assumes that the level of damage can be associated with a characteristic of the hazard. For an example, the proportion of damage to infrastructure is correlated to flood depth at a specific location and time. Examples of natural hazard types and their corresponding characteristic units are given in Table 3.

Table 3 Example units of measures of hazard severity level

Hazard	Characteristic Unit and Sample Measure
Flooding	Flood depth (mm)
Hurricane	Wind speed (km/hr)

A hazard can be described as a function of the impacted area, time, and severity. It is important to have the ability to consider multiple forms of hazards, as they impact infrastructure differently. For example, wind damage has been cited as having caused the most electrical faults in the UK based on a study that looked at climate change impacts on electrical networks (Mccoll et al., 2012).

3.3 Impact Assessment (P3)

As hazards are formalized, it is necessary to relate a hazard's severity and the damage it causes to exposed infrastructure. When the hazard loading exceeds certain system thresholds, the system response can shift (Linkov & Palma-Oliveira, 2017). The exceedance of this system threshold is the beginning of the loss of system functionality. In Simonovic and Peck's (2013) approach, a hazard’s damage affects resilience and system performance through performance loss, as demonstrated in equation (36).

$$\rho L_{Func}^{\phi} = f(t, H^{\tau}, SE_{n^{\phi},e^{\phi},pa^{\phi}}) \quad \textbf{(36)}$$

where ρL_{Func}^{ϕ} refers to the functional performance loss of an infrastructure element, t is time, H^{τ} is a hazard of type τ, and $SE_{n^{\phi},e^{\phi},pa^{\phi}}$ represents a specific system element. In an actual model, the impact relationship can take the form of an equation, a graph, or a table.

An example from the literature of a flood impact on the traffic speed relationship is provided in Figure 9.

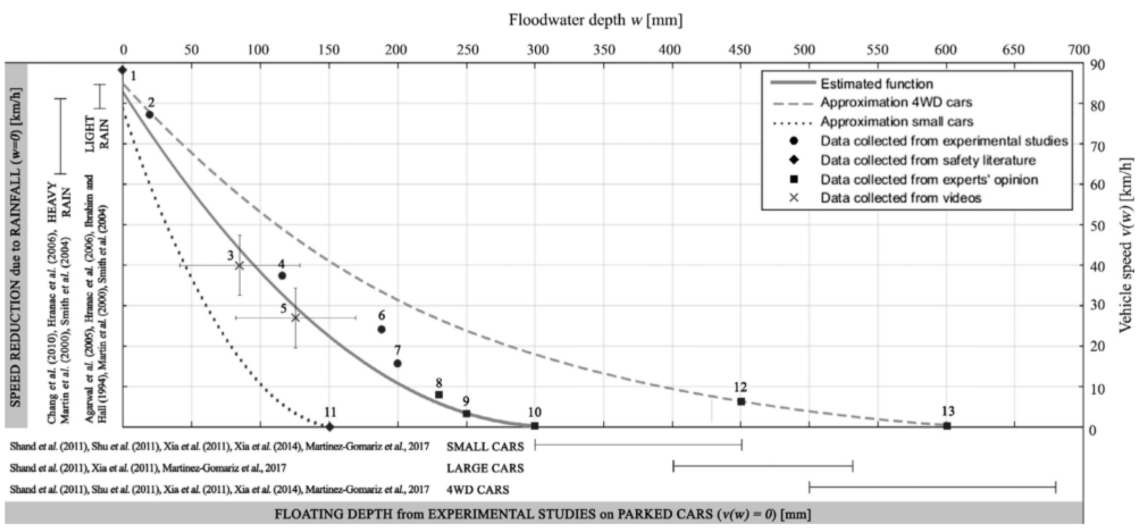

Figure 9 Reduction of the flood depth to vehicle speed relationship on roads. This figure is the property of the original authors of Pregnolato et al. (2017) CC-BY.

Thus, for each road edge that has an impact from standing water depth, speed performance can be adjusted, resulting in an impact on overall system performance and resilience.

Another form of an impact relationship is captured by fragility curves. Fragility curves relate a hazard’s magnitude, such as peak ground acceleration in the case of earthquakes, or wind speed for hurricanes, with a certain level of probabilistic damage for a specific building type. An example taken from the US Hazus 2.1 Hurricane Module is shown in Figure 10.

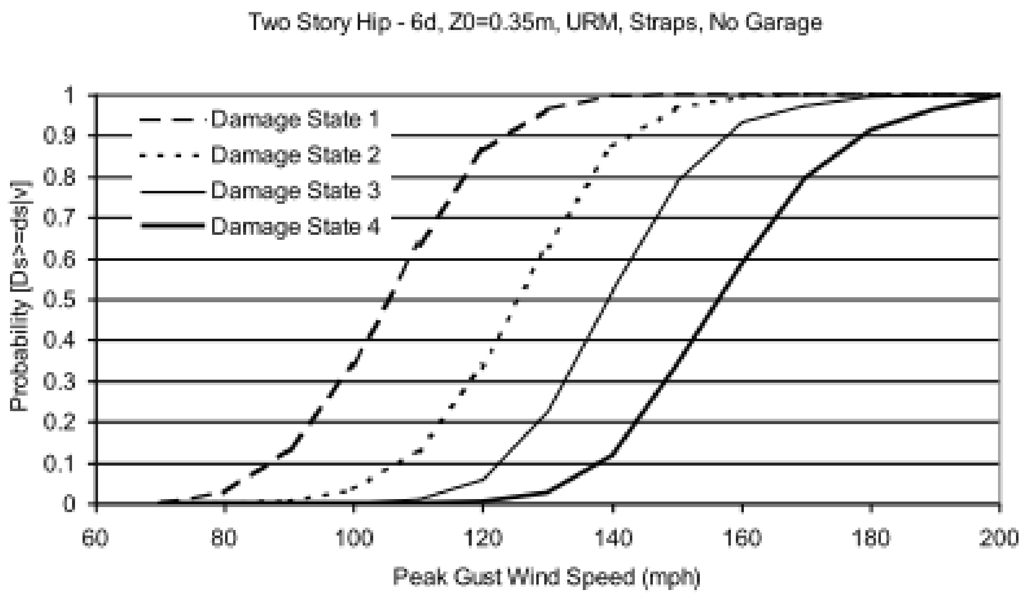

Figure 10 Example of a fragility curve for a hurricane hazard. This figure is the property of the original authors of Federal Emergency Management Agency, (n.d.).

The damage states refer to the following conditions, as shown in

Table 4.

Table 4 Example of damage state classification for residential buildings. This table is the property of the original authors of Federal Emergency Management Agency, (n.d.).

Damage State	Qualitative Damage Description	Roof Cover Failure	Window Door Failures	Roof Deck	Missile Impacts on Walls	Roof Structure Failure	Wall Structure Failure
0	**No Damage or Very Minor Damage** Little or no visible damage from the outside. No broken windows, or failed roof deck. Minimal loss of roof cover, with no or very limited water penetration.	≤2%	No	No	No	No	No
1	**Minor Damage** Maximum of one broken window, door or garage door. Moderate roof cover loss that can be covered to prevent additional water entering the building. Marks or dents on walls requiring painting or patching for repair.	>2% and ≤15%	One window, door, or garage door failure	No	<5 impacts	No	No
2	**Moderate Damage** Major roof cover damage, moderate window breakage. Minor roof sheathing failure. Some resulting damage to interior of building from water	>15% and ≤50%	> one and ≤ the larger of 20% and 3	1 to 3 panels	Typically 5 to 10 impacts	No	No
3	**Severe Damage** Major window damage or roof sheathing loss. Major roof cover loss. Extensive damage to interior from water.	>50%	> the larger of 20% & 3 and ≤50%	>3 and ≤25%	Typically 10 to 20 impacts	No	No
4	**Destruction** Complete roof failure and/or, failure of wall frame. Oss of more than 50% of roof sheathing	Typically >50%	>50%	>25%	Typically >20 impacts	Yes	Yes

When impact relationships are unavailable, the functionality of a system element can be reduced to a binary state of one and zero, representing whether the component is functioning properly or not, respectively.

When combined with expert judgement, thresholds can be used. For example, Taiwan High Speed Rail set thresholds to determine hazard conditions that affect the performance of their infrastructure. During a severe wind storm event, wind speeds of 20 m/s require careful monitoring, a 25 m/s wind speed results in a decision to reduce the speed of railway services, and a 30 m/s wind speed causes a suspension of services (Quinn et al., 2017).

The approach proposed in this thesis generally uses a deterministic method of estimating performance loss. At the same time, probabilistic methods can be partially incorporated as with the case of fragility curves. Figuring out how uncertainty can be conceptualized is key in supporting decision making for complex infrastructure compared to pure random uncertainty (Francis & Bekera, 2014).

When the hazard impacts have been considered for a single time step for each system component, performance losses as a result of interdependencies are invoked prior to the next time step. As this dependent relationship can come in various forms, equation (37) generalizes this phenomenon.

$$\rho L_{Func}^{\phi} = f(t, SE_{\rho_{Func}^{n}, \rho_{Func}^{e}, \rho_{Func}^{pa}}) \qquad \textbf{(37)}$$

$SE_{\rho_{Func}^{n}, \rho_{Func}^{e}, \rho_{Func}^{pa}}$ represents other system elements' functionalities that are depended on by the component of interest. Naturally, a constraint exists for the performance state of any single infrastructure component in that it cannot be a negative value.

3.4 Adaptation Options (P4)

Boyle et al. (2013) conducted a literature review on climate change impacts on critical infrastructure in Canada, and one of their conclusions was that adaptive measures can positively affect the resiliency of infrastructure. Furthermore, an increase in resiliency can translate to a reduction in future costs in the form of maintenance, repair, and replacement.

Adaptation options provide a means for the overall system to reduce performance loss in the event of a disruption, or the recovery of system performance when loss has already occurred. In the context of the resilience approach, adaptation measures can affect any of the following: (i) a decrease in the slope of the system performance curve during its decline stage, (ii) an increase in the recovery rate slope, (iii) an increase in the minimum performance that would have occurred without the adaptation measure, and (iv) a decrease in the time required to reach an acceptable system performance level.

The choice of which adaptation measures to consider and implement is dependent on a given scenario. The resilience approach used in this thesis is flexible as it allows consideration of various adaptation measures. Sample adaptation measures are shown in Table 5. Measures can be classified as proactive or reactive. Proactive measures are characterized as actions that require preparation, typically with prior consideration. Once a hazard strikes, they are very difficult to adjust, if at all, during the event. Reactive measures are characterized by decisions that occur after a hazard warning has been issued. They typically occur due to a judgement call during the hazard event. A brief description of the measures and their effects on resilience are presented in Table 5.

Table 5 Sample adaptation options classified into proactive and reactive measures

Proactive Measures	**Reactive Measures**
a) Structural reinforcement/design	g) Temporary dikes and embankments
b) Land use planning	h) Pumping out floodwaters
c) Maintenance/drainage	i) Declaration of disaster escalation
d) Backup generators/energy storage	
e) Action/emergency plan	
f) Efficient access to insurance	

a) Structural reinforcement and design refer to changes to the composition of the engineered infrastructure. For example, the engineered design can reinforce infrastructure through the use of a different building material, effectively changing how components interact with the surrounding environment. An example pertaining to electrical systems is the application of looped or networked configurations compared to radial designs. This type of measure is likely to decrease the rate of system performance decline and increase the robustness of the system.

b) Land use planning refers here to the physical placement of infrastructure. For example, a piece of infrastructure located outside of a floodplain area would not incur the same risks as it would if it were located in a floodplain area. This measure can mitigate exposure to a hazard and thereby reduce loss of resilience.

c) Regular maintenance of infrastructure can prolong its lifespan and increase its functional state. For example, debris can accumulate in drainage pipes over time, reducing their capacity to convey floodwater. The removal of debris can restore functionality and optimize drainage capacity. This measure is likely to decrease the rate of decline of system performance and increase the robustness of the system.

d) Backup generators are another source of energy for certain infrastructure in place of electricity. For example, backup generators enable pumps to function even if electricity from the grid is temporarily unavailable. In an electrical network setting, other examples include energy storage options or distributed energy generation. This effectively builds redundancy into the system and prevents a loss of pump system performance.

e) An effective emergency plan provides a set strategy in response to a hazard event. This provides a rational logic by which resources can be properly allocated in the case of poor decision making that may have ensued because of emotional pressure. This measure is likely to increase the resourcefulness aspect of resilience and decrease the time to full recovery.

f) Efficient access to insurance provides additional financial resources in a timely manner. Its effective allocation boosts the recovery rate and decreases the time required to achieve a fully recovered state.

g) Temporary dikes and embankments may be created in response to a flood warning. These can be in the form of sandbags or earth berms that act as a barrier to prevent large quantities of water from entering protected areas. They decrease the loss of system performance and increase the minimum performance that would have occurred.

h) Pumps can be used to move floodwater from a vulnerable location containing critical infrastructure to another location that is more adept at handling stormwater. For example, floodwater may be moved from an evacuation center location to a nearby stormwater management pond. Depending on the deployment timing of the pumps, this measure can reduce the loss of system performance or increase the recovery rate of an infrastructure system.

i) Municipal governments are generally expected to handle an incoming hazard to the best of their ability. However, if the situation is deemed unmanageable given their current level of resources, they may opt to declare the hazard a disaster. This categorization compels higher levels of government to aid in the recovery efforts.

3.5 Assessment of System Performance and Resilience (P5)

The basic definition of system resilience used in the thesis (Sections 2.2 and 2.3) integrates the impacts of hazards (Section 3.3.) and choice of adaptation options (Section 3.4). System performance can change as a result of hazards and the system's adaptive capacity, which affects system resilience. This occurs at the level of individual element for each time step. Subsequently, the common individual elements of a single type are aggregated. For example, the system performance of all water network nodes are combined, and the infrastructure elements are aggregated based on the different types of infrastructure (nodes, edges, or polygon areas). Figure 11 illustrates this calculation process.

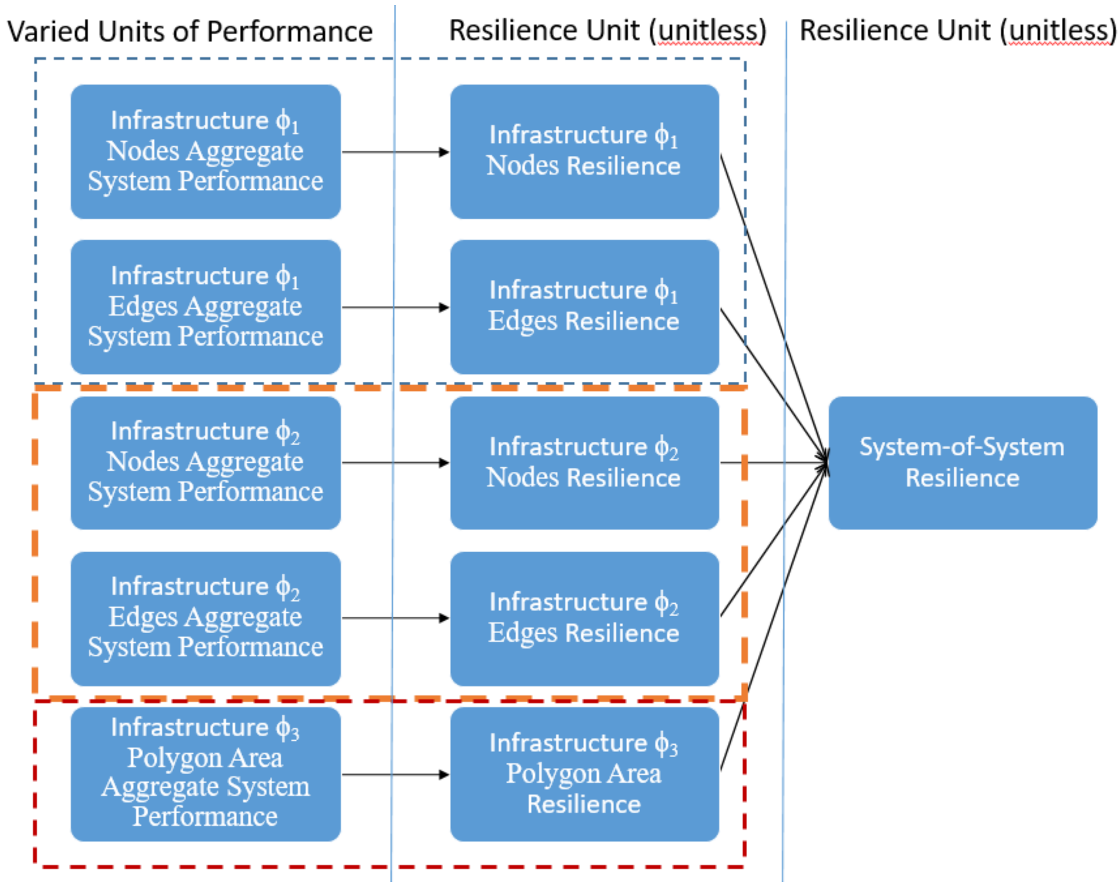

Figure 11 Calculation of overall resilience from aggregated system performance

Below are mathematical formulations for the combined system performance of nodes, edges, and polygon areas within a single network or layer. This formulation assumes that the system performance shares the same unit for a specific infrastructure system and element class.

$$\rho_{Func}^{\phi n}(t) = Sum\ of\ functional\ capacity\ of\ nodes\ in\ network\ or\ layer$$
$$= \sum_{i=1}^{N^{\phi}} \rho_{i,Func}^{\phi n}(t) \qquad \textbf{(38)}$$

Equation (38) shows the system performance for nodes within a network or layer. The formulation assumes that all nodes within the same network or layer are equally important. The symbol N^{ϕ} is used to denote the number of nodes within the network or layer. If the nodes were to be represented as a binary state, the formulation is simplified to equation (39).

$$\rho_{Func}^{\phi n}(t) = Number\ of\ active\ nodes\ in\ network\ or\ layer = n_{op}^{\phi}(t) \qquad \textbf{(39)}$$

The network or layer system performance for nodes is regarded as the sum of operating nodes at a specific point in time. For example, the system performance of a water network node is determined to be functional or non-functional, represented as a value of one or zero, respectively. Following this, all water network nodes are combined into a single value for the water network.

$$\begin{aligned}\rho_{Func}^{\phi e}(t) &= Sum\ of\ functional\ capacity\ of\ edges\ in\ network\ or\ layer \\ &= \sum_{i=1}^{E^{\phi}} \rho_{i,Func}^{\phi e}(t)\end{aligned} \qquad \textbf{(40)}$$

Equation (40) shows the system performance for edges within a network or layer. Similar to nodal formulation, it assumes that all edges within the same network or layer are equally important. However, the functional state of the edge is not limited to a binary state, and the functional state is allowed to vary. This formulation provides the flexibility to represent edges in a semi-optimal functional state. For example, during an extreme precipitation event, drivers may reduce their speed but still gradually approach their destinations. Alternatively, one lane may be closed due to a road block while other lanes remain functional. The total system performance of the edges within a single network or layer is calculated to be the summed functional capacity at a specific time, as represented by the term $\sum_{i=1}^{E^{\phi}} \rho_{i,Func}^{\phi e}(t)$. The symbol E^{ϕ} is used to denote the number of edges within the network or layer.

$$\rho_{Func}^{\phi PA}(t) = \sum_{i=1}^{PA^{\phi}} \rho_{i,Func}^{\phi pa}(t) \times IA_i \qquad \textbf{(41)}$$

Equation (41) shows the system performance for polygon areas within a layer. Unlike nodal and edge formulation, this assumes that the size of the polygon area is directly proportional with the system performance of the layer. Again, the functional state of individual polygon areas, $\rho_{i,Func}^{\phi pa}(t)$, is allowed to vary, similar to edges. However, the polygon areas are assigned an importance weight for the overall system performance of the polygon area layer based on their influence area, IA. The system performance of the polygon area layer is the total system performance of polygon areas at time t. Note the symbol PA^{Φ} is used to denote the number of polygon areas within the layer.

The resilience of an individual infrastructure type can be computed using equation

(42**)** through equation (44), which are the resilience formulations for nodes, edges, and polygon areas, respectively. They all use a similar concept of determining the ratio between the area underneath their system performance curve to the potential capacity performance area that could have occurred, as shown in Figure 1 in Section 2.2. Through this formulation, their unique system performance units are standardized into a unitless resilience measure.

$$r^{\phi n}(t) = \frac{Area\ under\ system\ performance\ curve\ for\ nodes\ of\ specific\ type}{Total\ Potential\ Area\ \ for\ nodes\ of\ specific\ type} = \frac{\int_{t_0}^{t} \rho_{Func}^{\phi n}(t)}{\rho_{Func}^{\phi n}(t_0) \times t} \quad \textbf{(42)}$$

$$r^{\phi e}(t) = \frac{Area\ under\ system\ performance\ curve\ for\ edges\ of\ specific\ type}{Total\ Potential\ Area\ \ for\ edges\ of\ specific\ type} = \frac{\int_{t_0}^{t} \rho_{Func}^{\phi e}(t)}{\rho_{Func}^{\phi n}(t_0) \times t} \quad \textbf{(43)}$$

$$r^{\phi PA}(t) = \frac{Area\ under\ system\ performance\ curve\ \ spatial\ area\ of\ specific\ type}{Total\ Potential\ Area\ \ for\ polygon\ areas\ of\ specific\ type} = \frac{\int_{t_0}^{t} \rho_{Func}^{\phi PA}(t)}{\rho_{Func}^{\phi PA}(t_0) \times t} \quad \textbf{(44)}$$

Once the resilience values of individual infrastructure networks or layers for a certain class of elements are obtained, they are combined to form the set of resilience values over time for a system-of-systems. Multiple quantitative metrics of resilience exist in the literature, as evidenced in Section 2.3; however, the one applied to this methodology is shown in equation (45):

$$R(t) = \left\{\prod_{\phi=1}^{M} r^{\phi}(t)\right\}^{\frac{1}{M}} \tag{45}$$

where $r^{\phi}(t)$ represents the set of resilience values at various times for a unique infrastructure type and element. M denotes the total number of unique infrastructure types and elements present within the modelled system-of-systems.

Characteristics of resilience are embedded within the quantitative process. These include robustness, redundancy, resourcefulness, and rapidity. Their explicit quantitative values can provide additional information on the disruption caused by and recovery after an event.

Zobel (2011) pointed out that one of the original drawbacks of Bruneau et al.'s (2003) quantitative formulation is that the same resilience quantity can be achieved through different paths. A system that suffers a large performance loss but recovers quickly could theoretically have the same resilience value as another system that suffers a small performance loss but recovers slowly, as demonstrated in Figure 12.

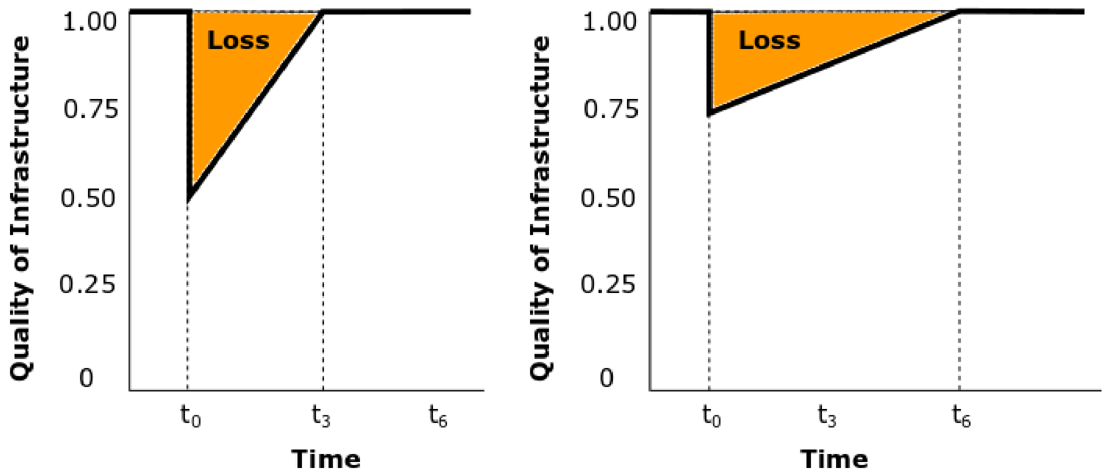

Figure 12 Two scenarios with the same loss and resilience but different curves. Adapted from Zobel (2011)[4].

The introduction of adapted dynamic resilience in this thesis addresses the aforementioned issue as it provides a sense of progression and magnitude of change. The explicit values of robustness, rapidity, redundancy, and resourcefulness can also be used as valuable indicators for the decision support process. For the purposes of this thesis, robustness is defined as the minimum performance state associated with a scenario. Two robustness formulations are used. The first is introduced here and applied to a particular type of element within a specific network or layer. The second is based on Simonovic & Arunkumar (2016) and is applied to the overall system. They both share the same concept of identifying the worst system state but have a different dependent, y-axis variable.

$$R_{rob}^{\phi}(t_{dmax}^{\phi}) = \rho_{Func}^{\phi}(t_{dmax}^{\phi}) \tag{46}$$

[4] Republished, with permission obtained by Howard Tong, from "Representing Perceived Tradeoffs in Defining Disaster Resilience", Zobel (2011), Volume 50; permission conveyed through Copyright Clearance Center, Inc.

Equation (46) shows that the robustness of a particular network or layer element type, R_{rob}^{ϕ}, is the performance, ρ_{Func}^{ϕ}, at time, t_{dmax}^{ϕ}, associated with the lowest system performance for a specific infrastructure system.

$$R_{rob}^{SA}\,(t_{dmax}) = R(t_{dmax}) \tag{47}$$

Equation (47) shows the system-of-systems robustness value, R_{rob}^{SA}, is equal to the lowest overall system-of-systems resilience value encountered, $R(t_{dmax})$.

Rapidity, shown in equation (48), is expressed as the amount of time that has elapsed since the disruption until the overall system reaches a recovered state.

$$R_{rap} = t_r - t_d \tag{48}$$

The variable t_r is the time at which the system-of-systems reaches a stable, recovered state. Note that during a simulation, it is possible for rapidity to have not yet occurred. Compared to the previous rapidity formulation proposed by Kong and Simonovic (2016), this formulation relaxes the requirement that resilience must return to full system performance.

The formulations of redundancy and resourcefulness are expressed in equation (49) and (50), respectively, taken from Simonovic and Arunkumar (2016).

$$R_{red} = \frac{R(t_{dmax}) - R(t_d)}{t_{dmax} - t_0} \tag{49}$$

$$R_{Res} = \frac{R(t_r) - R(t_{dmax})}{t_r - t_{dmax}} \tag{50}$$

Both represent the slopes of the resilience curve but on different sides of the maximum disruption time. Prior to maximum disruption, the declining slope is considered to represent redundancy, where a flatter slope indicates that infrastructure elements have substitutes or have low impact on system performance. The rising slope after the maximum disruption time is termed “resourcefulness”, an indicator of the amount and effective usage of resources available for recovery.

This concludes the methodology of deterministically quantifying infrastructure resilience. The methodology section began by describing infrastructure systems in the form of networks and layers. Hazards, adaptations, and their respective subsequent impacts were described next. Finally, resilience and its properties were quantitatively derived from the resulting system performance at each time step. The primary features that extend Kong and Simonovic's (2016) original methodology include the use of spatial infrastructure elements, new subdivision development, infrastructure network expansion, and adjustable damage representation. This effectively makes the resilience formulation more robust.

Given the high costs of natural disasters, disaster management should be integrated into infrastructure planning, design, operations and maintenance policies to mitigate losses. The web-based infrastructure decision support tool can help with this endeavor. It uses quantitative resilience to assess how well an urban system responds to natural hazards. Knowing the baseline of the system response, decision makers can visualize and quantify the added resilience from incorporating different adaptation measures. Therefore, the web-based tool can assist decision makers in the selection of the best adaptation measures to apply for a given scenario to increase community resilience. This can be applied in infrastructure planning, design, and operations and maintenance. Dr. Andre Schardong has been leading efforts to use the methodology described in this thesis to create a web-based infrastructure decision support tool. The tool, named ResilSIMt, is in the public domain and can be accessed at http://resilsimt-uwo.ca. The system architecture of this web-based tool and a brief user's manual are in Appendix A. A detailed tool description is available in the technical manual (Schardong et al. 2018). The following section uses the tool to show the main extended features that are the focus of this thesis through a case study situated in the City of Toronto.

Section 4

4 Infrastructure Resilience to Flooding and Wind – City of Toronto Case Study

Section 3 described the proposed methodology for calculating the resilience of municipal infrastructure. This thesis modifies Kong and Simonovic's (2016) approach by introducing (i) spatial impact areas, (ii) adjustable damage representation, (iii) a new subdivision infrastructure development method, and (iv) an infrastructure expansion capability for existing networks. This section presents an application of the method through a newly developed web-based tool in the form of a case study in the City of Toronto. Note that the thesis focuses on the implementation of the adapted methodology and the case studies are used for illustrative purposes only.

The section begins by describing the background on the reasons the City of Toronto is interested in improving resilience. Subsequently, five case study simulations are presented, illustrating the main contributions of the thesis.

4.1 Background

Toronto is the capital of Ontario, Canada. The City of Toronto had a population of 2,929,886 as of July 2017 and a land area of 630 km^2 (City of Toronto, 2018b). Similar to other Canadian cities, its critical infrastructure serves as the foundation of the lives of its citizens, providing functions that are essential in emergencies and are critical for urban community resilience (Simonovic & Peck, 2013).

In this section, facts and statistics on the City of Toronto’s critical infrastructure and buildings are presented. In terms of its road transportation, Toronto has 9,500 streets that cover 5,604 km. Streets are classified further into collectors, expressways, local roads, major arterials, minor arterials, and laneways. There are 2,164 traffic signals and 530 bridges located throughout the city. Approximately $5.1 million is spent on maintenance and energy for Toronto’s municipal transportation systems each year (City of Toronto Transportation Services, 2018).

Toronto’s municipal water infrastructure can be divided into three categories, namely potable water, wastewater, and stormwater. Toronto’s 2018 water budget backgrounder document provides a statistical summary of the city’s existing infrastructure. For potable water, this consists of four filtration plants, 11 reservoirs, four elevated storage tanks, 5,551 km of distribution watermains, 550 km of trunk watermains, 64,913 valves, 41,505 hydrants, 511,452 water service connections, and 18 pumping stations. For wastewater, this includes four wastewater treatment plants, 3,730 km of sanitary sewers, 1,411 km of combined sewers, 253 km of sanitary trunk, 121 km of combined trunk, 57,772 sanitary maintenance holes, 24,748 combined maintenance holes, 507,548 sewer service connections, 67 sanitary pumping stations, and eight combined pumping stations. For stormwater infrastructure, this consists of seven storage and detention tanks, 4,981 km of storm sewers, 27 km of trunk sewers, 76, 331 maintenance holes, 371 km of watercourses, 84 stormwater management ponds, 1,864 outfalls, 173,370 catch basins, and 12 stormwater pumping stations (Gironimo, 2017).

Electrical energy is provided through Toronto Hydro. The infrastructure, as of Dec. 31, 2017 consists of 178,800 poles, 15,540 km of overhead wires, 13,220 km of underground wires, 17,350 primary switches, and 60,540 distribution transformers (Toronto Hydro, 2018b). In 2011, 28% of underground assets had a fair or lower rating in the Asset Condition Assessment program. These assets are expected to require replacement within the next 10 years. In comparison, 50% of overhead assets had a fair or lower rating. Overall, 53% of station assets had a fair or lower rating (Toronto Hydro-Electric System Limited, 2011).

Section 2.1 previously discussed infrastructure problems that owners and managers may face. Here, the subset of infrastructure problems that are relevant to the City of Toronto is discussed. This relates to the electricity distribution, water, and road transportation sectors.

When heat waves occur, there is a spike in electrical demand because of cooling needs (Toronto Hydro, 2018a). This overloads the electrical distribution system and can cause functional performance loss. Much of the current distribution system is composed of

4.16kV lines. These lines have limited capacity and were not designed to handle neither the higher voltages of the forecasted service load growths from a larger population, nor the consumption of more energy because of increased average temperatures. The issue is worsened given the assets' aged condition and legacy design (Toronto Hydro-Electric System Limited, 2011). Distribution designs can consist of radial, looped, or network configurations. Radial configurations are less robust, as a component disruption could lead to the failure of the entire service line. However, they are generally chosen for their cheaper costs. As a result of all these combined factors, 40% of outages are attributed to the city's aged electrical distribution infrastructure (Toronto Hydro, 2018a).

Water infrastructure refers to potable water distribution and stormwater and wastewater collection systems. The main issues encountered include stricter regulatory reform and a continual accumulation of aging infrastructure. Stricter regulatory reforms mean that additional funds need to be allocated to accommodate the required changes. Aging infrastructure refers to the increased backlog of assets that are in need of repair. These issues are further exacerbated with a declining budget due to decreases in water consumption (Gironimo, 2017). All these factors contribute to stressing the overall water system, which can create vulnerabilities that lead to performance loss when a hazard is faced. As a result of improper design of the urban drainage system for the current flows and the lack of adequate upkeep, certain consequences may occur, such as flooded basements, which are seen as a major problem.

The road transportation sector in Toronto faces an issue with congestion, a form of performance loss, because of insufficient capacity. This insufficient capacity has arisen due to multiple factors. Currently, the existing road infrastructure cannot keep up with travel demand within the city. The resulting congestion is estimated to cost the average commuter 81 hours annually (City of Toronto, 2013). They also cited that it would be impractical to build enough roads to meet projected travel demand in the future, implying an infrastructure planning issue.

A key Future Weather and Climate Drivers Study commissioned by Toronto in 2011 predicted heat waves, extreme precipitation, and higher annual temperatures as future weather concerns. These weather-related hazards are expected to have impacts on municipal infrastructure and services. As an example, the City of Toronto experienced a heavy rainstorm on July 8, 2013 that resulted in, “Over $70 million cost to the city while the Insurance Bureau of Canada reported about $1 billion in insurance claims” (Chief Corporate Officer, 2016). Given the potential damage and risk associated with these events, the report urged all agencies in Toronto to collaborate to reduce this risk. Toronto’s city council has made enhancing infrastructure and service resilience a top priority. The expected outcome is a reduction in the risk of costs and injuries that can occur if extreme weather patterns persist (Chief Corporate Officer, 2016).

A report by the Toronto Chief Corporate Officer to the Parks and Environment Committee in November 2016 summarized the current progress that Toronto has made to increase resilience and the next key steps that are planned. In the timeframe between 2014 and 2016, the cross-corporate Resilient City Working Group implemented a policy that identified and assessed potential weather risks, defined interdependencies between key infrastructure, and outlined adaptation actions that can be taken to reduce risks. The policy follows a thematic area high level risk assessment approach, applying it to three initial thematic areas, including utilities, transportation, and water. Various City of Toronto divisions and partner agencies continue to undertake actions related to this initiative that help resilience decision making overall. These include gathering and applying GIS information, having a better understanding of flood information, and improving communications and outreach. Flood information is improving as the TRCA updates the vulnerable flood areas database using hydraulic model outputs, exposure, and vulnerability relationships within the GIS environment. Toronto Water is also undertaking environmental assessments through their Basement Flooding Protection Program to determine the effect of extreme rainfall events on sewer system capacity. The Environment and Energy Division launched their Extreme Weather Portal, a website that educates residents and businesses on weather-related risks and steps that can be taken to improve their resilience (Chief Corporate Officer, 2016).

The City of Toronto joined the 100 Resilient Cities network in May 2016 (City of Toronto, 2016). In a December 2016 workshop that comprised key stakeholders, including representatives from the 100 Resilient Cities, they began to build stronger relationships with each other and identified issues, needs, and priorities related to the essential functions of the city. One of the key findings from the workshop was that a resilience approach provides common ground to address the chronic stressors and shocks faced by different stakeholders. The stakeholder workshop also alluded that Toronto has great working policies but that implementation was perceived as lacking. Chicago's chief resilience officer advised the City of Toronto in a panel discussion that there were challenges in measuring progress related to resilience. He indicated that interdependent relationships between shocks and stressors were challenging to model, highlighting a need for resilience (City of Toronto, 2016).

The City of Toronto is interested in building resilience for their city and has taken initial steps towards this. However, no quantitative resilience metric has yet been employed (Chief Corporate Officer, 2016). The proposed collaborative research project can help the City of Toronto quantitatively measure resilience, allowing for future decision-making support. The quantitative resilience metric offers advantages in multiple forms. These include identifying vulnerable risk areas and their severity, creating a baseline measurement of resilience for future comparison, and comparing progress to other municipalities to improve infrastructure management best practices. The model behind the resilience calculation can capture the unique situations that each municipality faces when it comes to their existing infrastructure, geospatial placement, and interdependencies.

The project complements the initiatives already underway by the city staff. Specifically, the project makes use of the identified interdependencies, converts them into a quantitative relationship, and treats them as valuable model input. By explicitly inputting the various first-order relationships that exist among infrastructure components, among hazard and infrastructure, and among infrastructure systems, the model can reveal resilience, or lack of, in a given scenario. The model's value grows as more infrastructure components and more accurate relationships are captured as input. The computational powers are highlighted as the amount of information grows to a point at which it becomes difficult for humans to retain the collective data and the associated relationships. This limited human capability is where hidden cascading failures occur.

4.2 Experiments and Scenarios

This section applies the methodology from Section 3. Each subsection below illustrates a modification of Kong and Simonovic's (2016) infrastructure resilience methodology developed in this thesis. Section 4.2 culminates with a case study set in the City of Toronto that applies these added features in the case of a flood and wind hazard.

4.2.1 Experiment 1: Introduction of Spatial Impact Areas as a Data Format

Originally, Kong and Simonovic's (2016) model only captured infrastructure as a networks, representing infrastructure components as nodes or edges. If industrial or residential buildings were to be converted into this format, each building footprint would likely be represented by a single node. While this may be adequate in certain cases, nodes cannot accurately reflect a building's footprint. This inaccuracy within the model can potentially underestimate the damage suffered due to a hazard.

This thesis introduces the option of spatial impact areas as a data format in addition to the network form. Spatial impact areas can be visualized as polygon areas. The application of spatial impact areas has multiple benefits, including the added flexibility of capturing a more realistic geospatial representation on a map, enabling a more accurate hazard interaction compared to the original model as well as a mechanism to illustrate service areas. To illustrate some of the benefits of spatial impact areas, this experiment uses the newly developed ResilSIMVt web tool to simulate the impact of a hypothetical flooding scenario on residential buildings. The residential building footprints were retrieved from Open Street Maps (OSM), an open data source (OpenStreetMap Wiki contributors, 2014).

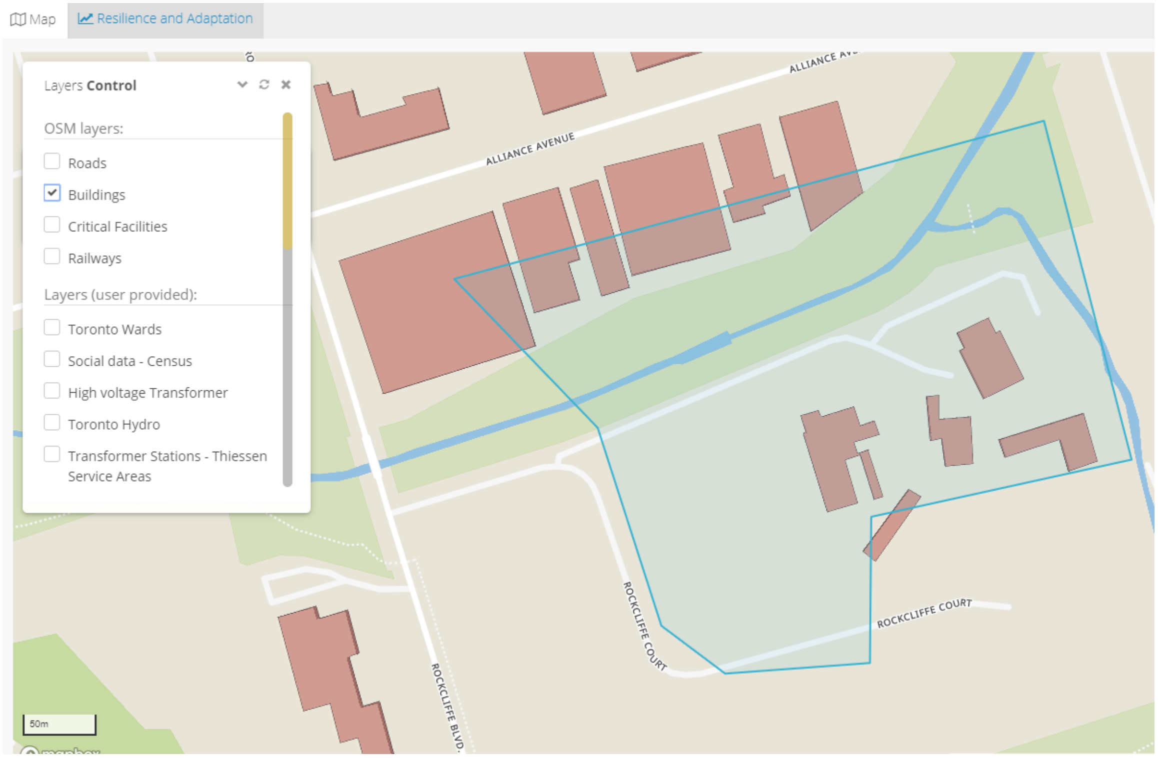

Figure 13 An application of spatial impact areas as a potential data format

In Figure 13, buildings within the area are shown as red polygon areas. The blue polygon represents a hypothetical example of the extent of a flooded area. It is apparent that the flooding extent may not entirely overlay some of buildings or the center of their location. Hypothetical effective flood water magnitudes, referring to the level of water above the ground surface, are displayed in Figure 14.

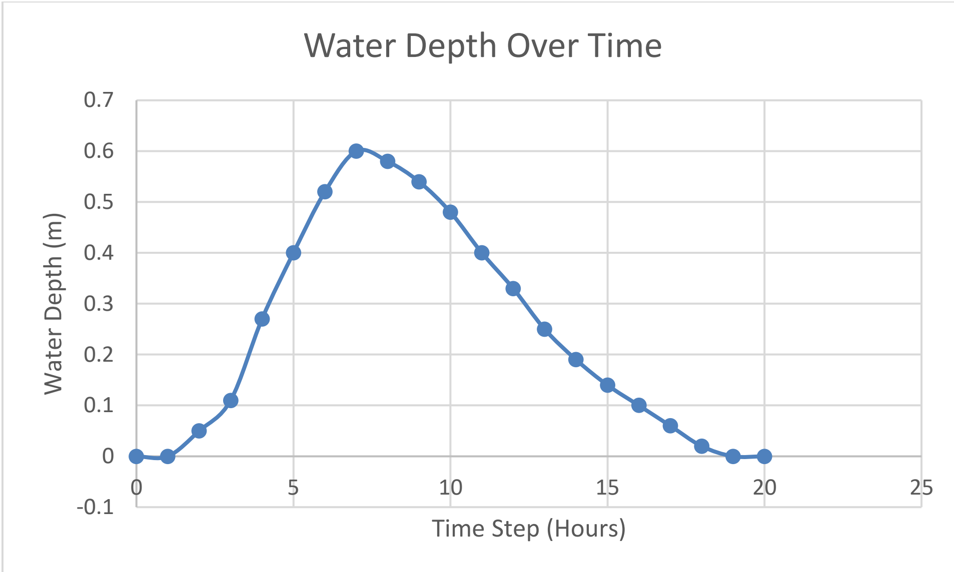

Figure 14 Case study effective flood depths

Flood damage to buildings is captured through tabulated stage-damage curves. All buildings in the case study are assumed to be residential and have the same characteristics. The stage-damage curve values, obtained from field inspections by qualified architectural experts accompanied by local building industry representatives, are shown in Table 6 (Natural Resources Canada, 2017). All residential buildings in the case study were assumed to be two-story Class A residential buildings. While it is acknowledged that other building types exist and can be implemented as separate layers or subclasses, considering this would require additional building and impact relationship data. The performance metric for these buildings is their estimated structural and inner content economic value. This experiment used the economic value in $/m^2 as the performance metric.

The initial value, $\rho_{0,Phys}^{Residential\_Building}$, was assumed to be the maximum potential recorded damage of $2,863/m^2. Equation (51) shows the remaining performance level, $\rho_{i,Phys}^{Residential\_Building}$, when a flood loss of $\rho_{i,Loss}^{Residential\_Building}$ occurs. Given that damage can occur when flood depth is zero, due to basement contents, the calculation of loss was only invoked in areas where flood hazard input is inserted.

$$\rho_{i,Phys}^{Residential\_Building} = \rho_{0,Phys}^{Residential\_Building} - \rho_{i,Loss}^{Residential\_Building} \quad \textbf{(51)}$$

Table 6 Stage damage for a two-story Class A residential building (Adapted from Natural Resources Canada, 2017)

Depth Relative to Main Floor (m)	Main Floor Contents ($/m²)	Main Floor Structure ($/m²)	Basement Contents ($/m²)	Basement Structure ($/m²)	Total Damage ($/m²)
0	0	0	523	522	1045
0.1	343	665	523	522	2053
0.3	545	676	523	522	2266
0.6	663	826	523	522	2534
0.9	748	1051	523	522	2845
1.2	766	1051	523	522	2862
1.5	767	1051	523	522	2863
1.8	767	1051	523	522	2863
2.1	767	1051	523	522	2863
2.4	767	1051	523	522	2863
2.7	767	1051	523	522	2863

With the introduction of polygon areas as a data format, the system performance of a layer that consists of multiple polygons assumes that their individual impact to the overall layer performance is proportional to the sizes of the polygons. In effect, a larger polygon area with a similar base system performance has a greater effect on the overall layer's system performance.

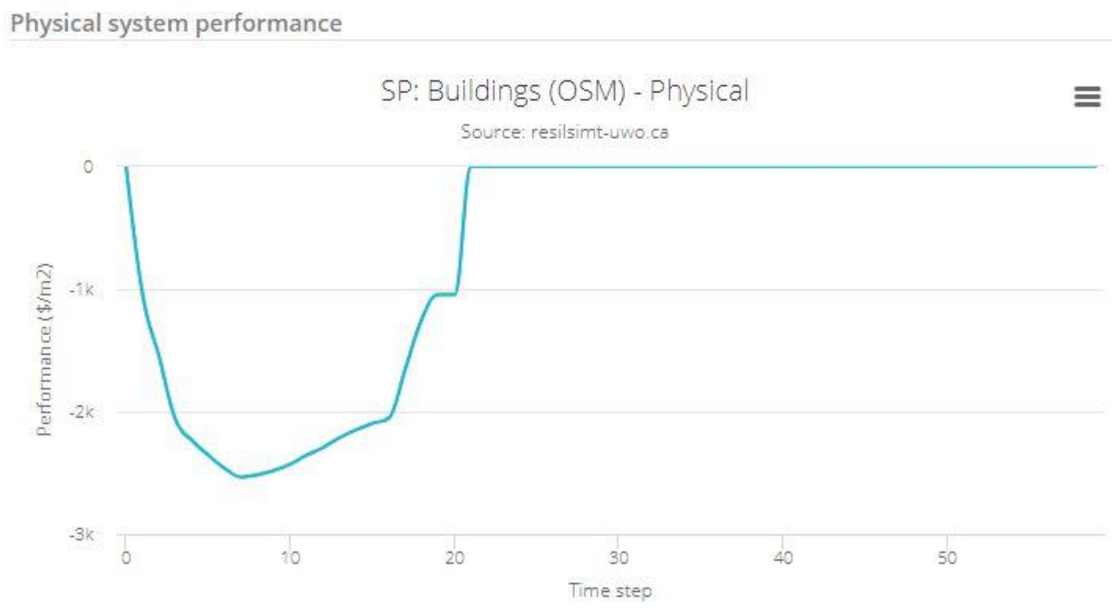

Figure 15 Experiment 1 - building performance curve

Figure 15 displays the result of the simulation and shows that building performance decreases when flooding occurs and that the building recovers as flooding recedes. The figure demonstrates that spatial impact areas successfully capture system performance over time. Figure 16 shows that the overall resilience is based on the single interaction between buildings and flooding. The cursor on ResilSIMt can be used to identify system performance and resilience at each time step, allowing robustness values to be easily extracted.

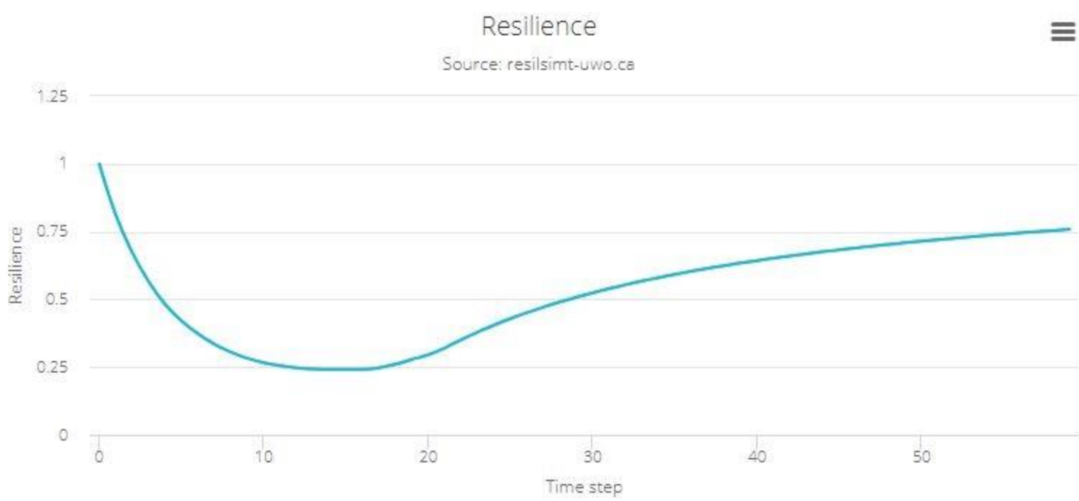

Figure 16 Experiment 1 - overall resilience curve for building layer

Given a dataset that includes spatial impact areas of other building types (i.e., commercial, industrial, institutional) and their respective impact relationships to floods or other hazards, infrastructure managers can determine their individual resilience values.

As individual system components can have suboptimal states and yet remain functional, the loss of system performance caused by a direct hazard impact is assumed to be proportional to the hazard's intensity. For example, building damage may be directly proportional to the height of flooding. When applying stage-damage curve tables, or their equivalent, if an intensity value is not explicitly expressed but is within the available range, linear interpolation is used to calculate the impact. From a hazard impact perspective, the method assumes that if the hazard area interacts with any portion of the edge or polygon area, the impact is applied to the whole individual system component.

The application of spatial impact areas in this scenario provides practical benefits in terms of accuracy by capturing the damage that can be incurred as a result of floodwaters entering parts of a building. However, this does not make the use of network representation inferior in all cases. One example where it is useful is the application of the infrastructure expansion algorithm, shown in Experiment 4, which currently relies on infrastructure being represented as nodes and edges.

4.2.2 Experiment 2: Adjustable Damage Representation for Network Components

In Kong and Simonovic (2016), both nodes and edges within a network have binary performance values. They are either functional or non-functional. One of the contributions of this thesis allows each individual network component to have a variable performance state in order to illustrate how infrastructure can have partial functionality. This can increase the accuracy and better capture complex infrastructure behaviour.

The tool was used to illustrate the application of adjustable damage utilizing street network information, the streets' geographical locations, and maximum speed limits. The change in maximum speed limits was used as a performance metric for the network. Flooding was used as a hazard input, based on a 100-year return-period floodplain area identified by the TRCA (2018). This area is shown in Figure 17.

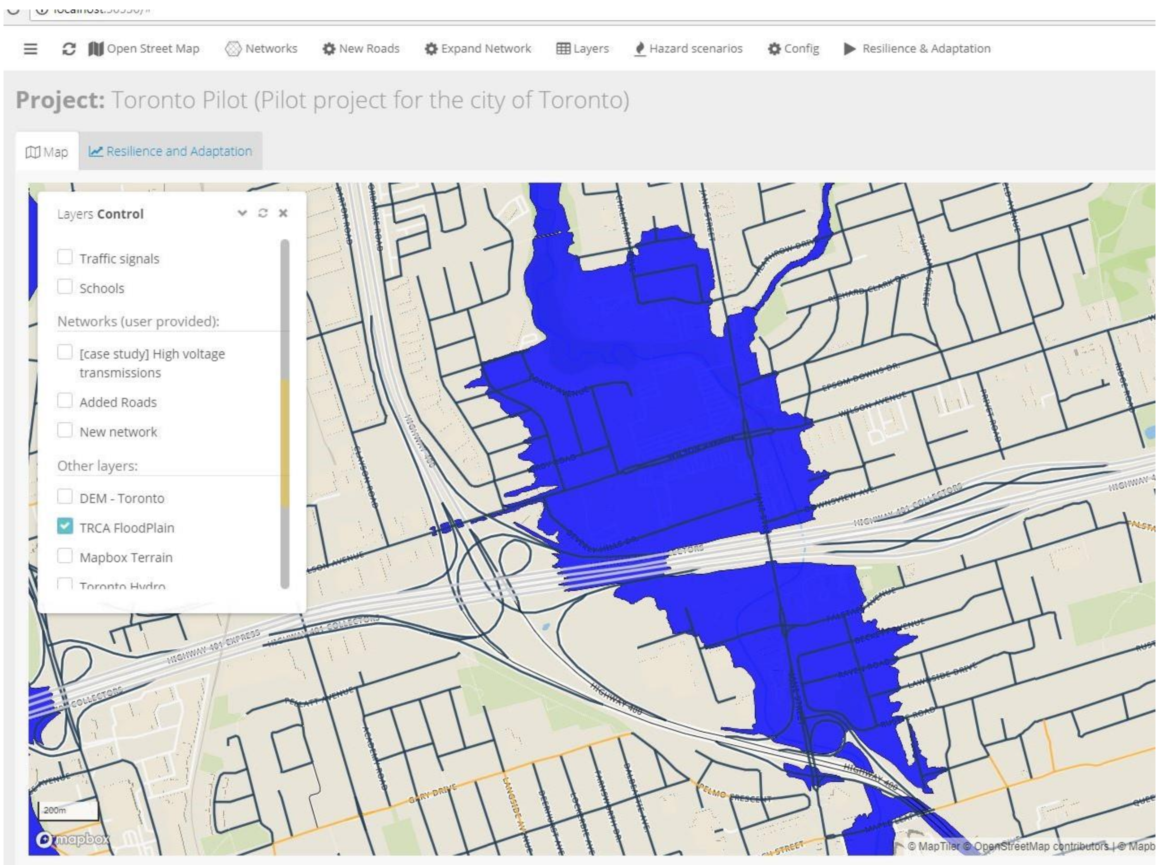

Figure 17 100-year return-period floodplain area from the Toronto Region Conservation Authority

A flood-depth impact relationship from Pregnolato et al. (2017) was applied to show the varied loss of performance and remaining functionality. The impact relationship was previously depicted in Figure 9, and the equational form is shown in equation (52).

$$v(w) = 0.0009w^2 - 0.5529w + 86.9448 \quad \textbf{(52)}$$

where v(w) is the maximum vehicle speed in km/h as a function of flood depth w in mm.

Within equation (52), there are a few assumptions. First, in the original study, data was gathered from various sources that included experimental studies, safety literature, experts' opinions, and videos to develop an approximated function between two classes of cars: four-wheel-drive vehicles and small cars. Subsequently, all the data sources were aggregated for an estimated function for cars in general (Pregnolato et al., 2017). The inherent assumption in this estimated function implies that the maximum vehicular speed is 86.9 km/h when there is zero flood depth. In this thesis, this function is applied to the designated road speeds available in the road network edges, assuming the roads are constantly used and all vehicles are cars. As the maximum road speed varies depending on the stretch of road, the above equation was transformed using equation (36). The speed reduction of roads is shown in equation (53).

$$\rho L_{Func}^{Road} = \rho_{0,Func}^{Road} - (1 - \frac{v(w)}{86.9448}) \times \rho_{0,Func}^{Road} \quad \textbf{(53)}$$

where ρL_{Func}^{Road} is the road performance loss using car speed reduction as a proxy, $\rho_{0,Func}^{Road}$ is the initial road performance using maximum road speed as a proxy, and $(1 - \frac{v(w)}{86.9448})$ serves as a coefficient representing the percentage of road speed reduction. The variable v(w) is taken from equation (52).

A threshold of 30 cm flood depth was originally used to determine a non-functional state for road infrastructure based on the binary assessment for edges. Figure 18 illustrates this result. By comparison, Figure 19 illustrates the effect of a varied edge state approach. Given a flooding scenario and the impact relationship from (52), the edges in Figure 19 show varied performance and capture functionality loss when floodwater is on the road surface.

As system components can have varied performance instead of functional or non-functional states, it is assumed that the summation of individual components' varied performance is a good indicator of the system performance for a given network or layer. As an example, consider flow in a water distribution network as a performance metric. In this case, system performance of the network is directly proportional to the summation of water flow throughout individual pipes of the network.

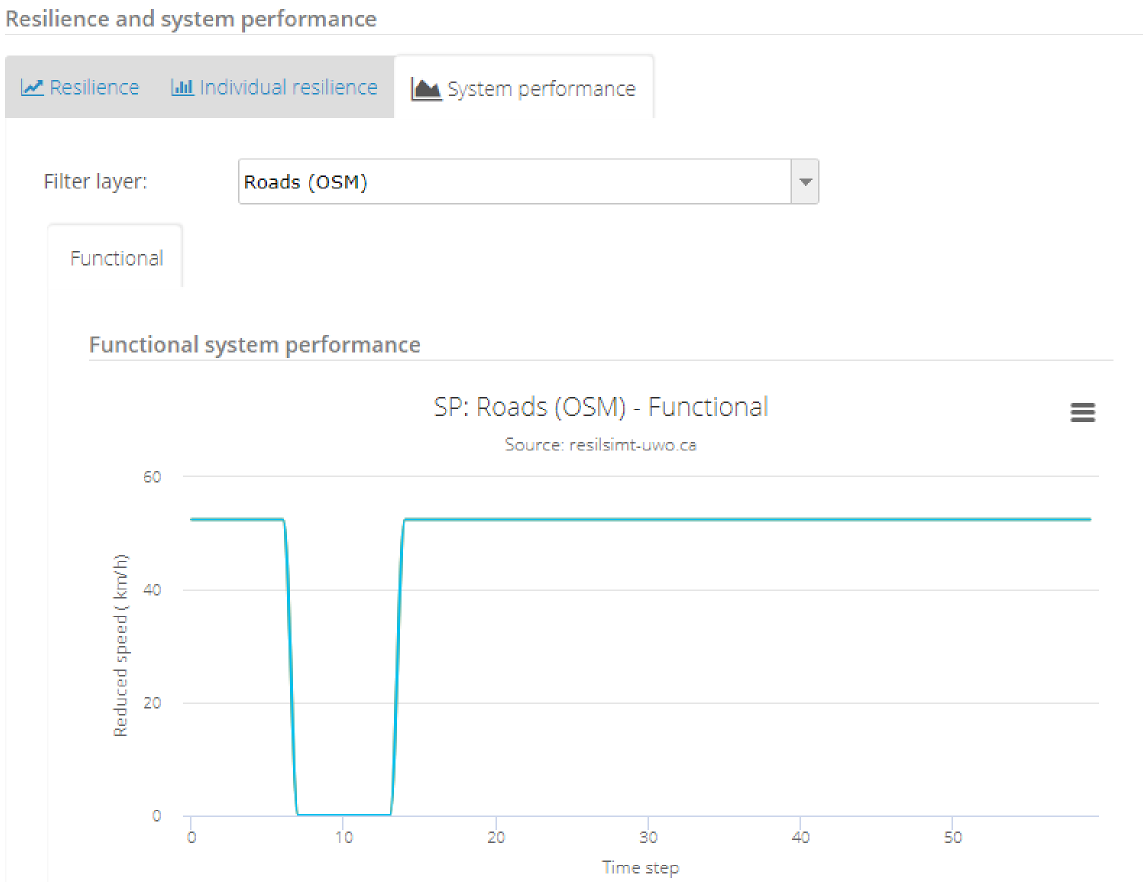

Figure 18 A binary functional state for road edge components

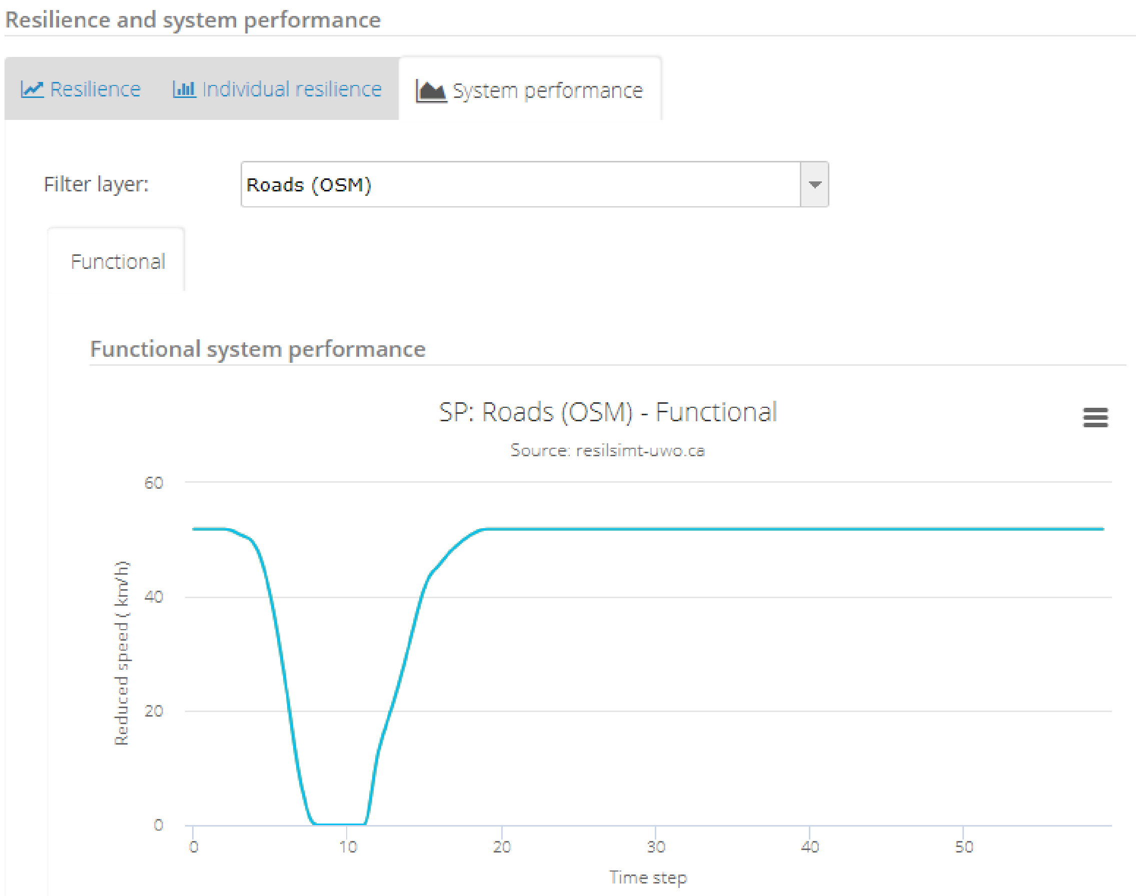

Figure 19 A varied functional state approach for road edge components

The flexibility of allowing edges to have adjustable damage representation makes the infrastructure representation more realistic. Removing the constraint that forces system performance to be either functional or non-functional acknowledges that certain system components can have partial functionality.

4.2.3 Experiment 3: New Subdivision Road Infrastructure Development

Given that one of the infrastructure management challenges is urban growth, it is important for infrastructure managers to have access to a method that can simulate new infrastructure development. In Section 3.1.4., Wickramasuriya et al.'s (2011) algorithm is presented in the context of new subdivision development. This experiment shows how road infrastructure can be developed on a hypothetical empty lot of land that has been set aside for a new subdivision development. Following this, three resilience scenarios are considered in the context of hypothetical flooding for new development. This demonstrates the potential effect that infrastructure development has on system resilience.

The inputs for the new subdivision road development include a spatial area to be developed, typical lot dimensions, and street width. Figure 20A illustrates an empty plot of land near the intersections of Steeles Avenue East and Tapscott Road prior to applying the algorithm. The input lot size is 127ft by 43ft, based on a housing brokerage firm, for a detached three bedroom house worth $900,000 to $1,100,000 (TheRedPin, 2015). The lot dimensions were converted to an input of 38.7m by 13.1m. Given a residential setting, two curb lanes were assumed. Each curb lane that carries traffic speeds of 50km/h or lower has a dimensional width of 3.3m (City of Toronto Transportation Services, 2017). Figure 20B illustrates the result of application of the new subdivision development algorithm for a planned road infrastructure network.

Figure 20 Comparison of before and after images of roads added in a subdivision development scenario. Figure A is an empty lot bounded by Steeles Avenue East, Tapscott Road, and Passmore Avenue. Figure B is the same location with the proposed road infrastructure.

A hypothetical flood hazard was created to showcase the effect that infrastructure development can have on resilience. The flood area is illustrated in Figure 21, and the progression of flood depths over time is shown in Figure 22.

Figure 21 Hypothetical flooded region in the newly developed area

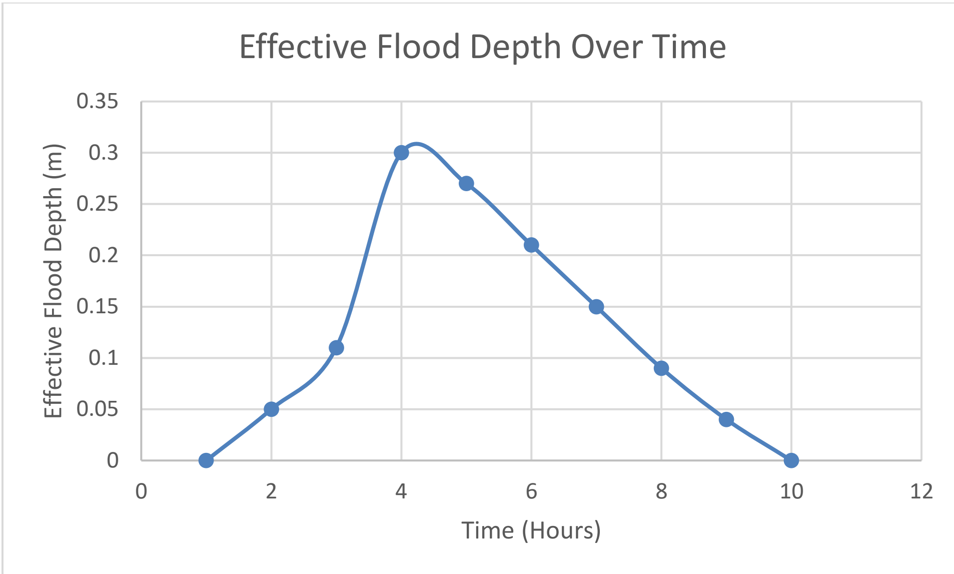

Figure 22 Hypothetical effective flood depth input for Experiment 3

Three scenarios were considered. The first scenario demonstrates the effect that the flood hazard would have on only the existing road infrastructure system shown in Figure 20A. Pregnolato et al.'s (2017) flood depth to traffic speed impact is used here. The results of the simulation yielded the resilience curve in Figure 23.

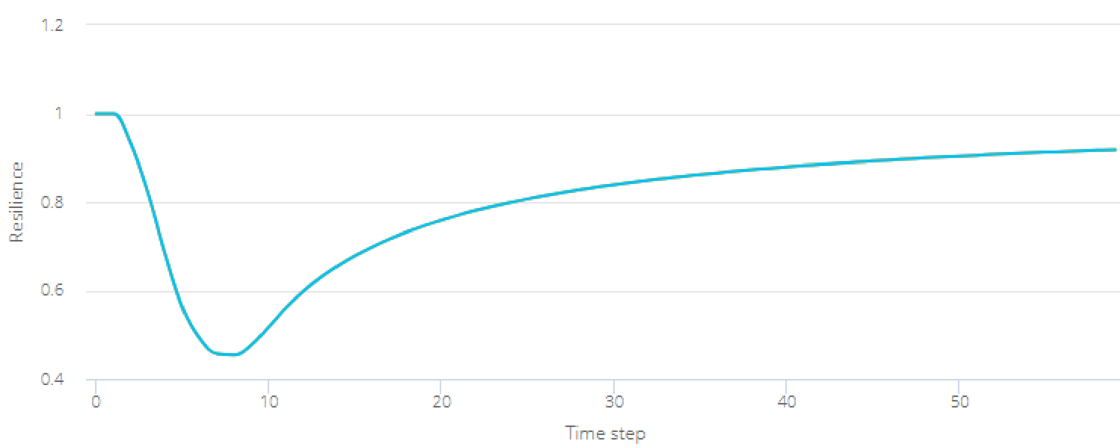

Figure 23 Resilience curve output for no new subdivision road development

The second scenario has an overall infrastructure system that consists of both the existing road network and the newly developed road network shown in Figure 20B. The newly developed road network was assumed to have the same build and drainage characteristics as the existing road network. Again, the same flood impact was used for both networks. The third scenario uses the same infrastructure components as the second scenario, but an adjusted flood depth to traffic speed impact relationship was used for the newly developed road network. This models a scenario where an adaptation measure, such as permeable pavement, is implemented. In this scenario, it is assumed that permeable pavement would allow more water to infiltrate the ground compared to the existing road network. Thus, a 10% flood depth reduction is assumed. For example, if the flood depth was 30 cm for an existing road segment, then permeable pavement would reduce it to 27 cm.

The resilience values for each of the three scenarios are illustrated in Figure 24.

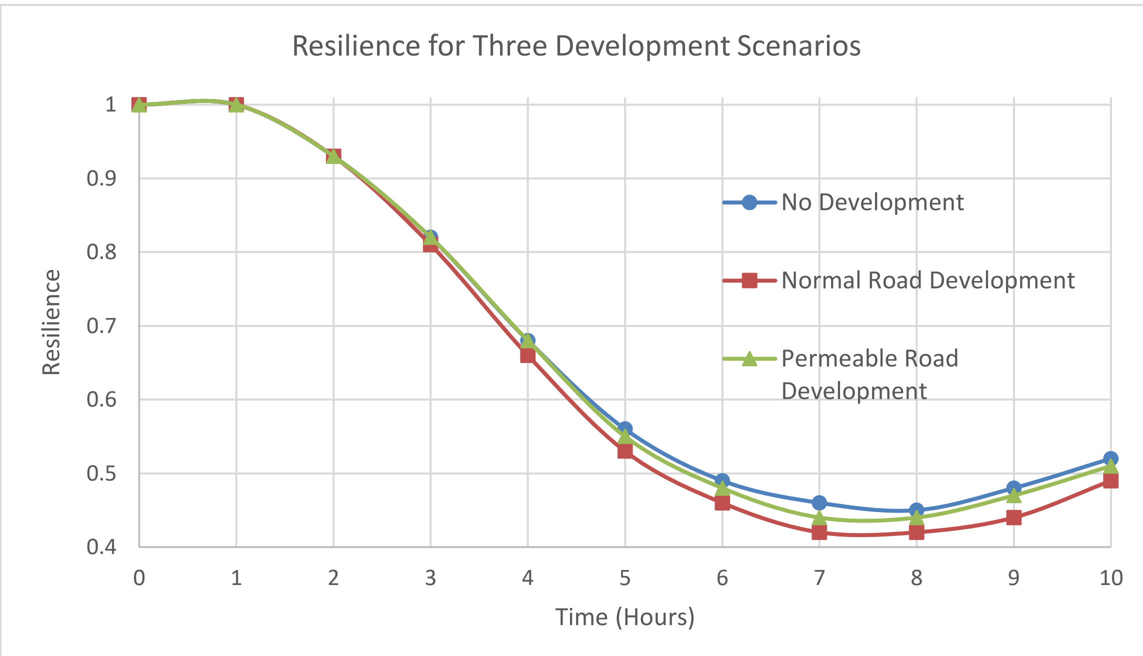

Figure 24 Comparison of resilience values for the three new development scenarios

The no new road development scenario yielded the highest set of resilience values. Normal new road development combined with existing roads was the worst of the three scenarios in terms of resilience values. The third scenario had resilience values closer to the no new development option.

While the no new road development yielded the highest set of resilience values, it is unlikely that this is the case in all scenarios. However, the experiment results do suggest that the placement of new infrastructure networks is important. If the new networks were developed in an area unaffected by hazards, the overall resilience would likely be different. Second, the implementation of adaptation options can help to greatly reduce the loss of system performance while satisfying new infrastructure growth, as demonstrated in the third scenario.

Overall, the added feature of new network development provides infrastructure managers with the ability to simulate one form of subdivision development. When this feature is added to a resilience assessment, it can help managers determine the impact that the planned networks have on overall system resilience.

4.2.4 Experiment 4: Infrastructure Network Expansion

Given that one of the infrastructure management challenges is urban growth, it is important for infrastructure managers to have access to a method that can simulate existing infrastructure expansion. Infrastructure network expansion is based on the process presented by Fu et al. (2016) and was described in Section 3.1.5. For this experiment, the algorithm is applied to a high-voltage transmission network. Subsequently, the expanded network is faced with a wind storm hazard. The inputs required for the expansion of an existing network include: population density data to simulate electricity demand, the spatial area of interest to expand, the number of nodes to add, and $\gamma, \alpha\ and\ \beta$ parameters from Fu et al.'s (2016) methodology.

High-voltage transformer stations were extracted from the Transformer Station Region file from DMTI spatial, which is available through Scholars Geoportal (DMTI Spatial Inc., 2017). The polygon areas available were converted into a nodal format. Additional nodes were added based on the transmission station map from the Integrated Regional Resource Plan document (Ontario Power Authority, 2015). Edges were added based on the electrical transmission file, which is also available through the Scholars Geoportal. All of these data were combined to form the existing high-voltage network input. Figure

25A illustrates the electrical transmission network consisting of nodes and edges before expansion.

Population density data were obtained from Toronto ward census data (City of Toronto, 2018a). The central to southern parts of Toronto were selected as the area for potential expansion. Two nodes were added. $\gamma, \alpha\ and\ \beta$ parameters took the values of 0.579, 0.034, and 0.0, respectively, based on Fu et al. (2016).

Figure 25B illustrates the same electrical transmission network after it was expanded based on this methodology. Two edges were created, as shown in the pink colour in Figure 25B. Note that the area is magnified to show the added nodes and edges.

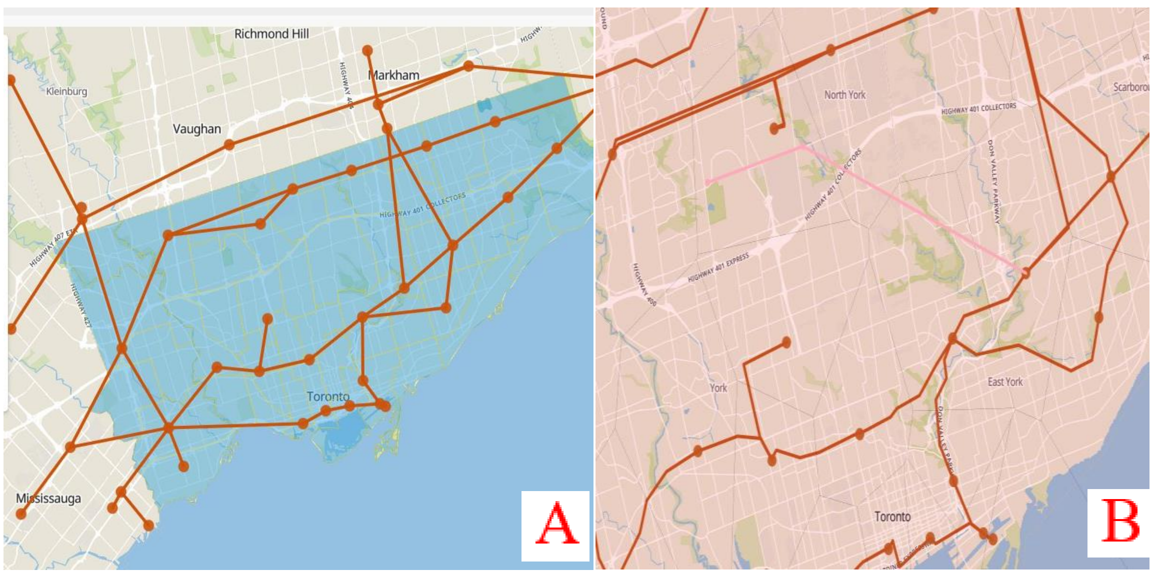

Figure 25 Comparison of before and after images for the expansion of the high-voltage transmission network

The expanded high-voltage transmission tower network was subjected to a hypothetical wind storm that encompassed the entire electrical network displayed. The performance metric for the high-voltage towers are binary, with the options of either functional or non-functional. The overall unit of measure for the network is the percentage of components still functional. The wind storm magnitude over time is shown in Figure 26.

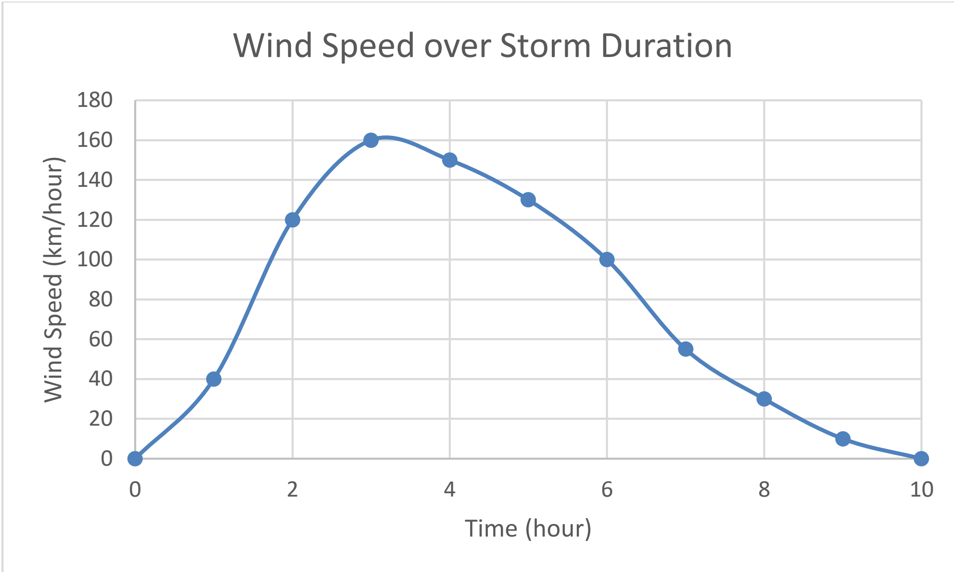

Figure 26 Hypothetical wind storm event

The relationship between wind damage and high-voltage transmission towers was determined through the use of a fragility curve. The fragility curve applied was taken from Fu et al. (2017). The authors derived the fragility curve through an analytical approach by applying wind loads on the modelled tower structure using the commercial software ABAQUS (Fu et al., 2017; Panteli, Pickering, Wilkinson, & Dawson, 2017). Figure 27 shows the wind fragility curve used in this case study. It was assumed that the transmission towers were equivalent to the L2 towers used in the UK.

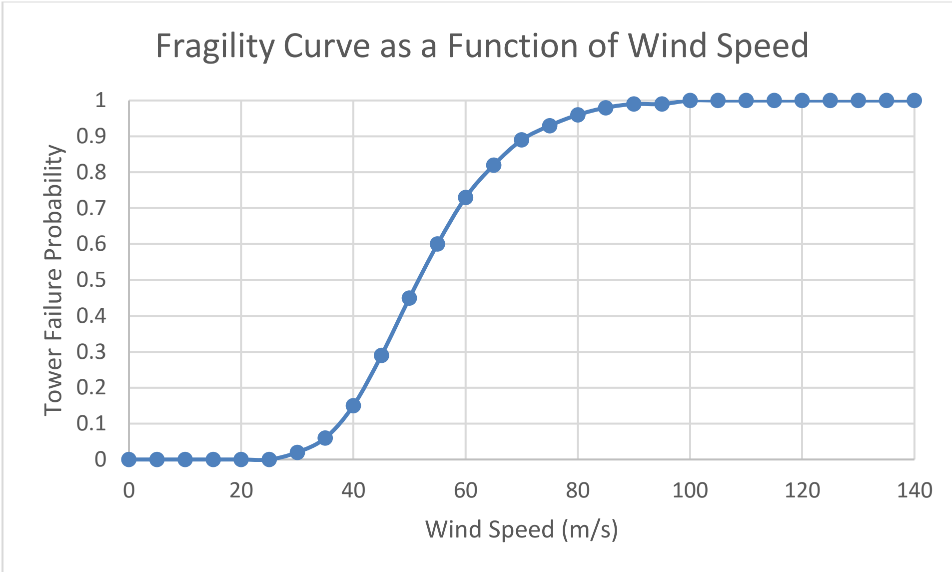

Figure 27 Fragility curve for transmission tower failure. This work belongs to Fu et al. (2017). ©[2017] IEEE

If a high-voltage transmission network component is damaged, it is considered permanent in the sense that it requires external resources to recover the unit. This simulates the occurrence of high transmission tower failure. This is in contrast to the flood damage introduced earlier, where the loss in functionality of roads reduces as the hazard recedes. The results of the experiment are visualized in Figure 28 and Figure 29.

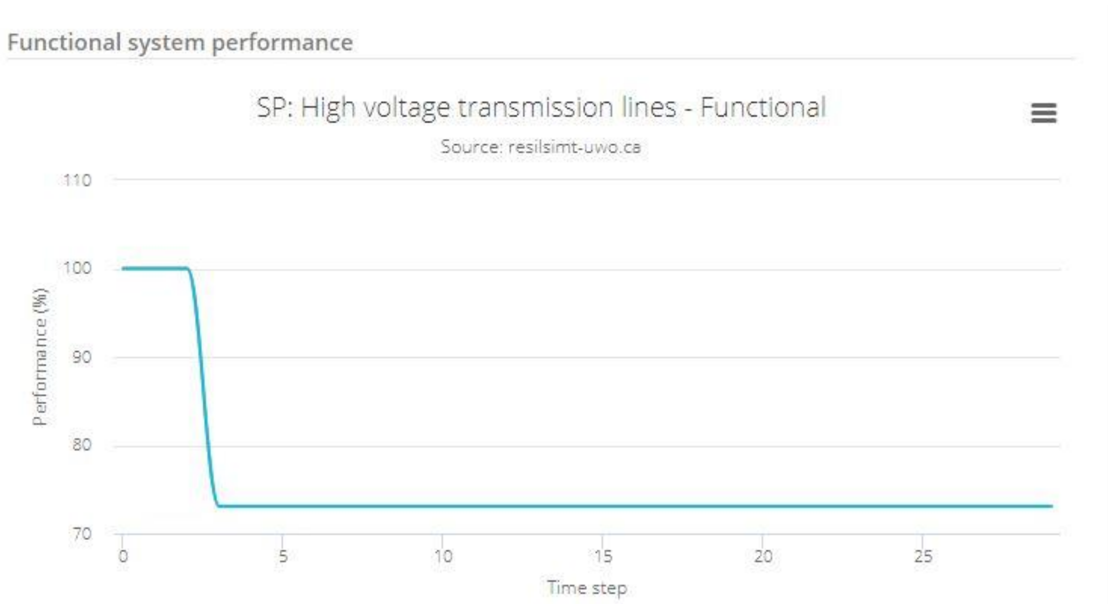

Figure 28 Experiment 4 high-voltage transmission tower system performance

Figure 29 Experiment 4 resilience curve

This experiment would normally have similar results as the one involving new network development previously presented, highlighting the importance of infrastructure location. However, there is a key difference between the last experiment and the current one. The hazard in the current scenario encompasses the entire network. Given the uniformity of a single infrastructure network and the all-encompassing nature of the hazard, the components behave identically. If not for the stochastic nature embedded in the fragility curves, the resilience results would be the same for an expanded infrastructure network and its original form. The proportion of system performance loss compared to overall potential performance remains the same.

Nonetheless, an infrastructure expansion component remains useful to infrastructure managers if a hazard is localized or there are differences in the behaviour of infrastructure components.

4.2.5 Experiment 5: Use of ResilSIMt - City of Toronto Case Study

The features described in Sections 4.2.1 through 4.2.4 were combined into a case study set in Toronto with flood and wind hazard scenarios. The purpose of the case study is to showcase the full capacity of the ResilSIMt web-based tool. However, as there is lack of real infrastructure and impact relationship data that can be adapted into this tool at this time, the quantified resilience output here cannot be used to draw meaningful conclusions for decision making. Nonetheless, the case study still illustrates the adapted methodology and its potential usefulness in infrastructure decision support should sufficient data be made available.

Network and layer data for roads and buildings, introduced earlier, were combined with the new roads from the subdivision development, the high-voltage network and its expansion, spatial hazard impact areas representation, and adjustable damage. Traffic signal data were also added in this case study. Traffic light locations in the form of nodes were obtained from the City of Toronto open data catalogue (City of Toronto, 2018a). Interdependencies were linked between certain networks. Adaptation measures were also explicitly implemented.

Figure 30 illustrates the impact relationships that hazards can have with infrastructure networks and layers in this experiment. The impact summary is provided directly from ResilSIMt. Beginning with the flood and wind hazards, these relationships can have direct impacts on infrastructure. The high-voltage transmission network can affect traffic signals, which can subsequently affect roads through interdependent relationships.

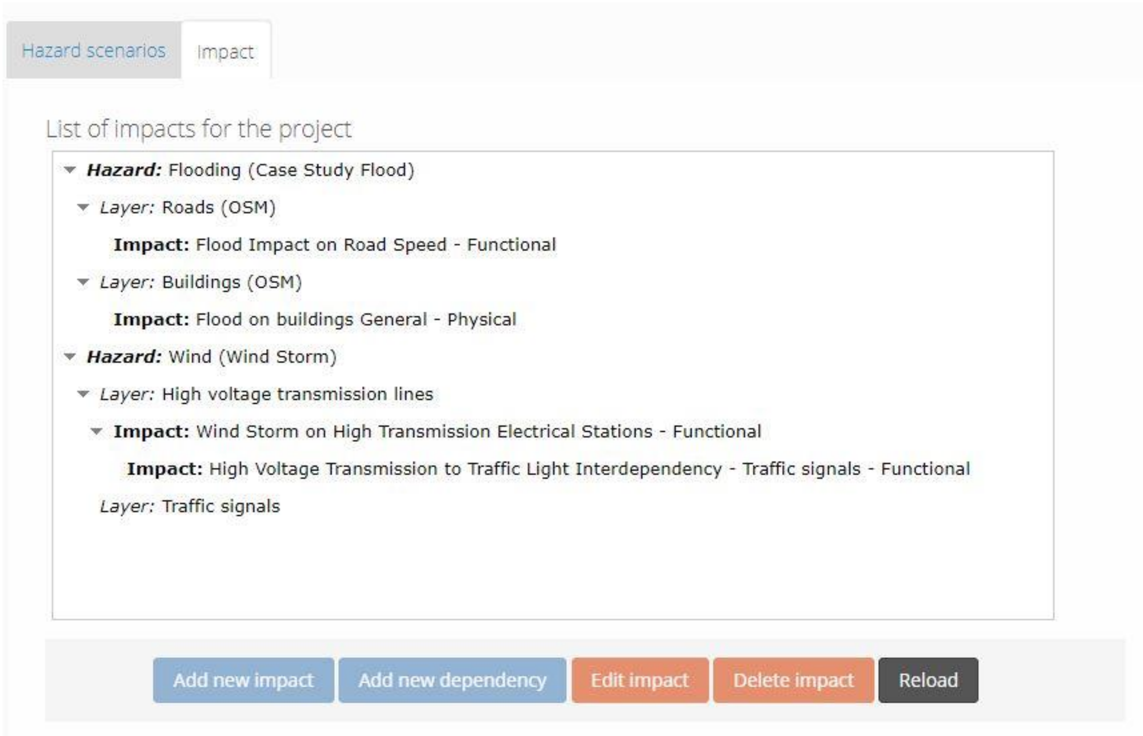

Figure 30 Summary of impact relationships in Experiment 5

4.2.5.1 Experiment 5 Inputs

Each network and layer cited has its own performance measure to indicate its functionality. The performance measure for road networks was maximum speed in km/hr. The performance measure for electrical components was described as either functioning or non-functioning, and they were assigned the values of one and zero respectively. This is applicable for the high-voltage network components and traffic light signals. Buildings had a performance measure of economic value in $/m^2.

Two hazards are applied to this case study, namely flooding and wind. The blue area in Figure 31 refers to the TRCA 100-year floodplain (TRCA, 2018). The two purple spatial areas represent flooded areas for this illustrative case study.

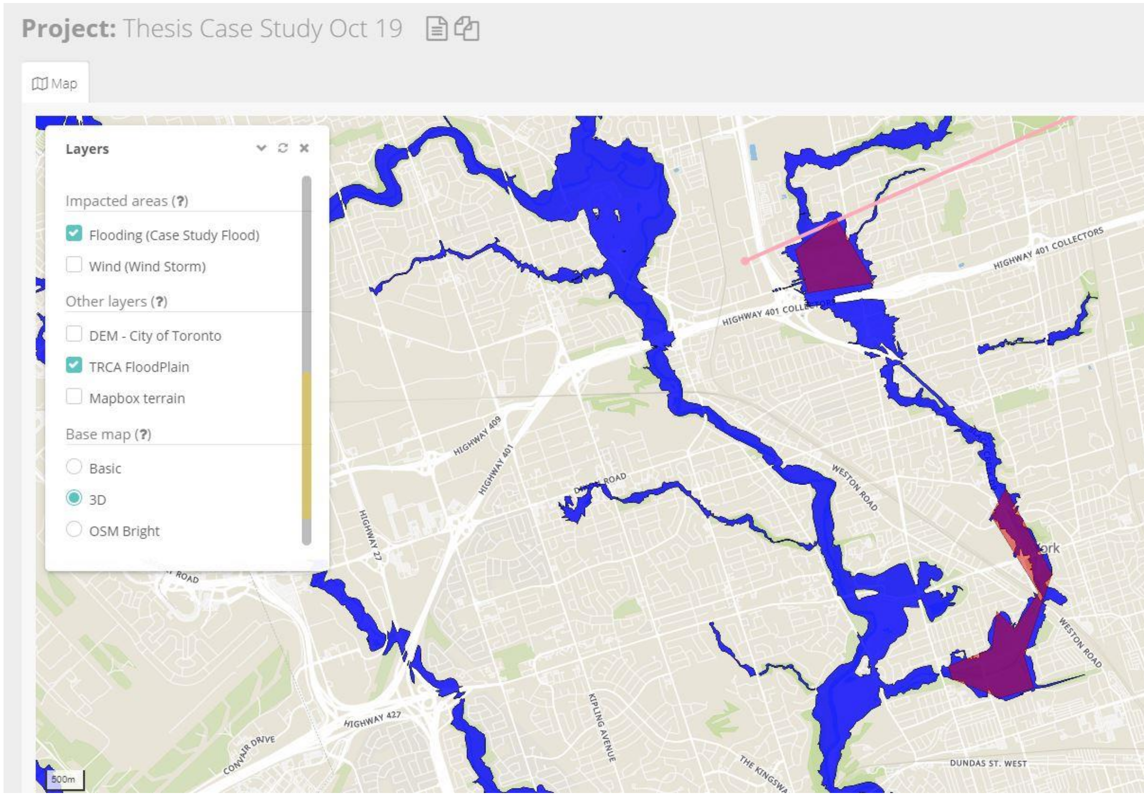

Figure 31 Capturing realistic flood hazard areas for a simulation

Hypothetical effective flood depth magnitudes for each time step were the same as those provided in Figure 14. For both flooded areas, the same flood depth magnitude over time was applied.

Hypothetical wind storms were also simulated in two spatial areas as shown in Figure 32. The wind direction was from the southwest towards the northeast and was characterized by two wind bands (with different wind speeds).

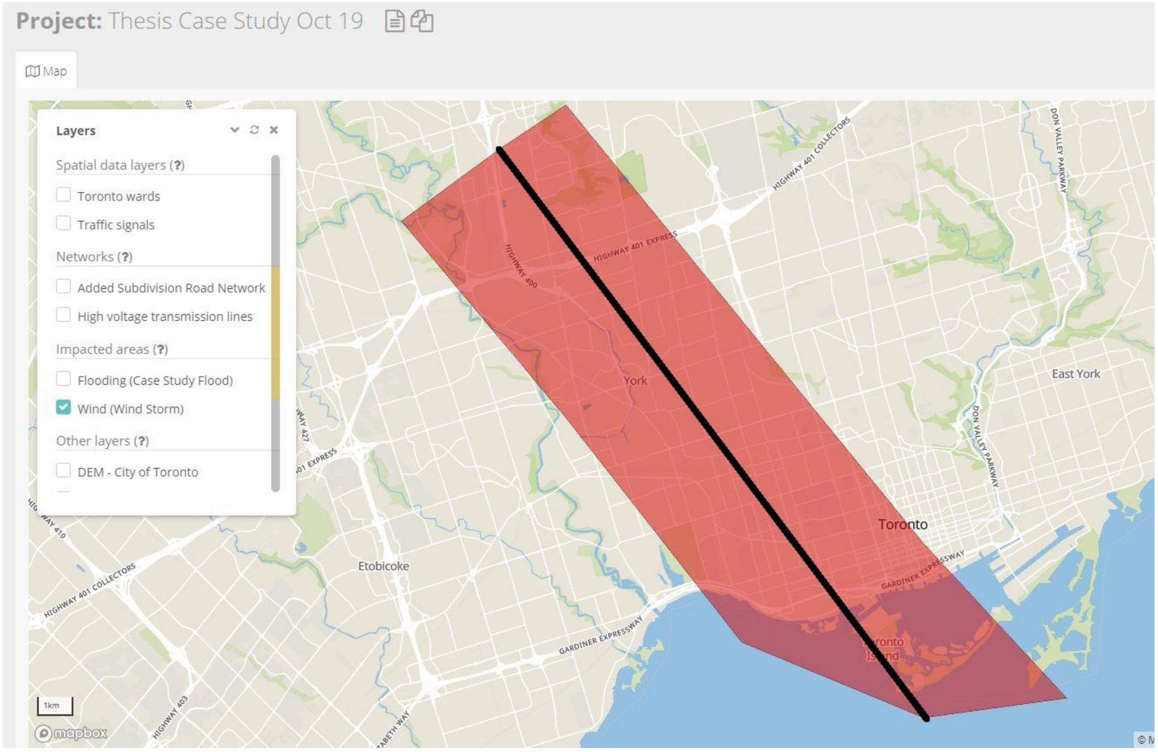

Figure 32 Case study wind storm areas

Hypothetical wind speeds over the duration of the simulation are provided in Figure 33. The second wind band was assumed to have the same magnitude as the first wind band but with a one-hour time delay.

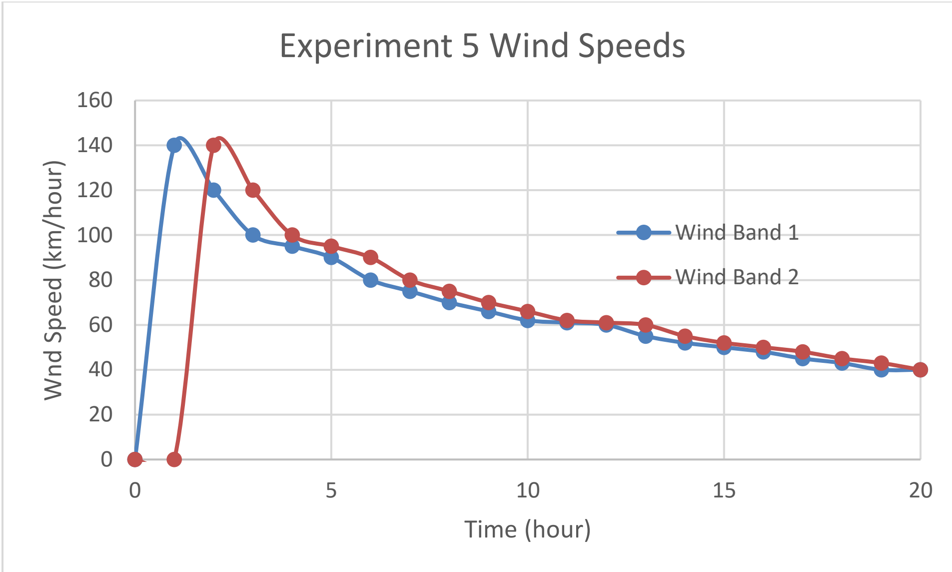

Figure 33 Case study wind speeds over time

Quantitative deterministic and probabilistic relationships were used to describe the impacts of each hazard on each infrastructure system considered. Table 7 summarizes the hazard impact relationships in this case study.

Table 7 Hazard impact relationships applied to the City of Toronto case study

Hazard	Infrastructure Impacted	Relationship Input
Flood	Roads	Equation
Flood	Buildings	Stage-damage curve
Wind	High-voltage transmission towers	Fragility curves

The relationship between flood depth and traffic speed was the same as that described in Section 4.2.4.

Similar to Experiment 1, it was assumed that all buildings are residential and have the same build. The stage-damage curve relationship displayed in Figure 22 was also used in this experiment. Wind storms applied the same fragility curves as Figure 27 to determine the impact to high-voltage transmission towers.

Two interdependent relationships were captured in this experiment. First, when a node in the transmission network was no longer functional, it was assumed to directly affect the surrounding electrical service area. As a result, traffic lights within this service area were assumed to be non-functional. The Thiessen Polygon method was used to create the electrical service areas from the high-voltage transmission network.

Second, non-working traffic lights affect the roads, and it was assumed that this decreases traffic speed by 3km/hr. This value is based on a 2009 study by the Greater London Authority (2009) on the economic impact of traffic lights. They found that traffic signals affect vehicular speeds differently depending on factors such as road type, timing, and background traffic. The highest recorded average speed delay for a non-roundabout area was 2 mph (rounded to 3km/hr), which was used in this case study.

These interdependent relationships illustrate cascading failure effects.

4.2.5.2 Experiment 5 Outputs and Adaptation Measures

The outputs of the simulation include system performance over time and infrastructure resilience values for each infrastructure system (i.e., roads, traffic signals, high-voltage network, and buildings). The system performance for various infrastructure systems is shown in Figure 34 through Figure 37.

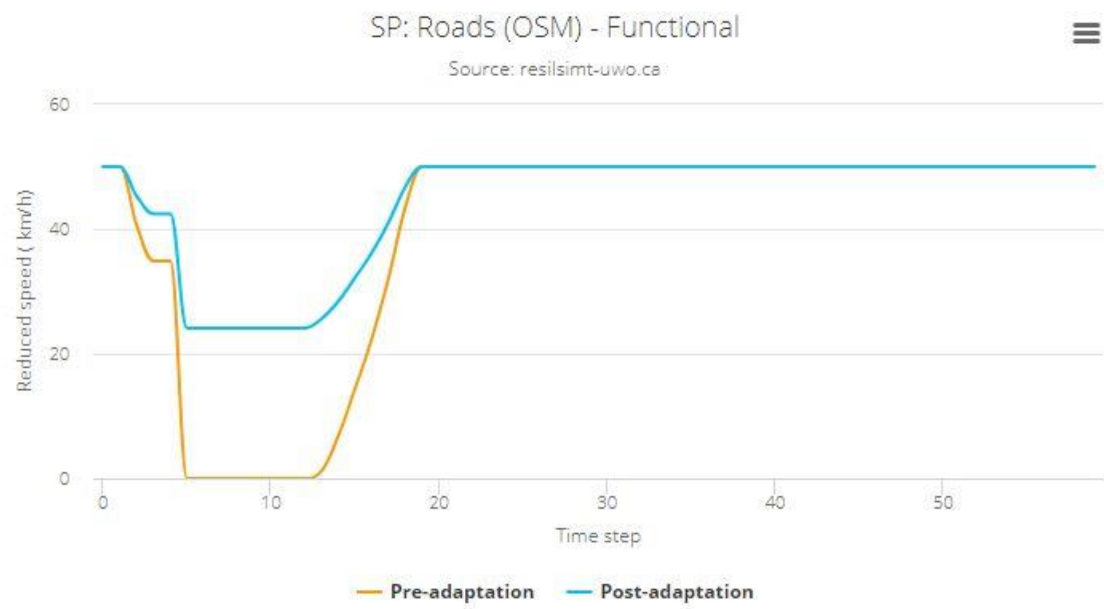

Figure 34 Case study average road speed performance over time

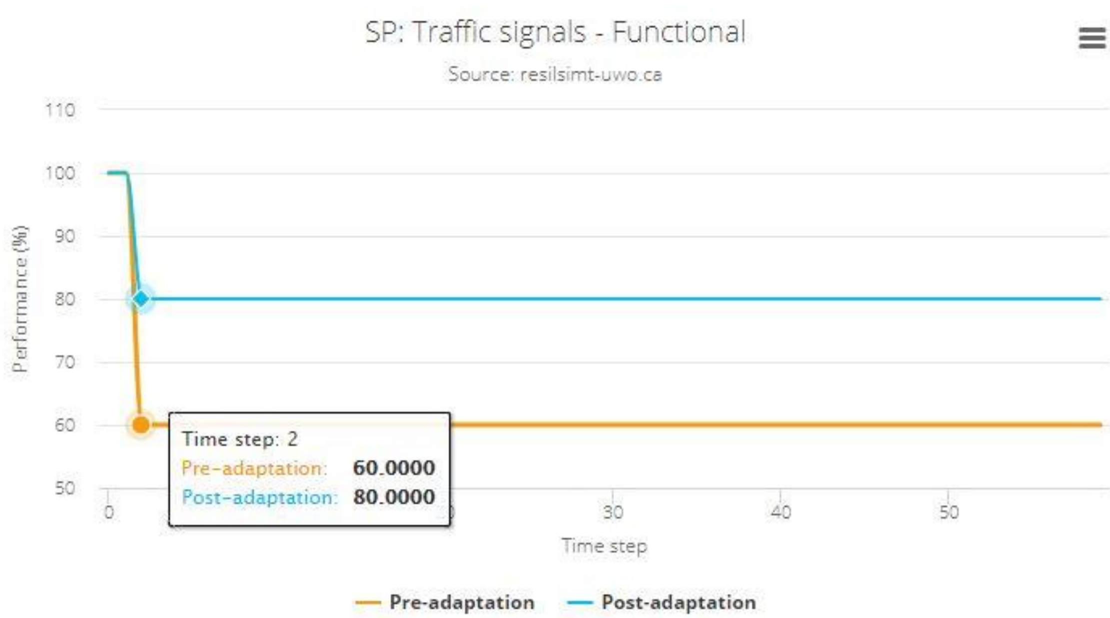

Figure 35 Case study traffic signal performance over time

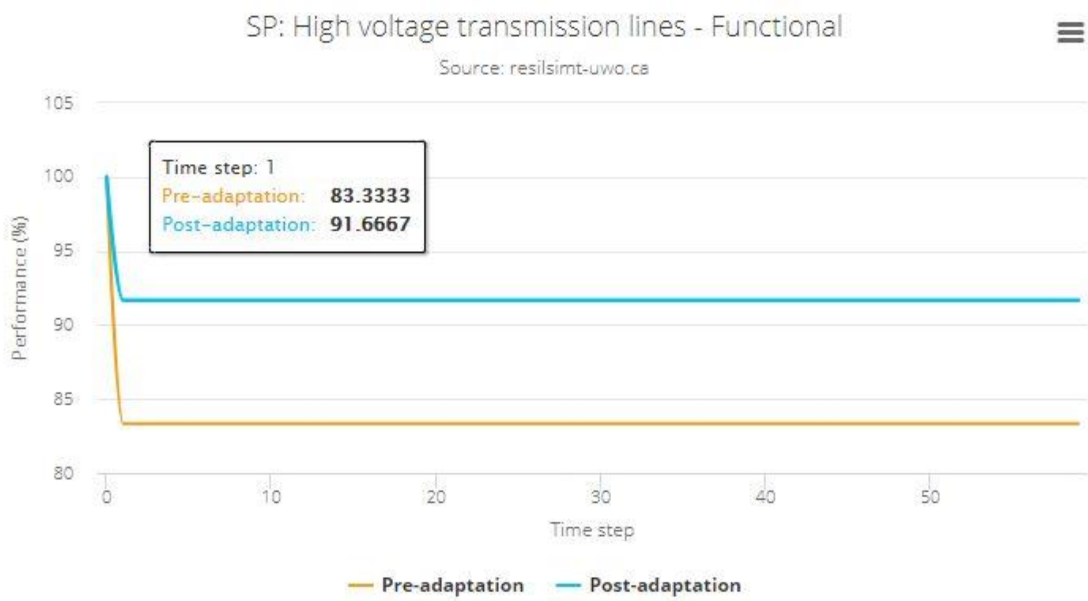

Figure 36 Case study high-voltage transmission lines performance over time

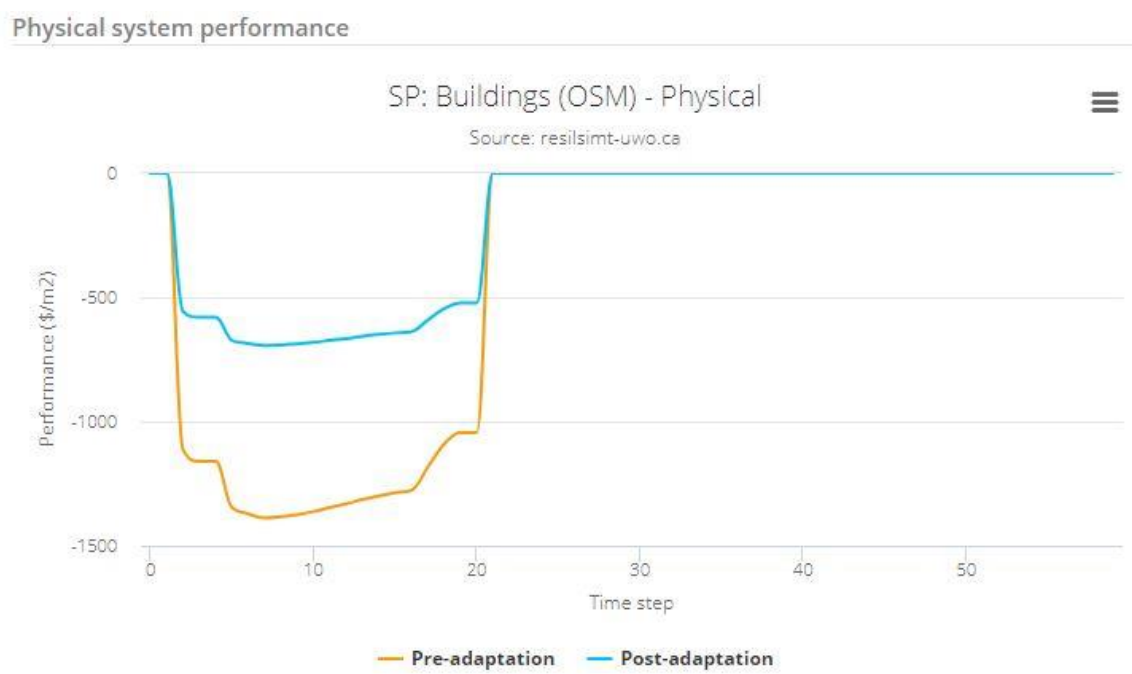

Figure 37 Case study building performance over time

The orange lines represent system performance without any adaptation options. The blue lines represent functionality with a mixture of adaptation options. As previously presented in Section 3.4, adaptation options can be classified as proactive or reactive. ResilSIMt follows this classification scheme. Adaptation measures are user-generated, meaning that the user can control which infrastructure a measure affects. Additionally, the user controls the magnitude of an adaptation's effect through the use of sliders in the tool. Further information on ResilSIMt's implementation of adaptation options, including how input magnitudes are converted to system performance improvement, can be found in Appendix A2.4 and Schardong et al. (2018).

Proactive adaptation measures were implemented in the study. These include permeable surfaces, percentage of houses with backwater valves, transmission tower network hardening, and backup power for traffic signals. The adaptation options listed in Figure 38 affect the road network, buildings, high-voltage transmission network, and traffic signal infrastructure, respectively, in this case study. Each adaptation option was implemented at 50%, where the option of a maximum 100% adaptation magnitude was capable of fully mitigating an infrastructure's performance loss.

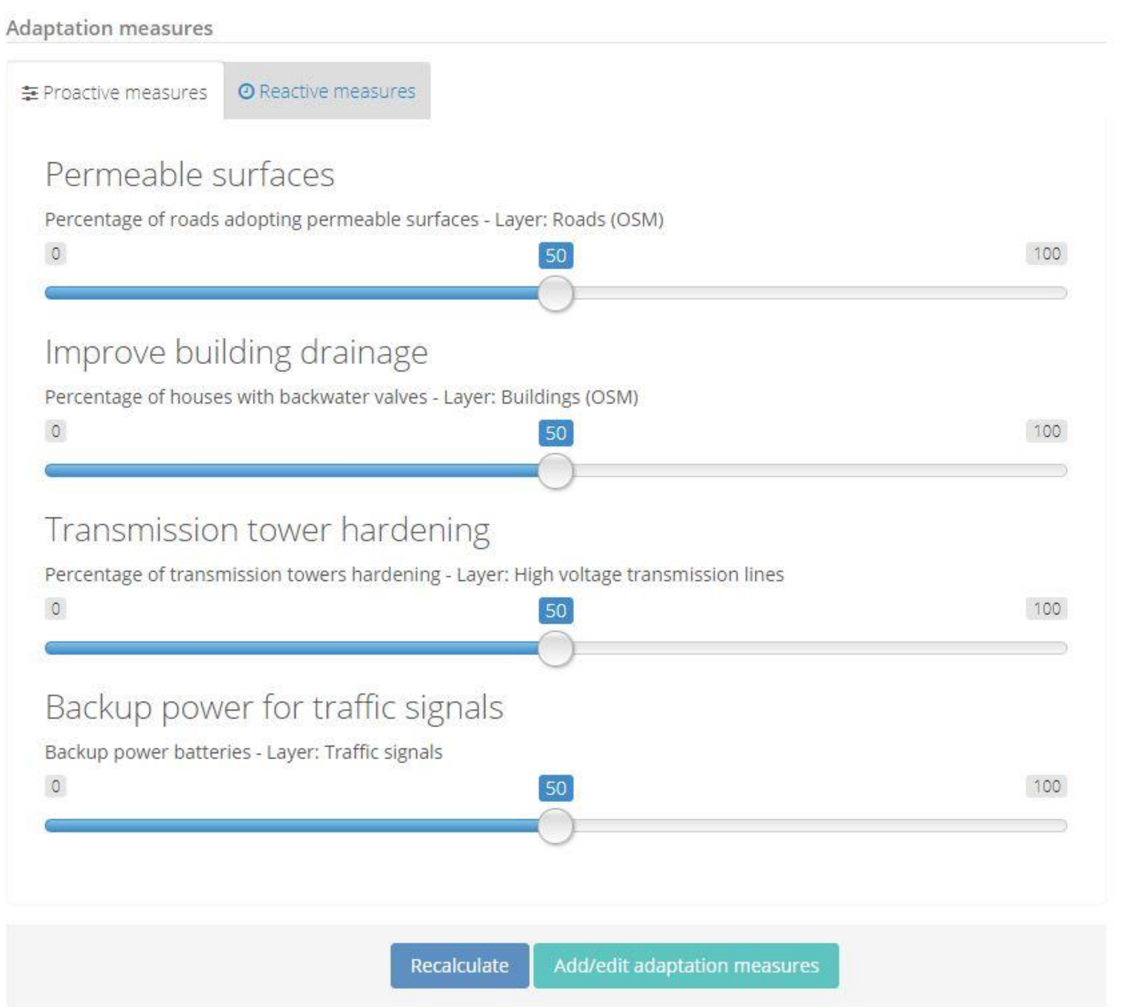

Figure 38 Experiment 5 adaptation options

It is noteworthy that the tool can capture temporary and permanent damage. Temporary damage relates to the idea that once a hazard recedes, the system performance of infrastructure can return to normal. Road infrastructure and building performance nicely illustrates this point, as traffic delays caused by flooding return to zero after the floodwaters recede. In contrast, a network of high-voltage transmission lines presents a nice example of permanent damage. If the wind is strong enough to cause a transmission tower to fall, the damage does not disappear after the hazard unless resources are allocated to fix the issue. The tool allows the user the flexibility to indicate whether the damage is temporary or permanent. The experiment also nicely illustrates that as traffic signals depend on electricity, their permanent absence can have lasting effects on infrastructure.

The infrastructure resilience for each infrastructure system shown above is presented in Figure 39 to Figure 42, respectively.

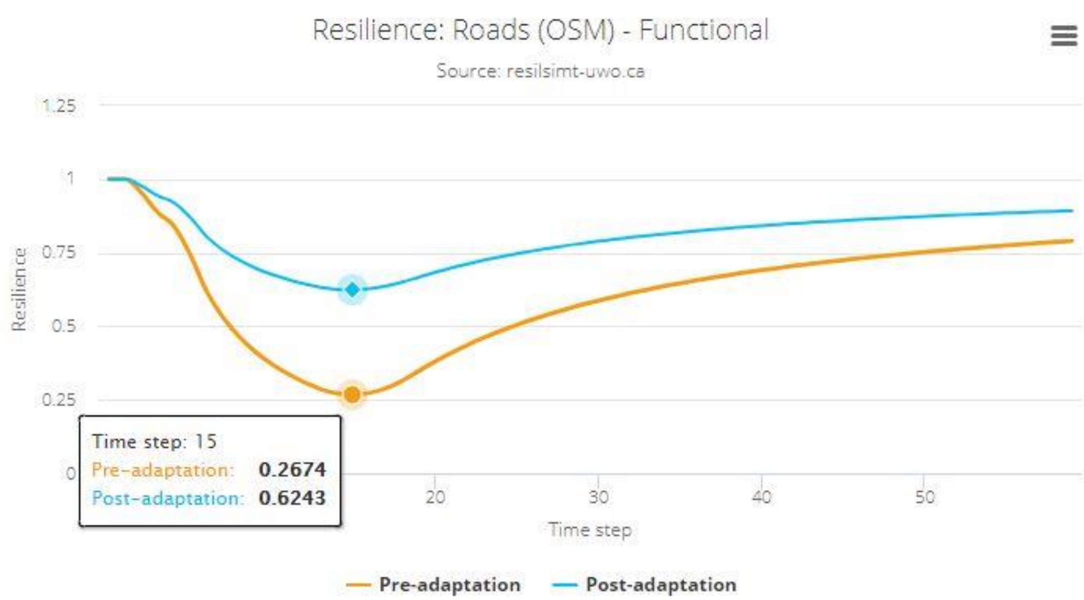

Figure 39 Case study road network resilience

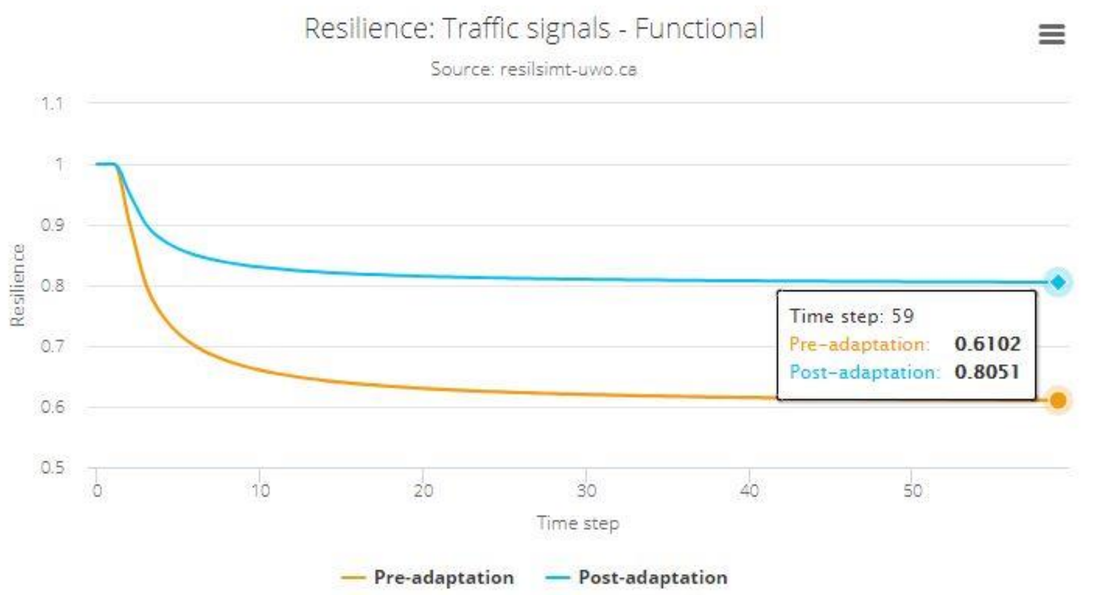

Figure 40 Case study traffic light resilience

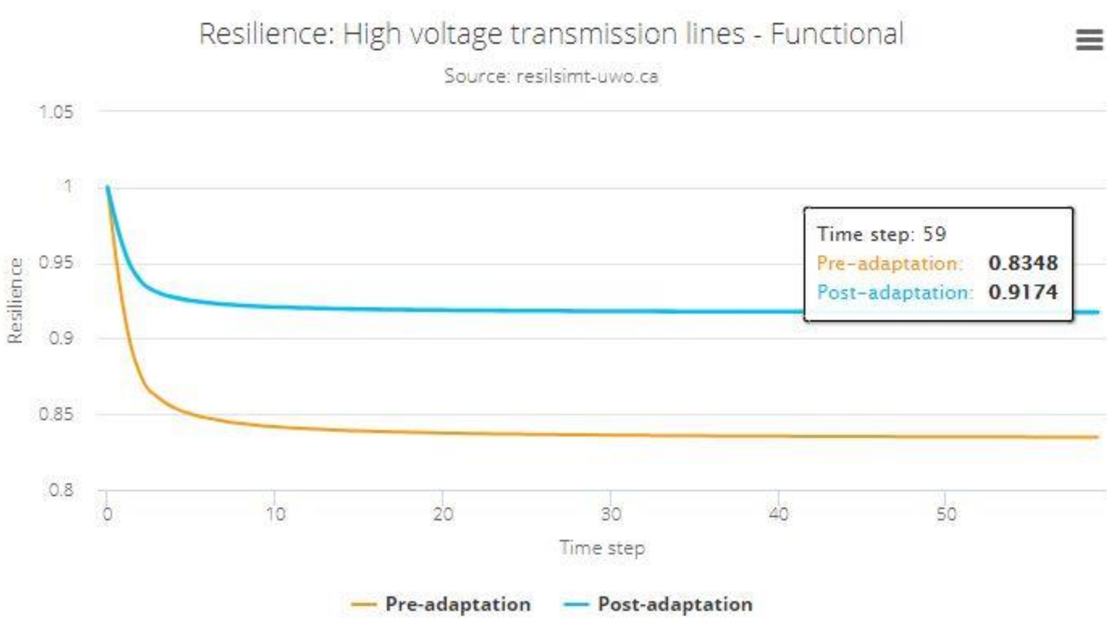

Figure 41 Case study high-voltage network resilience

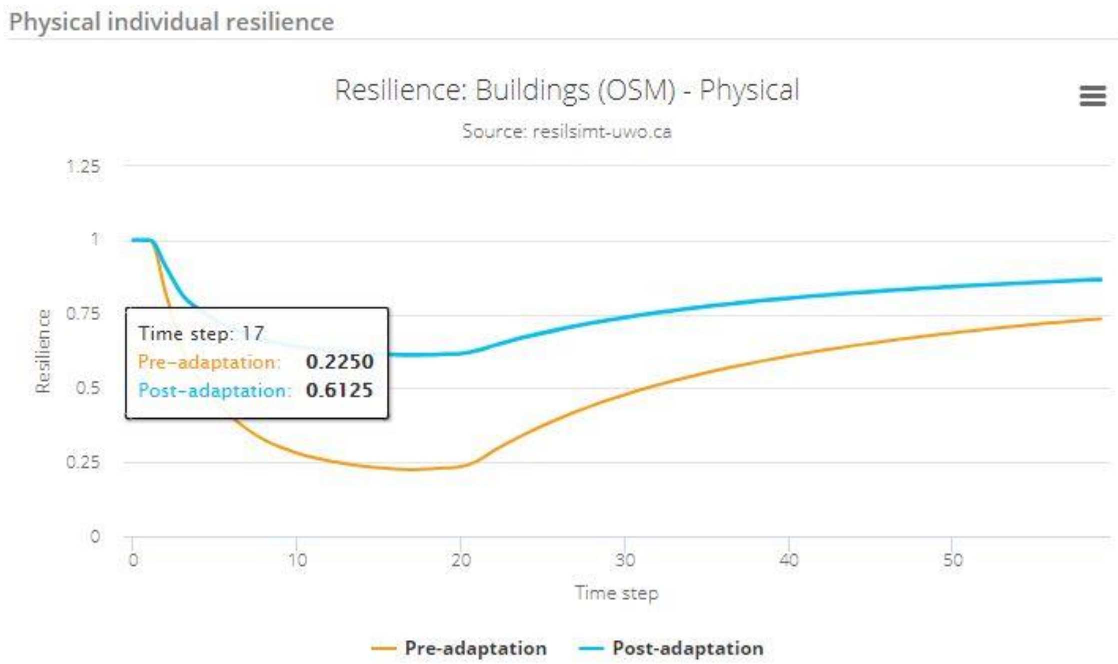

Figure 42 Case study building infrastructure layer resilience

When all of the infrastructure resilience values are combined, an overall system-of-systems resilience curve can be developed. The resultant curve is shown in Figure 43.

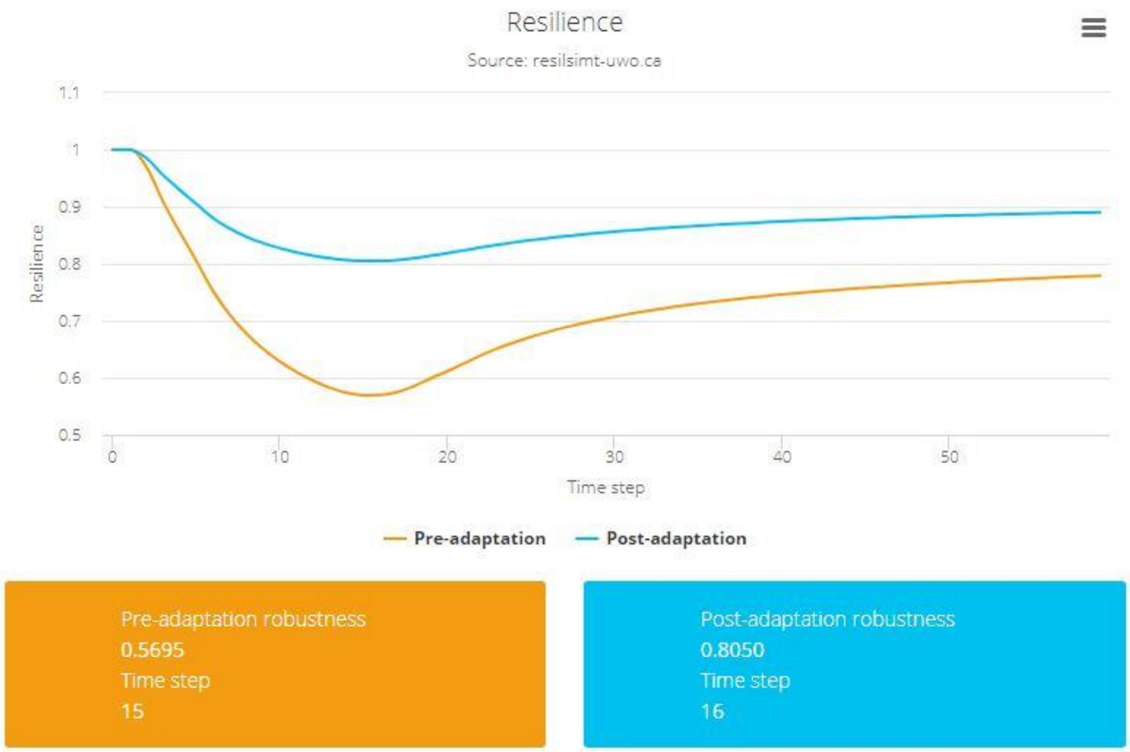

Figure 43 Case study system-of-systems resilience curve

Similar to the other curves, the tool displays an orange line for resilience values without adaptation measures and a blue line for those with adaptation measures. In both cases, resilience does not return to the pre-hazard state. The system-of-systems robustness value for each scenario is also provided.

The ability to connect infrastructure through interdependencies proves useful in modelling complex phenomena. It adds an additional layer of nuance to a system's behaviour. ResilSIMt provides infrastructure managers a means to input and compare different adaptation measures, along with their effects on system performance and overall system-of-systems resilience. Finally, the web-based tool further supports decision support by providing the option of easily downloading system performance and resilience values for individual infrastructure systems.

Section 5

5 Conclusions

Natural hazards are becoming a greater threat to municipal infrastructure. This is arguably due to three primary changes, namely increased urbanization leading to higher vulnerability, a changing climate, and aging infrastructure. From a societal viewpoint, it is necessary to buffer against natural hazards and to recover efficiently when disruptions do occur. This thesis explores the use of resilience in infrastructure management. Quantifiable resilience measures for infrastructure decision making, however, are currently lacking.

This thesis extends Kong and Simonovic's (2016) approach to quantifying resilience as a criterion for adaptation of municipal infrastructure to changing conditions. The current approach is based on the complex network theory and is applied to a City of Toronto case study involving some of its key infrastructure systems. The methodology treats key infrastructure as networks and layers, with each data type having its own indicator of system performance. The networks and layers are interconnected with user-defined interdependency relationships, such that the level of functionality of one system component can affect another system component. Hazards are introduced to simulate the decrease in functionality of systems or loss of system performance. The remaining system performance over time is defined as resilience and used as a municipal infrastructure decision-making criterion.

The main contributions of the thesis include: (i) the introduction of spatial impact areas as a data type that can hold system performance values; (ii) use of variable impact values for network components and spatial-area system performance; (iii) subdivision infrastructure (roads) development mechanism for application with new networks; and (iv) a network expansion mechanism. The main contributions to the methodology are tested using the ResilSIMt web-based tool in a case study set in the City of Toronto.

The first two experiments demonstrated the improved accuracy that can be obtained by incorporating spatial impact areas as a data format and allowing infrastructure components to have partial functionality. In Experiment 1, spatial impact areas were able to represent buildings' footprint more accurately compared to nodes; thus, this could better reveal when a flood impact occurred. In Experiment 2, road components were shown to have partial functionality during a flood hazard.

The third and fourth experiments demonstrated the incorporation of infrastructure growth on overall system resilience. In Experiment 3, a comparison of three different growth scenarios revealed that the placement of new road network infrastructure in a hazard-vulnerable area can lead to lower resilience than a no development option. The third scenario showed that the effects can be partially mitigated if permeable road pavements are applied as it can better handle floodwaters. The fourth experiment conveyed that resilience would not change if the existing network and its expanded components were subjected to a wind storm hazard.

Finally, the fifth experiment showed the potential usefulness of the ResilSIMt web tool for infrastructure managers. A system-of-systems was formed from four infrastructure networks or layers. Along with individual hazard impacts, some had interdependencies with other infrastructure networks. The multi-hazards of wind and flooding illustrated the cascading failure that can occur within the system-of-systems. Proactive adaptation options provided a means to showcase the enhancement of resilience that can occur if the web tool is implemented. ResilSIMt further supports infrastructure management by enabling users to download tabulated system performance and resilience values that can be used for decision making.

Section 6

6 Methodology Limitations and Future Research Directions

The proposed methodology does have limitations, beginning with the heavy data requirements. The power of the methodology relies on the interdependencies between various system components, allowing it to simulate complex phenomenon of cascading failures. As with all simulations, the results are only as good as the input data. Restrictions on the data input exist, such as the data must be in a network or layer-type form of nodes, edges, and polygon areas in order to simulate resilience. In the case study, the acquisition of this data posed a considerable challenge. With each data format and type of infrastructure, an appropriate system performance metric for each impact type is needed. The impact relationships and interdependencies play a critical role in evaluating system performance and the resulting resilience. With the case study that was presented earlier, it does not have the level of rigor that is typically expected for practical infrastructure decision making as the data requirements have not been met.

The impact relationships are currently dependent on a single characteristic of a hazard. In reality, other factors play a role. For flooding, this might be the velocity of the floodwaters. For wind damage, the surrounding objects, the environment, and debris play important roles in the calculation of damage. Although the methodology is flexible enough to consider another characteristic of the hazard as an indicator, the resulting system component performance would be calculated as the sum of independent losses. Complex phenomena demonstrate it is possible for the whole to be not merely the sum of its parts. In the context of this discussion, the methodology is limited in the sense that different hazard characteristics cannot be combined in such a manner that system performance depends on both hazard characteristics simultaneously.

Similar to the above hazard impact relationship, the same holds true for interdependencies. One of the limitations can be found in the case study of road speed and how it depends on both flood levels and traffic lights. Currently, the loss of performance, in terms of decreased road speed, is calculated individually and added together to determine the total impact. However, one could argue that if a vehicle has slowed down as a result of traffic light outage, the speed reduction from ponding water is already partially considered, resulting in a possible overestimation. In other cases, underestimation is a possibility.

While much work has been completed in this thesis in regard to increasing the capabilities of the resilience methodology for municipal infrastructure decision making, there are many different directions that could further increase these capabilities. These directions can be grouped into adaptation, cost considerations, optimization, and capability enhancement.

Adaptation is an essential aspect of resilience quantification. As identified earlier in the discussion, one of the limitations of this study was the lack of a clearly defined mathematical formulation for adaptation. Given a proactive and reactive adaptation measure classification, proactive measures can be incorporated by changing the impact relationships. However, reactive adaptation measures need to be developed further in future work.

Given that the quantitative representations of resilience can be further improved, it may be helpful to link the resilience metric to other infrastructure decision-making criteria. Cost is one example. It may be desirable to know how much resilience can be gained through applying various adaptation measures to a specific scenario and the costs required to implement these measures. Another example is incorporating a cost estimation to increase resilience values for a given scenario when hazard disruptions occur. The latter example is helpful for incorporating resilience into traditional decision-making methods, namely cost-benefit analysis.

The resilience methodology presented provides only a simulation of a specific scenario given the networks, layers, interdependencies, impact relationships, and hazards. It can be beneficial to adapt the resilience quantification into an optimization formulation, where one attempts to maximize the user’s objectives in addition to resilience, thus explicitly serving as a decision-making support tool.

The following minor suggestions are various ways that the capabilities of the methodology and its implementation can be improved. The first suggestion is relaxing the constraints on variables allowed for impact relationships. Currently, the state of a network component is dependent on other network components that are defined, hazard intensity, and time. However, in reality, the functionality or state of a network component can be influenced by other key variables that are not captured. One example is the velocity of water flow in flood scenarios, which can cause erosion damage.

References

100 Resilient Cities. (2018). About Us. Retrieved May 23, 2018, from https://www.100resilientcities.org/about-us/

Agostino, G. D., & Scala, A. (Eds.). (2014). *Networks of Networks : The Last Frontier of Complexity*. Springer Complexity. https://doi.org/10.1007/978-3-319-03518-5

Ahmad, I. (2015). *The State of Ontario's Roads and Bridges: An Analysis of 93 Municipalities*. Retrieved from https://www.amo.on.ca/AMO-PDFs/Gas_Tax/Roads-and-Bridges/Roads-and-Bridges-Study-March-2015.aspx

Alderson, D. L., Brown, G. G., & Carlyle, W. M. (2014). Assessing and Improving Operational Resilience of Critical Infrastructures and Other Systems. *Informs*. https://doi.org/http://dx.doi.org/10.1287/educ.2014.0131

Amaral, L. A. N., & Ottino, J. M. (2004). Complex networks. *The European Physical Journal B*, *38*(2), 147–162. https://doi.org/10.1140/epjb/e2004-00110-5

American Society of Civil Engineers. (2017). *2017 Report Card for american infrastructure: A Comprehensive Assessment of America's Infrastructure*. Retrieved from https://www.infrastructurereportcard.org/wp-content/uploads/2016/10/2017-Infrastructure-Report-Card.pdf

ASCE. (2013). Policy Statement 518 - Unified Definitions for Critical Infrastructure Resilience. Retrieved September 21, 2018, from https://www.asce.org/issues-and-advocacy/public-policy/policy-statement-518---unified-definitions-for-critical-infrastructure-resilience/

Ayyub, B. M. (2015). Practical Resilience Metrics for Planning, Design, and Decision Making. *ASCE-ASME Journal of Risk and Uncertainty in Engineering Systems, Part A: Civil Engineering*, *1*(3), 11. https://doi.org/10.1061/AJRUA6.0000826

Baker, B., Sklokin, I., Coad, L., & Crawford, T. (2011). *Canada's Electricity Infrastructure: Building a Case for Investment*. *The Conference Board of Canada*. Retrieved from http://www.scribd.com/doc/52488546/Canada-s-Electricity-Infrastructure-Building-a-Case-for-Investement

Bhatia, U., Kumar, D., Kodra, E., & Ganguly, A. R. (2015). Network science based quantification of resilience demonstrated on the indian railways network. *PLoS ONE*, *10*(11), 1–18. https://doi.org/10.1371/journal.pone.0141890

Boyle, J., Cunningham, M., & Dekens, J. (2013). *Climate Change Adaptation and Canadian Infrastructure: A review of the literature*. Retrieved from http://www.iisd.org/pdf/2013/adaptation_can_infrastructure.pdf

Brown, S., & Dawson, R. (2016). Building network-level resilience to resource disruption from flooding: Case studies from the Shetland Islands and Hurricane Sandy. In *3rd European Conference on Flood Risk Management (FLOODrisk 2016)* (Vol. 7, p. 8). EDP Sciences. https://doi.org/10.1051/e3sconf/201 60704008

Bruneau, M., Chang, S. E., Ronald, T., Lee, G. C., Rourke, T. D. O., Reinhorn, A. M., … Winterfeldt, D. Von. (2003). A Framework to Quantitatively Assess and Enhance the Seismic Resilience of Communities. *Earthquake Spectra*, *19*(4), 733–752. https://doi.org/10.1193/1.1623497

Canadian Construction Association et al. (2016). *Canadian Infrastructure Report Card: Informing the Future*. Retrieved from http://canadianinfrastructure.ca/downloads/Canadian_Infrastructure_Report_2016.p

df
Chief Corporate Officer. (2016). *Resilient City - Preparing for a Changing Climate*. Toronto. Retrieved from https://www.toronto.ca/legdocs/mmis/2016/pe/bgrd/backgroundfile-98049.pdf
Chin, D. A. (2006). *Water Resources Engineering* (2nd ed.). Pearson Education Inc.
City of Stratford. (2016). *Infrastructure Standards and Specifications*. Stratford. Retrieved from https://www.stratfordcanada.ca/en/insidecityhall/resources/InfrastructureDevelopmentServices/Building/Stratford-Infrastructure-Manual-Mar-2016.pdf
City of Toronto. (2013). *City of Toronto congestion management plan 2014-2018*. Retrieved from https://www.toronto.ca/wp-content/uploads/2017/08/963e-congetion-managment-plan-2014-2018.pdf
City of Toronto. (2016). *Resilient Toronto Agenda Setting Workshop Summary*. Retrieved from https://www.toronto.ca/wp-content/uploads/2017/11/912e-ResilientTO-Agenda-Setting-Workshop-Summary-December-2016.pdf
City of Toronto. (2018a). Open Data Catalogue. Retrieved December 12, 2018, from https://www.toronto.ca/city-government/data-research-maps/open-data/open-data-catalogue/
City of Toronto. (2018b). Toronto at a Glance. Retrieved August 2, 2018, from https://www.toronto.ca/city-government/data-research-maps/toronto-at-a-glance/
City of Toronto Transportation Services. (2017). *Road Engineering Design Guidelines: Lane Widths*. Retrieved from https://www1.toronto.ca/City Of Toronto/Engineering and Construction Services/Standards and Specifications/Files/pdf/Road Design Guidelines/Lane_Widths_Guideline_Version_2.0_Jun2017.pdf
City of Toronto Transportation Services. (2018). Transportation Services statistics - facts - number of roads - bike lanes - bus shelters. Retrieved August 13, 2018, from https://www.toronto.ca/311/knowledgebase/kb/docs/articles/transportation-services/transportation-infrastructure-management/operational-planning-and-policy/operational-planning-and-policy/transportation-services-statistics-facts-number-of-roads-bike-lanes-
CSA Group. (2012). *National Survey of Canada's Infrastructure Engineers about Climate Change*. Retrieved from https://www.egbc.ca/getmedia/4e003686-63dd-41c2-a5d6-27df561b76e4/Engineers-Canada-National-Survey-of-Canada-Infrastructure-Engineers-about-Climate-Change.pdf.aspx
Cutter, S. L., Barnes, L., Berry, M., Burton, C., Evans, E., Tate, E., & Webb, J. (2008). A place-based model for understanding community resilience to natural disasters. *Global Environmental Change*, *18*(4), 598–606. https://doi.org/10.1016/j.gloenvcha.2008.07.013
DMTI Spatial Inc. (2017). Transformer Station Point - 2017. Retrieved December 12, 2018, from http://geo1.scholarsportal.info
Federal Emergency Management Agency. (2013). *Multi-hazard Loss Estimation Methdology Hurricane - Hazus - MH 2.1 Technical Manual*. Washington. Retrieved from https://www.fema.gov/media-library-data/20130726-1820-25045-9850/hzmh2_1_hr_tm.pdf
Flyvbjerg, B. (2009). Survival of the unfittest: Why the worst infrastructure gets built-and what we can do about it. *Oxford Review of Economic Policy*, *25*(3), 344–367.

https://doi.org/10.1093/oxrep/grp024
Francis, R., & Bekera, B. (2014). A metric and frameworks for resilience analysis of engineered and infrastructure systems. *Reliability Engineering and System Safety*, *121*, 90–103. https://doi.org/10.1016/j.ress.2013.07.004
Friedman, Y., & Lee, T. (2017). *Cities Taking Action How the 100RC Network is Building Urban Resilience*. Retrieved from http://100resilientcities.org/wp-content/uploads/2017/07/WEB_170720_Summit-report_100rc-1.pdf
Fu, G., Wilkinson, S., & Dawson, R. J. (2016). A Spatial Network Model for Civil Infrastructure System Development. *Computer-Aided Civil and Infrastructure Engineering*, *31*(9), 661–680. https://doi.org/10.1111/mice.12204
Fu, G., Wilkinson, S., Dawson, R. J., Fowler, H. J., Kilsby, C., & Panteli, M. (2017). Integrated Approach to Assess the Resilience of Future Electricity Infrastructure Networks to Climate Hazards. *IEEE SYSTEMS JOURNAL*, *12*(4), 1–12. https://doi.org/10.1109/JSYST.2017.2700791
Gironimo, L. Di. (2017). *2018 Toronto Water Budget*. Retrieved from https://www.toronto.ca/legdocs/mmis/2017/bu/bgrd/backgroundfile-108694.pdf
Graham, S., & Marvin, S. (2001). *Splintering urbanism: networked infrastructures, technological mobilities and the urban condition*. New York: Routledge. https://doi.org/10.4324/9780203452202
Greater London Authority. (2009). *Economic impact of traffic signals*. London. Retrieved from https://www.london.gov.uk/sites/default/files/gla_migrate_files_destination/traffic-signals.pdf
Harvey, R., de Lange, M., McBean, E., Trenouth, W., Singh, A., & James, P. (2017). Asset condition assessment of municipal drinking water, wastewater and stormwater systems–Challenges and directions forward. *Canadian Water Resources Journal*, *42*(2), 138–148. https://doi.org/10.1080/07011784.2016.1224684
Henry, D., & Ramirez-marquez, J. E. (2012). Generic metrics and quantitative approaches for system resilience as a function of time. *Reliability Engineering and System Safety*, *99*, 114–122. https://doi.org/10.1016/j.ress.2011.09.002
Heracleous, C., Kolios, P., Panayiotou, C. G., Ellinas, G., & Polycarpou, M. (2017). Hybrid systems modeling for critical infrastructures interdependency. *Reliability Engineering and System Safety*, *165*(August 2016), 89–101. https://doi.org/10.1016/j.ress.2017.03.028
Holling, C. S. (1973). Resilience and stability of ecological systems. *Annual Review of Ecology and Systematics*, *4*, 1–23. https://doi.org/10.1146/annurev.es.04.110173.000245
Homeland Security Council. (2007). *National Strategy for Homeland Security*. Washington. Retrieved from https://www.dhs.gov/xlibrary/assets/nat_strat_homelandsecurity_2007.pdf
Hosseini, S., Barker, K., & Ramirez-marquez, J. E. (2016). A review of definitions and measures of system resilience. *Reliability Engineering and System Safety*, *145*, 47–61. https://doi.org/10.1016/j.ress.2015.08.006
Ip, W. H., & Wang, D. (2011). Resilience and friability of transportation networks: Evaluation, analysis and optimization. *IEEE Systems Journal*, *5*(2), 189–198. https://doi.org/10.1109/JSYST.2010.2096670

Irwin, S., Schardong, A., Simonovic, S. P., & Nirupama, N. (2016). ResilSIM — A Decision Support Tool for Estimating Resilience of Urban Systems. *Water*, *8*(9). https://doi.org/10.3390/w8090377

Irwin, S., Simonovic, S. P., & Nirupama, N. (2016). *Introduction to ResilSIM : A Decision Support Tool for Estimating Disaster Resilience to Hydro- Meteorological Events*. London. Retrieved from https://www.eng.uwo.ca/research/iclr/fids/publications/products/94.pdf

Kelman, L., & Soberman, R. M. (2010). *"Getting it Right" Lessons from the St. Clair Streetcar for the Implementation of Transit City*. Toronto. Retrieved from https://www.ttc.ca/About_the_TTC/Commission_reports_and_information/Commission_meetings/2010/Jan_20_2010/Reports/Transit_City_Impleme.pdf

Kong, J., & Simonovic, S. (2016). *Interdependent Infrastructure Network Resilience Model with Joint Restoration Strategy*. London. Retrieved from https://www.eng.uwo.ca/research/iclr/fids/publications/products/96.pdf

Linkov, I., & Palma-Oliveira, J. (2017). *Resilience and Risk Methods and Application in Environment, Cyber and Social Domains*. (I. Linkov & J. Palma-Oliveira, Eds.) (1st ed.). Dordrecht: Springer. https://doi.org/10.1007/978-94-024-1123-2

Little, R. G. (2010). Managing the Risk of Cascading Failure in Complex Urban Infrastructures. In S. Graham (Ed.), *Disrupted Cities When Infrastructures Fails* (1st ed., pp. 27–39). Routledge.

Mcaslan, A. (2010). *The Concept of Resilience Understanding its Origins, Meaning and Utility*. Retrieved from http://www.flinders.edu.au/centres-files/TRI/pdfs/resilience origins and utility.pdf

Mccoll, L., Palin, E. J., Thornton, H. E., Sexton, D. M. H., Betts, R., & Mylne, K. (2012). Assessing the potential impact of climate change on the UK's electricity network. *Climate Change*, *115*(3–4), 821–835. https://doi.org/10.1007/s10584-012-0469-6

MCEER. (2006). MCEER's Resilience Framework: Resilience Concept Drives Development of New Knowledge, Tools & Technologies. Retrieved September 21, 2018, from http://mceer.buffalo.edu/research/resilience/Resilience_10-24-06.pdf

Merz, B., Elmer, F., & Thieken, A. H. (2009). Significance of "high probability/low damage" versus "low probability/high damage" flood events. *Natural Hazards and Earth System Sciences*, *9*(3), 1033–1046. https://doi.org/https://doi.org/10.5194/nhess-9-1033-2009

Mostafavi, A. (2017). A System-of-Systems Approach for Integrated Resilience Assessment in Highway Transportation Infrastructure Investment. *Infrastructures*, *2*(4), 22. https://doi.org/10.3390/infrastructures2040022

National Infrastructure Advisory Council. (2009). *Critical Infrastructure Resilience Final Report and Recommendations*. Retrieved from https://www.dhs.gov/sites/default/files/publications/niac-critical-infrastructure-resilience-final-report-09-08-09-508.pdf

Natural Resources Canada. (2017). *Canadian Guidelines and Database of Flood Vulnerability Functions*. Retrieved from http://hazuscanada.ca/sites/all/files/nrc-canadianguidelines-final_2017-03-30_draft.pdf

Ontario Ministry of Environment. (2003). *Stormwater Management Planning and Design Manual*. Toronto: Ontario Ministry of Environment. Retrieved from http://www.ontla.on.ca/library/repository/mon/5000/10302166.pdf

Ontario Power Authority, IESO, Hydro One, & Toronto Hydro. (2015). *Central Toronto Integrated Regional Resource Plan Discussion Workbook*. Retrieved from https://www.torontohydro.com/sites/electricsystem/GridInvestment/Documents/IRRP Narrative_August 25_HIGHRESr.pdf
Ontario Sewer & Watermain Construction Association. (2018). *The State of Ontario's Water and Wastewater Infrastructure*. Retrieved from http://www.oswca.org/uploads/2-the-state-of-ontario-s-water-and-wastewater-infrastructure_march29-min_001.pdf
OpenStreetMap Wiki contributors. (2014). Main Page. Retrieved December 12, 2018, from https://wiki.openstreetmap.org/w/index.php?title=Main_Page&oldid=1060762
Panteli, M., Pickering, C., Wilkinson, S., & Dawson, R. (2017). Power System Resilience to Extreme Weather: Fragility Modeling, Probabilistic Impact Assessment, and Adaptation Measures. *IEEE Transactions on Power Systems*, *32*(5), 3747–3757. https://doi.org/10.1109/TPWRS.2016.2641463
Park, J., Seager, T. P., Rao, P. S. C., Convertino, M., & Linkov, I. (2013). Integrating Risk and Resilience Approaches to Catastrophe Management in Engineering Systems. *Risk Analysis*, *33*(3), 356–367. https://doi.org/10.1111/j.1539-6924.2012.01885.x
Pregnolato, M., Ford, A., Wilkinson, S. M., & Dawson, R. J. (2017). The impact of flooding on road transport: A depth-disruption function. *Transportation Research Part D: Transport and Environment*, *55*, 67–81. https://doi.org/10.1016/j.trd.2017.06.020
Quinn, A., Jack, A., Hodgkinson, S., Ferranti, E., Beckford, J., & Dora, J. (2017). *RAIL ADAPT Adapting the railway for the future*. Paris. Retrieved from https://uic.org/railadapt-report
Rankine, W. J. M. (1867). *A Manual of Civil Engineering* (Fifth Edit). London: Charles Griffin and Company.
Reed, D. A., Kapur, K. C., & Christie, R. D. (2009). Methodology for Assessing the Resilience of Networked Infrastructure. *IEEE SYSTEMS JOURNAL*, *3*(2), 174–180. https://doi.org/10.1109/JSYST.2009.2017396
Sánchez-silva, M., Frangopol, D. M., Padgett, J., & Soliman, M. (2016). Maintenance and Operation of Infrastructure Systems: Review. *Journal of Structural Engineering*, *142*(1), 1–16. https://doi.org/10.1061/(ASCE)ST.1943-541X.0001543.
Schardong, A., Simonovic, S. P., & Tong, H. (2018). *Use of Quantitative Resilience in Managing Urban Infrastructure Response to Natural Hazards: A Web-Based Decision Support Tool - ResilSIMt*. London. Retrieved from https://www.eng.uwo.ca/research/iclr/fids/publications/products/105.pdf
Sela, L., Bhatia, U., Zhuang, J., & Ganguly, A. (2017). Resilience Strategies for Interdependent Multiscale Lifeline Infrastructure Networks. In *ASCE International Workshop on Computing in Civil Engineering 2017* (pp. 265–272). Seattle, Washington. https://doi.org/doi:10.1061/9780784480847.033
Simmins, G. (2011). Urban and Regional Planning. Retrieved March 12, 2018, from http://www.thecanadianencyclopedia.ca/en/article/urban-and-regional-planning/
Simonovic, S. P. (2016). FROM RISK MANAGEMENT TO QUANTITATIVE DISASTER RESILIENCE – A PARADIGM SHIFT. *International Journal of Safety and Security Engineering*, *6*(2), 85–95. https://doi.org/10.2495/SAFE-V6-N2-85-95

Simonovic, S. P., & Arunkumar, R. (2016). Comparison of static and dynamic resilience for a multipurpose reservoir operation. *Water Resources Research*, *52*(11), 77–116. https://doi.org/10.1002/2016WR019551

Simonovic, S. P., & Peck, A. (2013). Dynamic Resilience to Climate Change Caused Natural Disasters in Coastal Megacities Quantification Framework. *British Journal of Environment & Climate Change*, *3*(3), 378–401. https://doi.org/10.9734/BJECC/2013/2504

Thacker, S., Pant, R., & Hall, J. W. (2017). System-of-systems formulation and disruption analysis for multi-scale critical national infrastructures. *Reliability Engineering and System Safety*, *167*, 30–41. https://doi.org/10.1016/j.ress.2017.04.023

The White House. (2013). Presidential Policy Directive - Critical Infrastructure Security and Resilience, PPD-21. Retrieved September 21, 2018, from https://www.whitehouse.gov/the-press-office/2013/02/12/presidential-policy-directive-critical-infrastructure-security-and-resil

TheRedPin. (2015). What does the average detached home look like in the GTA's most prominent cities? Retrieved May 31, 2018, from https://blog.theredpin.com/blog/what-does-the-average-detached-home-look-like-in-12-cities-in-the-greater-toronto-area/

Tierney, K., & Bruneau, M. (2007). Conceptualizing and Measuring Resilience: A Key to Disaster Loss Reduction. *TR News*, 14–15. https://doi.org/10.17226/23168

Toronto Hydro-Electric System Limited. (2011). *DISTRIBUTION SYSTEM – SYSTEM CHALLENGES*. Toronto. Retrieved from http://www.torontohydro.com/sites/electricsystem/documents/2012edr/d1_t07_s05.pdf

Toronto Hydro. (2018a). About Outages. Retrieved August 7, 2018, from http://www.torontohydro.com/sites/electricsystem/PowerOutages/Pages/aboutoutages.aspx

Toronto Hydro. (2018b). Facts at a glance. Retrieved August 13, 2018, from https://www.torontohydro.com/sites/corporate/AboutUs/Pages/FactsataGlance.aspx

TRCA. (2018). Flood Plain Map. Retrieved December 12, 2018, from https://trca.ca/conservation/flood-risk-management/flood-plain-map-viewer/

UNISDR (United Nations Office for Disaster Risk Reduction). (2017). Terminology. Retrieved September 21, 2018, from https://www.unisdr.org/we/inform/terminology

Upadhyaya, J. K., Biswas, N., & Tam, E. (2014). A review of infrastructure challenges: assessing stormwater system sustainability. *Canadian Journal of Civil Engineering*, *41*(6), 483–492. https://doi.org/10.1139/cjce-2013-0430

Van Wee, B., & Tavasszy, L. A. (2008). Ex-ante evaluation of mega-projects: methodological issues and cost-benefit analysis. In *Decision-Making on Mega-Projects: Cost-Benefit Analysis, Planning and Innovation*. Edward Elgar Publishing Limited.

Vugrin, E. D., Warren, D. E., Ehlen, M. A., & Camphouse, R. C. (2010). A Framework for Assessing the Resilience of Infrastructure and Economic Systems. In K. Gopalakrishnan & S. Peeta (Eds.), *Sustainable and Resilient Critical Infrastructure Systems: Simulation, Modeling, and Intelligent Engineering* (pp. 77–116). Berlin, Heidelberg: Springer Berlin Heidelberg. https://doi.org/10.1007/978-3-642-11405-2

Wakchaure, A. S. (2001). *An ArcView tool for simulating Land Subdivision for Build Out Analysis*. Virginia Polytechnic Institute and State University. Retrieved from https://vtechworks.lib.vt.edu/handle/10919/37156

Wickramasuriya, R., Chisholm, L. A., Puotinen, M., Gill, N., & Klepeis, P. (2011). An automated land subdivision tool for urban and regional planning: Concepts, implementation and testing. *Environmental Modelling and Software*, *26*(12), 1675–1684. https://doi.org/10.1016/j.envsoft.2011.06.003

Wickramasuriya, R., Chisholm, L., Puotinen, M., & Gill, N. (2010). Parcel subdivision automation for agent-based land use modelling. In D. Swayne, W. Yang, A. Voinov, A. Rizzoli, & T. Filatova (Eds.), *International Congress on International Environmental Modelling and Software* (pp. 1–8). Ottawa. Retrieved from https://www.researchgate.net/publication/228576374_Parcel_subdivision_automation_for_agent-based_land_use_modelling

Woods, D. D. (2015). Four concepts for resilience and the implications for the future of resilience engineering. *Reliability Engineering and System Safety*, *141*, 5–9. https://doi.org/10.1016/j.ress.2015.03.018

World Economic Forum. (2014). *Strategic Infrastructure Steps to Operate and Maintain Infrastructure Efficiently and Effectively*. Retrieved from http://www3.weforum.org/docs/WEF_IU_StrategicInfrastructureSteps_Report_2014.pdf

Zhao, T., & Tseng, C. (2003). Valuing Flexibility in Infrastructure Expansion. *Journal of Infrastructure Systems*, *9*(3), 89–97. https://doi.org/https://doi.org/10.1061/(ASCE)1076-0342(2003)9:3(89)

Zobel, C. W. (2011). Representing perceived tradeoffs in defining disaster resilience. *Decision Support Systems*, *50*(2), 394–403. https://doi.org/10.1016/j.dss.2010.10.001

Appendix A - Implementation of Resilience in Infrastructure Management

Appendix A refers to the development of a tool that can implement this thesis's methodology and apply it to real infrastructure management problems. The tool has been developed by the research group of Prof. Simonovic at Western University under the leadership of Dr. Andre Schardong. The tool is in the form of a web-based application and is in the public domain: http://resilsimt-uwo.ca/ .

This appendix focusses on how to implement the methodology to bridge its theoretical and application value and thereby realize its potential as a decision support tool. The presentation is divided into two parts. The first part provides an overview of the tool's system architecture. The second part examines how the tool operates from a user's perspective and provides a brief user's manual. The tool is designed with the intent of helping infrastructure managers estimate the difference in resilience values as a result of choosing various sets of adaptation options. A detailed technical description of the tool is available in Schardong et al. (2018).

A1 System Architecture of the Tool

The tool provides a service, which in this context refers to quantifying a resilience value based on the interactions of the infrastructure system, the hazard scenario, and the adaptations applied.

The interactions between software components are summarized in Figure 44. These interactions can be divided into three main software components: the user interface (UI), the application server, and the database. Beginning with the UI, the user provides input data and requests resilience values from the system. A request is then escalated to the server where it is processed. Data input is then added to the database. Open data is also retrieved from the database and used for processing by the server. The server applies the algorithms developed in the methodology coupled with the available data to calculate resilience values, which are then fed back to the UI to be presented to the user.

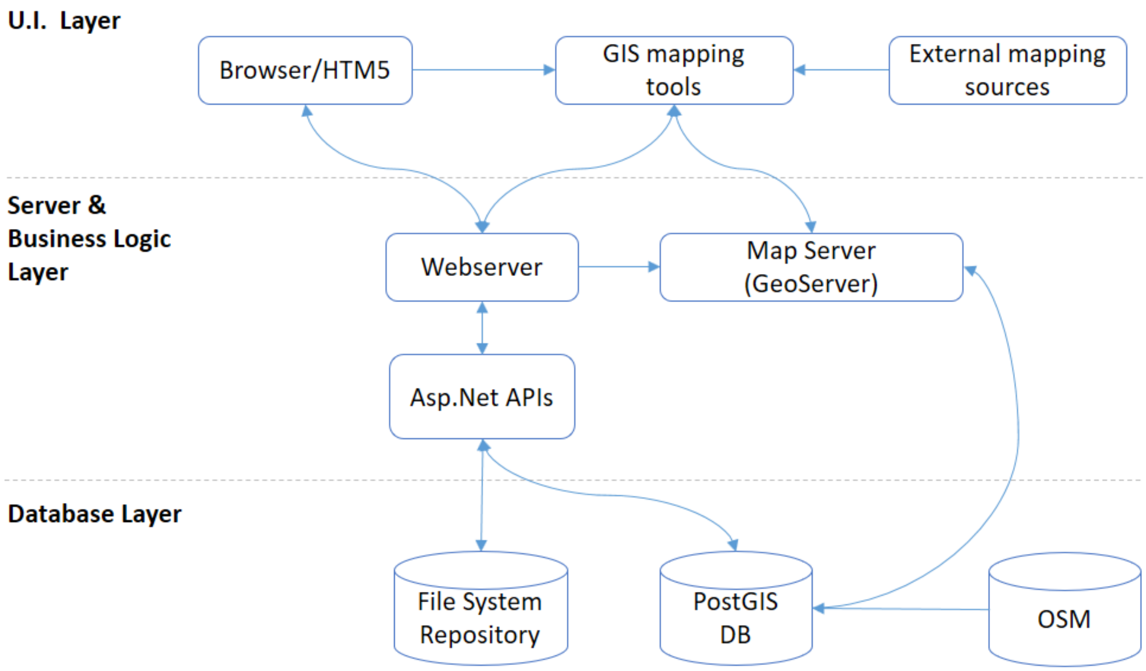

Figure 44 System architecture of the resilience tool. This figure is the property of the original authors of Schardong et al. (2018).

Within each main software component, there are multiple components that perform various tasks. For the resilience tool, HTM5 acts as the browser, displaying the information and results. Specifically, HTM5 is a combination of hypertext markup language (HTML) and cascading style sheet (CSS) that allows the design and placement of text on the screen for the user to see. This is also how the user is able to input adjustments to the extent of adaptation options. GIS mapping tools are employed to enhance the visualization process by providing a spatial sense of where infrastructure is located and where hazards occur. The GIS mapping tools use JavaScript to help with some of the local processing. In the context of inputting or editing infrastructure networks, this component controls their spatial placement. In the context of hazard input, the GIS mapping tools enable the user to draw polygon areas that represent where a hazard strikes. External mapping services are used to provide various maps, such as a base map, to give the user a sense of how infrastructure placement relates to the geographical surroundings. Additional geographic layers such as property boundaries, geopolitical boundaries, and municipalities are also available.

The database primarily comprises the PostgreSQL software with a PostGIS extension. The database allows for the storage of inputs and results. Open Street Maps (OSM) are one of the primary data sources made available in the tool. OSM contains various network and layer data such as road networks and locations of various critical facilities.

The process between the UI and the database is where most of the computation and processing occurs and consists of Asp.Net, which stores the code representing the methodology described earlier. Specifically, it uses C# programming language. The webserver is the component that enables the stored code to be executed on the net. In contrast, the map server enables the processing of geospatial imaging, such as zooming in and out of a mapped area. For example, whenever zooming in or out of the map image, the server is actually accessing different rectangular tiles at various resolutions and details. Some of these details are simplified and kept hidden depending on the spatial extent.

A2 User’s Manual

A2.1 Account Creation

The tool requires the user to create an account. This allows uploaded data to remain personalized and private and results to be saved.

A2.2 Infrastructure Network Input

There are two primary ways to create a network. These include manual input of nodes and edges, uploading existing networks through files, and creation via built-in methods within the tool.

The first method of creating a network is by uploading a shapefile that consists of nodes and edges. Note that the shapefile must be georeferenced as all data within the tool require GIS coordinates.

The second method of creating a network is using the defined expansion methodology described by Schardong et al. (2018). This typically requires the user to input a few parameters and draw an area, and the network is then automatically populated.

Some default data is available through OSM that can be used as networks or layers. Additional layers may be added by the user to represent nodes, edges, or polygon areas that can contribute to the resilience calculations. Having other layers for visual reference or boundaries can also be useful.

The interdependent relationships between different networks and layers that affect overall resilience are specified here. A relationship is assumed to be a one-directional relationship, where the state of one system component affects the state of another system component in a separate network or layer.

A2.3 Hazard and Impact Relationship Input

Once the overall infrastructure system has been defined, the user specifies the hazards and the respective impact relationships for each component type. A hazard is defined by its magnitude characteristic at every time step. For each time step, the user may draw an area affected by the hazard. The components that fall within this area then require a hazard impact relationship for that specific component. This relationship can take the form of an equational input or tabular input. In flood studies, this has a similar form to stage-damage curves. It is assumed that damage impact is not affected by any factors outside of this characteristic measure.

A2.4 Base Case Resilience Output and Adaptation Options

After the input of the hazard and impact relationship, the tool processes the inputs and shows the resultant system performance and associated resilience measures for individual systems and the overall system.

Adaptation measures come in various forms. The first are specified adaptation measures in the form of sliders that adjust the extent to which the measures are applied. These adaptation measures work by taking the difference in loss of performance for a specific component between the base case scenario and the scenario in which the component was unaffected by the storm. This performance loss forms the potential gain that could occur if the adaptation option was implemented. A maxed-out slider implies that the adaptation is used optimally and no performance loss occurred for the specific type of infrastructure component. An unchanged slider would have performance matching the base case scenario without an implemented adaptation.

Adaptation implementation can also come in the form of replacing infrastructure components, thereby adjusting the impact relationship with the hazard. This is completed in the infrastructure design when the user revisits the section.

A2.5 Downloading Outputs

The resilience data of scenarios that were run can be downloaded from the tool in the form of tables.

Graphs can only be displayed in the web browser

Curriculum Vitae

Name: Howard Tong

Post-secondary Education and Degrees:
University of Waterloo
Waterloo, Ontario, Canada
2010-2016 B.A.S

Western University
London, Ontario, Canada
2016-2018 M.E.Sc

Related Work Experience
Environmental Analyst
Canadian Imperial Bank of Canada
2015

Publications:

Schardong, A., Simonovic, S. P., & Tong, H. (2018). *Use of Quantitative Resilience in Managing Urban Infrastructure Response to Natural Hazards: A Web-Based Decision Support Tool - ResilSIMt*. London. https://www.eng.uwo.ca/research/iclr/fids/publications/products/105.pdf

Schardong, A., Simonovic, S. P., & Tong, H. (2019). Use of quantitative resilience in managing urban infrastructure response to natural hazards. *International Journal of Safety and Security Engineering*, *9*(1), 13–25. https://doi.org/10.2495/safe-v9-n1-13-25